NTRCI

NATIONAL TRANSPORTATION
RESEARCH CENTER, INCORPORATED
UNIVERSITY TRANPORTATION CENTER

Enhanced Finite Element Analysis Crash Model of Tractor-Trailers (Phase A)

This project was funded by the NTRCI University Transportation Center under a grant from the U.S. Department of Transportation Research and Innovative Technology Administration (#DTRT06G-0043)

Chuck Plaxico and James Kennedy – Battelle
Srdjan Simonovic – Oak Ridge National Laboratory
Nikola Zisi – University of Tennessee

TABLE OF CONTENTS

LIST OF TABLES

LIST OF FIGURES

EXECUTIVE SUMMARY

While many highway crashes involve vehicle-to-vehicle impacts, a substantial number of injuries and fatalities result from single vehicle impacts with roadside infrastructure such as guardrails, protective barriers, roadway signs and other fixed objects. The design and engineering of these structures strongly influence the injury-causing g-forces experienced by vehicle occupants and whether or not vehicles are redirected back into traffic. In recent decades, the highway community, including the U.S. Department of Transportation (USDOT), the Federal Highway Administration (FHWA), the Turner Fairbank Highway Research Center (TFHRC), and state Departments of Transportation have supported and conducted extensive full-scale passenger car-barrier crash tests to better understand crash performance of guardrails and barriers and to improve their design and to reduce the likelihood of vehicle-infrastructure crash fatalities and injuries. However, very limited work has been conducted on crash performance of barriers when impacted by medium and heavy duty trucks due to the cost and the complexity of full scale truck testing. Substantially more data and better understanding of truck-infrastructure crashes would enable the highway community to improve barrier design, to further reduce the likelihood of vehicle-infrastructure fatalities and injuries and to reduce highway congestion resulting from severe accidents.

In collaboration with the TFHRC, the National Transportation Research Center, Inc. (NTRCI) has taken an active role in enhancing industry understanding of truck-infrastructure crash behavior through funding the development and enhancement of advanced finite element (FE) computer simulation models of truck-infrastructure crashes. Recent NTRCI funded work on refinement and enhancement of models of single unit truck crashes into concrete barriers has demonstrated the ability of this advanced computer simulation technology to provide sorely needed high quality data and analysis results at substantially lower cost than full-scale crash tests. NTRCI is helping provide highway engineers with data to make better, more well-informed roadside infrastructure decisions that enhance the safety of the traveling public.

To build upon its success with single-unit truck crash simulation and analysis, NTRCI has funded the research team of Battelle, Oak Ridge National Laboratory (ORNL) and the University of Tennessee at Knoxville (UTK) to conduct a three-phase investigation to enhance and refine an FE model for simulating tractor-trailer crash events involving barriers and roadside safety hardware such as bridge rails and median barriers. The model was originally developed by the National Crash Analysis Center (NCAC) of George Washington University (GWU) and requires refinement and testing before it can be used by the engineering community for infrastructure design.

The objective of this current investigation led by Battelle is to validate and enhance computer models of a tractor-trailer combination that will be used in analysis, design, and evaluation of roadside safety hardware. The research team will evaluate the overall fidelity of the tractor-trailer model by verifying vehicle failure modes from simulation against those from actual truck crash tests. This effort will enable the tractor-trailer model to provide more realistic predictions of crash performance and significantly reduce the need for costly full-scale truck testing.

This report summarizes the results of the first phase of a three phase program. In general terms, the plan for conducting this effort over three phases is as follows:

1) Phase A - Conduct an in-depth evaluation of the NCAC tractor only FE model, implement selected modifications and develop a new trailer model.
2) Phase B - Complete preliminary modification of combined tractor-trailer models, provide them to the FHWA Center of Excellence (COE) community for beta testing, and validate them against suitable full-scale crash tests.
3) Phase C - Develop an online User's Manual / Website to facilitate the use of the model.

Following is an Executive Summary of the work conducted in Phase A of this program:

- Full-Scale Tractor-Trailer Crash Test Literature Review
- Tractor-Trailer Finite Model Evaluation and Enhancement
- Tractor-Trailer Material and Inertial Properties Evaluation
- Plans for Phase B of the Investigation

Full-Scale Tractor-Trailer Crash Test Literature Review. Chapter 2 of this report describes a literature search conducted by the research team to find and obtain reports and electronic data related to full-scale crash tests involving tractor-trailer vehicles. The data obtained from the literature review will be used in future activities as a gauge to measure fidelity of the tractor-trailer FE model by comparing simulation-vehicle failure modes with real vehicle crash test failure modes. For evaluation of the model, the study will focus on impacts with rigid barriers so that the mechanics of the impact can be isolated to the response of the vehicle.

The literature search identified some challenges. It was determined from the literature review that the vehicles used in the tests encompassed a wide range of vehicle makes and overall dimensions and none were consistent with the properties of the 1992 Freightliner FLD120 tractor upon which the FE model was based. Because the tests were focused on performance of the barrier, very little information was provided in the reports regarding damage and response of the vehicle. So, for the purposes of FE model validation, it will be necessary to obtain as much of the electronic data (e.g., accelerometer, rate gyros, photos, videos, etc.) corresponding to these tests and discern as much information as possible relating to the vehicles' response during impact.

In addition, all roadside safety hardware used on the National Highway System (NHS) must meet the testing requirements of National Cooperative Highway Research Program (NCHRP) Report 350 Recommended Procedures for the Safety Performance Evaluation of Highway Appurtenances[1]. This document contains recommended procedures for evaluating the safety performance of various highway safety features. It presents uniform guidelines for the crash testing of both permanent and temporary highway safety features and recommended evaluation

[1] Ross, H.E., D.L. Sicking, and H.S. Perrara, "Recommended Procedures for the Safety Performance Evaluation of Highway Appurtenances," *National Cooperative Highway Research Program Report No. 350*, Transportation Research Board, Washington, D.C., 1993.

criteria to assess test results. Guidelines are also presented for the in-service evaluation of safety features. These guidelines and criteria incorporate current technology and the collective judgment and expertise of professionals in the field of roadside safety design. They provide (1) a basis on which researchers and user agencies can compare the impact performance merits of candidate safety features, (2) guidance for developers of new safety features, and (3) a basis on which user agencies can formulate performance specification for safety features. Test levels 4, 5 and 6 in Report 350 are intended to evaluate strength of safety barriers for containing and redirecting heavy vehicles such as single-unit trucks and tractor-trailer vehicles. Report 350 does not require a specific make or model for the test vehicle, but rather provides recommended properties for test vehicles for representing various classes of vehicles.

Tractor-Trailer Finite Model Evaluation and Enhancement. Chapter 3 of this report describes the research team's evaluation of the tractor-trailer FE model and modifications made to enhance its fidelity. The team conducted a basic evaluation of the NCAC tractor model to identify critical model features that warranted improvement regarding the model's ability to accurately simulate vehicle response in impacts with roadside safety hardware. The accuracy of the enhanced tractor FE model (version 07-1226b) was assessed by comparing simulation results to a full-scale crash test of a Freightliner FLD120 tractor impacting a 42-inch tall F-shape concrete barrier. This test was conducted at the TFHRC Federal Outdoor Impact Laboratory (FOIL) under the auspices of the NCAC. This was the only test that has been conducted that involved a tractor without a trailer impacting a barrier at an oblique angle. The tractor vehicle used in the full-scale test was modified prior to the test, including removal of several parts. The exhaust stack and a section of the sleeper in the FE model were removed for the simulation to partially account for some of the modifications. The model of the barrier was idealized to be rigid, although the test barrier experienced some lateral displacement during impact. Although there were differences between the test and simulation, the FE model was able to effectively capture all the important phenomenological events during the impact related to vehicle kinematics. The vehicle experienced the highest accelerations between 0.1 and 0.2 seconds of the impact event. During this time range the maximum acceleration computed at the center of gravity of the tractor model was approximately 4 g's compared to approximately 5 g's in the full-scale test. After this time the accelerations drop to less than 1 g until approximately 0.67 seconds. This time corresponds to when the driver-side wheel impacts the ground and accelerations increase to slightly above 1 g in both the simulation and test. From the sequential views of the impact event, the kinematics of the tractor model correspond very well to the test vehicle regarding both magnitude and timing of events. The maximum roll angle of the tractor model measured at the tractor's center of gravity was higher in the simulation than the test (i.e., 10 degrees and 7.6 degrees respectively).

The deformations of the tractor during impact were isolated to the front, impact side of the vehicle in both the simulation and test. There was no noticeable damage to the frame rail in either the simulation or the test. The primary transfer of forces between the barrier and the vehicle appear to go through the front bumper and wheel assembly and it is these components that receive the majority of damage in the test and simulation. The response of the wheel assembly, in particular, has a significant affect on the kinematic behavior of the vehicle. The damage to the suspension in the full-scale test was limited to the fracture of the top leaf spring at the pinned connection at the front mounting bracket on the impact side and the fracture

of one U-bolt on the non-impact side. In the FE simulation, the top leaf spring on the impact side and the front U-bolt fractured at approximately 0.21 seconds.

While these preliminary results are promising, a more direct and detailed comparison is planned for Phase B in which all the components removed from the test vehicle will be removed from the model. The model will be modified to correspond as closely as possible to the test vehicle. Development of a modified barrier model is out of scope of this project and any influence of this discrepancy will have to be considered in the assessment of the tractor model's accuracy.

The development of a new semi-trailer was also accomplished during Phase A of this project. The original semi-trailer model developed by NCAC was determined to be inappropriate for use in NCHRP Report 350 simulations based on comparison of the model's geometry with the requirements specified in the report. The research team recommended and NTRCI approved a decision to create the new trailer model.

The new trailer model was developed based primarily on the geometry of a 53-ft Stoughton trailer. The CAD geometry was obtained through a collaborative effort between the NTRCI team and Digimation. Team members visited a local Freightliner dealer and surveyed the trailers on their lot. Photographs and measurements were taken and provided to Digimation for use in developing the CAD geometry. This geometry was then used by to develop the FE mesh of the semi-trailer.

Tractor-Trailer Material and Inertial Properties Evaluation. Chapter 4 of the report describes the analysis and enhancement of the material models and inertial properties of the enhanced FE tractor model conducted by the team. During a crash, parts undergo permanent, plastic, deformation that dissipates impact energy, and the model must have accurate material yield and flow stresses descriptions to achieve reasonable expectations of accuracy. In the new model, new materials and constitutive model parameters were assigned by the team to the following part systems:

1. Frame
2. Leaf springs
3. Driveshafts
4. Fasteners, brackets
5. Body, structural bumpers
6. Hood, aerodynamic bumpers, chassis side fairing

All the model modifications and model editing were implemented using computer programs and scripts. Such an approach allows for simple version control, modifications that can be turned on and off as needed, and that parametric studies can be performed automatically.

From the perspective of inertial properties and vehicle dynamics, the tractor-trailer vehicle can be viewed as an assembly of rigid bodies interconnected by suspensions and hitches. Springs connect two main characteristic sets of masses, unsprung and sprung, while hitches connect sprung masses of the tractor to the sprung mass of the trailer. In the tractor-trailer system, the tractor is only a small part of the total, fully laden heavy truck. However, its kinematics play an important role during the impact as it guides the load-dominant trailer mass through the hitch.

The enhancement of the inertia properties compared to the original model was modest. Markedly better performance of the enhanced model is primarily due to the vastly improved FEM sub-models for the suspension and models for deformation of the critical structural parts of the tractor. The distribution of masses can now be better handled due to our ability to evaluate inertial effect of parts modifications. The inertial modifications are primarily needed for the sprung mass with which we can tune the target inertial properties. This capability will be used in the next phase of the project to conduct parametric studies of the inertial properties on the tractor on its interaction with a roadside safety barrier.

Plans for Phase B of the Investigation. The preliminary evaluation of the modified tractor and trailer FE model initiated in Phase A will be completed in Phase B of the program. A major objective of Phase B of the project will be to validate the combined tractor-trailer models by simulating full-scale crash tests identified in the literature and comparing simulated vehicle behavior and failure modes to those reported in the crash tests. Details of the planned effort are described in the research team proposal for Phase B.

Once the performance of the tractor-trailer FE model is considered acceptable, the model will be provided to the other FHWA COEs in roadside safety. Use of the beta version by the COEs is encouraged so that further discrepancies can be brought forth to better improve the tractor-trailer FE model. The COEs may have applications for the tractor-trailer FEA model that could reveal previously unobserved kinematic behavior and/or failure modes of the tractor-trailer combination in impact situations. All comments and suggestions from the COEs will be assessed and discussed with NCAC and TFHRC for further action, including implementation into the model if deemed appropriate.

The vehicle dimensions in the model may also need to be altered to meet NCHRP Report 350 requirements before being applied in the analysis of roadside safety structures. NCHRP Report 350 does not require a specific make or model for the test vehicle, but rather provides recommended properties for the test vehicles to represent various classes of vehicles. For example, NCHRP Report 350 Test Level 5 requires that the maximum tractor wheel base not exceed 189 inches for the 36000V vehicle (79,366-lb tractor/van-trailer), whereas the current model's wheel base length is 217.2 inches (5.52 m) and includes a sleeper-cab. It is recommended that the enhancement of the model continue based on its current geometry. Once the model is validated, it can then be modified to meet length requirements of Report 350 by removing a section of the sleeper and the frame of the tractor. Any permanent changes to the FE model (such as reduced length) will be at the agreement of NTRCI, TFHRC, NCAC and the COEs.

CHAPTER 1. INTRODUCTION

In recent decades, the highway community, including the U.S. Department of Transportation (USDOT), the Federal Highway Administration (FHWA), the Turner Fairbank Highway Research Center (TFHRC), and state Departments of Transportation have supported and conducted extensive full-scale passenger car-barrier crash tests to better understand crash performance of guardrails and barriers and to improve their design and to reduce the likelihood of vehicle-infrastructure crash fatalities and injuries. Improved understanding of truck-infrastructure crashes would enable the highway community to improve barrier design, to further reduce the likelihood of vehicle-infrastructure fatalities and injuries and to reduce highway congestion resulting from severe accidents. In collaboration with the TFHRC, the National Transportation Research Center, Inc. (NTRCI) has taken an active role in enhancing industry understanding of truck-infrastructure crash behavior through funding the development and enhancement of advanced finite element (FE) computer simulation models of truck-infrastructure crashes. NTRCI is helping provide highway engineers with data to make better, more well-informed roadside infrastructure decisions that enhance the safety of the traveling public.

NTRCI has funded the research team of Battelle, Oak Ridge National Laboratory (ORNL) and the University of Tennessee at Knoxville (UTK) to conduct a three-phase investigation to enhance and refine an FE model for simulating tractor-trailer crash events involving barriers and roadside safety hardware such as bridge rails and median barriers. The model was originally developed by the National Crash Analysis Center (NCAC) of George Washington University (GWU) and requires refinement and testing before it can be used by the engineering community for infrastructure design.

The objective of this current investigation led by Battelle is to validate and enhance computer models of a tractor-trailer combination that will be used in analysis, design, and evaluation of roadside safety hardware. The research team will evaluate the overall fidelity of the tractor-trailer model by verifying vehicle failure modes from simulation against those from actual truck crash tests. This effort will enable the tractor-trailer model to provide more realistic predictions of crash performance and significantly reduce the need for costly full-scale truck testing.

This report summarizes the results of the first phase, Phase A, of a three phase program. In general terms, the plan for conducting this effort over three phases is as follows:

- Phase A - Conduct an in-depth evaluation of the NCAC tractor only FE model, implement selected modifications and develop a new trailer model.
- Phase B - Complete preliminary modification of combined tractor-trailer models, provide them to the FHWA Center of Excellence (COE) community for beta testing, and validate them against suitable full-scale crash tests.
- Phase C - Develop an online User's Manual / Website to facilitate the use of the model.

This report on the Phase A investigation is presented as six chapters, according to the organization of the work.

- Chapter 1. Introduction

- Chapter 2. Full-Scale Tractor-Trailer Crash Test Literature Review, led by Battelle
- Chapter 3. Tractor-Trailer Finite Element Model Evaluation and Enhancement, led by Battelle
- Chapter 4. Tractor-Trailer Material and Inertial Properties Evaluation, led by ORNL and UT
- Chapter 5. Summary of Plans for Phase B of the Investigation
- Chapter 6. References

CHAPTER 2. FULL-SCALE TRACTOR-TRAILER CRASH TEST LITERATURE REVIEW

The NTRCI Finite Element Analysis Team is conducting a study to enhance a finite element (FE) model of a tractor-trailer developed by the National Crash Analysis Center (NCAC). The model was developed for the purpose of simulating tractor-trailer crash events with particular emphasis on those crash events involving roadside safety hardware (e.g., bridge rails, median barriers, etc.). As part of this study, Battelle led the Team in conducting a literature search to find and obtain reports and electronic data related to full-scale crash tests involving tractor-trailer vehicles.

A primary objective of the study is to determine the overall fidelity of the tractor-trailer FE model by comparing simulation-vehicle failure modes with real vehicle failure modes. For evaluation of the model, the study will focus on impacts with rigid barriers so that the mechanics of the impact can be isolated to the response of the vehicle. The data obtained from these reports will be used as a gauge to measure model fidelity; however, the literature search has identified some associated challenges.

Testing requirements for evaluation of roadside safety barriers such as National Cooperative Highway Research Program (NCHRP) Report 350[1] do not require a specific make or model for the test vehicle but, rather, provide recommended properties for the test vehicles to represent various classes of vehicles. For example, NCHRP Report 350 Test Level 5 requires that the maximum tractor wheel base not exceed 189 inches for the 36000V vehicle (79,366-lb tractor/van-trailer), the overall length of the tractor-trailer not exceed 50 ft, the maximum overhang of the trailer not exceed 86.6 inches, the cargo bed height must fall within 50-54 inches, and the center of gravity must fall within 70.9-74.8 inches.

It was determined from the literature review that the vehicles used in the tests encompassed a wide range of vehicle makes and overall dimensions and none were consistent with the properties of the 1992 Freightliner FLD120 tractor on which the FE model was based. Because the tests were focused on performance of the barrier, very little information was provided in the reports regarding damage and response of the vehicle. So, for the purposes of FE model validation, it will be necessary to obtain the electronic data (e.g., accelerometer, rate gyros, photos, videos, etc.) corresponding to these tests and discern as much information as possible relating to the vehicles' response during impact.

LITERATURE OVERVIEW

To date, eleven (11) crash test reports have been obtained and one other identified. These tests were conducted over a span of 22 years starting in 1981. Of those reports obtained, nine tests were conducted at the Texas Transportation Institute (TTI) in College Station Texas, one test was conducted at the Federal Outdoor Impact Facility (FOIL) in McLean, Virginia by the NCAC, and one test was conducted at the Midwest Roadside Safety Facility (MwRSF) in Lincoln, Nebraska. The tests typically involved tractor-trailers with a nominal weight of 50,000 lbs or 80,000 lbs impacting a barrier at a nominal speed and angle of 50 mph and 15 degrees, respectively. The test videos, photos, and electronic data have been obtained for only two tests (i.e., MwRSF and FOIL/NCAC tests). The literature search is an ongoing task and the Research Team is still in the process of obtaining additional electronic test data.

Eight of the crash tests were qualification tests for concrete bridge rails and median barriers, which are classified as rigid-barriers in terms of roadside safety devices. The concrete barriers were typically 42 inches tall, except in two cases where a steel tube rail was installed on top of the concrete barrier to increase overall barrier height. Two of these tests were on "aesthetic" or open-faced, post-and-beam style designs. In most cases, barrier deflections were negligible except for the post-and-beam style designs. Damage to the barriers was reported as being only cosmetic except for the cases involving a steel rail installed on top of the concrete barrier and for the post-and-beam style design.

Two tests were conducted on an instrumented vertical wall to measure impact forces from tractor-trailer impacts. This type of data can be very useful for verification of the FE model results; however, the results also show that the magnitude of force is very dependent on the type of tractor and trailer and neither case corresponds to the current finite element model (conventional tractor with sleeper-cab and box-trailer). For example:

- In one test, a cab-over style tractor and a box-trailer with a mass of 80,000 lbs impacted the 90-inch tall wall at an impact speed of 55 mph and 15.3 degrees. The first peak load was approximately 66,000 lbs and corresponded to initial impact of the tractor; the second peak load was approximately 176,000 lbs and was associated with the rear tandem axles of the tractor and the front of the trailer; and the third peak load was approximately 220,000 lbs and was associated with the final impact of the trailer with the wall.
- The second test involved a conventional style tractor (with a sleeper unit) with a significantly longer wheel base and a tanker-trailer with a total mass of 80,000 lbs impacting the 90-inch tall wall at an impact speed of 54.8 mph and 16 degrees. Initial impact of the tractor resulted in a peak load of approximately 91,000 lbs; the impact of the rear tandem axles of the tractor resulted in a peak load of approximately 212,000 lbs; and the impact of the rear tandem axles of the trailer resulted in a peak load of approximately 408,000 lbs.

NCAC conducted a test specifically for the purpose of collecting crash performance/response data to use for validation of the NCAC tractor FE model. The test involved a 1992 Freightliner FLD120 tractor impacting into an F-shape concrete safety barrier at an impact speed of 31.25 mph at an angle of 25 degrees. A crash report was not written but accelerometer data was collected at several locations throughout the tractor, rate gyros were mounted near the center of gravity, and high-speed video was captured from several view points. The low mass and low impact speed of this test resulted in a relatively low impact severity compared to other tests,

which included a loaded van- or tanker-trailer but the data collected in the NCAC test may provide the most useful information for validation of the tractor because the tractor was isolated and the damage was only moderate

ASSESSMENT OF THE LITERATURE

An acceptable level of fidelity of the "bullet" model will need to be established based on expected applications. The current level of geometric detail limits the use of the model to applications involving low vehicle deformations (e.g., Roadside safety type applications-redirective impact on barriers) or applications involving the vehicle as simply a source of impact energy where results are not significantly sensitive to vehicle damage (e.g., homeland security type applications).

Validation criteria for assessing model performance will need to be established based on available data from the literature. Unfortunately, none of those tests involve the specific tractor type that the FE model was based on except for the test conducted by NCAC at the FOIL. Furthermore, most of the tests were focused on performance of a barrier system rather than the vehicle and consequently very little information was provided in the reports regarding damage and response of the vehicles. It will be necessary to obtain the electronic data (e.g., accelerometer, rate gyros, photos, videos, etc.) corresponding to these tests and discern as much information as possible relating to the vehicles' response during impact.

The final dimensions of the vehicle may need to be modified in order to meet FHWA crash testing criteria before being applied in the analysis of roadside safety structures. The current crash testing requirements of NCHRP Report 350 allow a maximum wheel base length of 189 inches, which cannot be attained with a traditional style tractor with a sleeper-cab. The current wheel base length of the FE model is 217.2 inches and includes a sleeper-cab. It is recommended that the development/enhancement of the model continue based on its current geometry and that the model be validated using data obtained from FOIL/NCAC test No. 03008. Once the model is validated, it can then be modified to meet length requirements of Report 350 by removing a section of the sleeper and the frame of the tractor.

HEAVY VEHICLE IMPACT LITERATURE REVIEW SUMMARIES

The following section compiles the results of the heavy vehicle crash test literature search. The entries contain the author(s), publishing date, and title along with a summary of the report. The articles are chronologically ordered with the most recent reports appearing first. Some of the reports contained additional information such as barrier design methodology or other crash test data relating to smaller vehicle impact with the barriers. Only the data pertinent to the heavy vehicle impact was report herein. Tables 1 and 2 provide a summary of test information and parameters for the tractor-trailer vehicle crash tests identified in the literature review. Tables 3 - 13 provide a summary of the test vehicles' dimensions and mass properties.

1.1 Hirsh, T.J. and A. Arnold, "Bridge Rail to Restrain and Redirect 80,000 lb Trucks," Report No. FHWA/TX-81/16+230-4F, Texas State Dept. of Highways & Public Transportation, Austin, Texas (prepared by Texas Transportation Institute, College Station, Texas), 1981.

TTI Test No. 6

Test Article:

- Texas C202 concrete parapet (post-and-beam style) with Texas C4 steel rail mounted on top
- 101.2 ft (30.84 m) long
- Barrier height = 54 in (1672 mm)

Test Vehicle:

- 1978 Auto car tractor
  - Wheel base from center of front axle to center of rear tandem axle was 162 in (411.5 cm)
- Van-semitrailer
  - Distance from center of tandem axle assembly on tractor to center of tandem axle on trailer was 29.25 ft (8.9 m)
  - Trailer was loaded with sandbags and secured with plywood boards and steel cables

Impact Conditions:

Mass = 79,770 lb
Velocity = 49.1 mph
Angle = 15 degrees

Vehicle Instrumentation:

- The vehicle was instrumented with x, y, and z accelerometers and rate gyros placed over the tandem axle of the tractor
- High-speed video
  - Overhead camera
  - Downstream camera aligned parallel to the barrier

A 36-inch (910 mm) high concrete parapet with a steel rail mounted on top was tested to determine if it would contain and redirect an 80,000 lb (36,300 kg) tractor/trailer. The overall height of the barrier was 54 inches. The test was conducted with a **1978 Auto car tractor/trailer** ballasted with sandbags to 79,770 lb (36,184 kg) impacting at a speed and angle of 49.1 mph (79.0 km/hr) and 15 degrees. The vehicle was safely contained and redirected.

The bridge deck supporting posts 1 through 8 were cracked and damaged.

The damage to the truck included right front and right tandem wheels. No further details were given in the report. From the photograph, it appears that the damage to the front was isolated to the impact side fender and suspension. The photo is too dark to discern any details.

The bridge rail was a modified version of the Texas traffic rail type C202. The design consisted of a concrete beam element 13 inches wide and 23 inches deep, mounted 36 inches high on concrete posts spaced at 10 ft center to center. The concrete posts are 7 inches deep and 5 ft long with a 5 ft opening between each post. The Texas steel rail type C4 was mounted on top of the concrete parapet to increase the height of the rail.

1.2. Hirsch, T.J., W.L. Fairbanks, and C.E. Buth, "Concrete Safety Shape with Metal Rail on Top to Redirect 80,000 LB Trucks," Report No. FHWA/TX-83, Texas State Department of Highways and Public Transportation, Austin, Texas, (prepared by Texas Transportation Institute, College Station, Texas), 1984.

TTI Test 2416-1

Test Article:

- Texas type T5 concrete safety shape with Texas C4 steel rail mounted on top
- 101.2 ft (30.8 m) long
- Barrier height = 50.0 in (1270 mm)

Test Vehicle:

- 1981 Kenworth tractor
  - Wheel base from center of front axle to center of rear tandem axle was 199.5 in (506.7 cm)
- Van-semitrailer
  - Distance from center of tandem axle assembly on tractor to center of tandem axle on trailer was 27.1 ft (8.25 m)
  - Trailer was loaded with sandbags

Impact Conditions:

Mass = 80,080 lb
Velocity = 48.4 mph
Angle = 14.5 degrees

Vehicle Instrumentation:

- The vehicle was instrumented with triaxial accelerometers and rate gyros placed over the tandem axle of the tractor
- High-speed video
  - Overhead camera
  - Downstream camera aligned parallel to the barrier

A modified 32-inch Texas T5 bridge rail (New Jersey concrete safety shape) with an 18 inch (457 mm) tall modified Texas type C4 metal rail mounted on top was tested with a 80,080-lb (36,356-kg) tractor/trailer impacting at 48.4 mph (77.9 km/hr) and 14.5 degrees.

The test vehicle was a **1981 Kenworth tractor** with a 40-ft (12-m) **van semitrailer** ballasted with sandbags. The test inertia weight of the vehicle was 80,080 lb (36,356 kg).

The vehicle was contained and redirected and came to rest on its side approximately 175 ft downstream of the impact point.

The concrete barrier damage was minimal but the steel rail mounted on top was damaged between post 5 and 8. The truck sustained damage to the front impact side and to the tandem wheels. The cab of the truck remained intact. No further details were provided in the report. The photograph in the report was too dark to discern any details of the damage.

1.3. Campise, W.L. and C.E. Buth, "Performance Limits of Longitudinal Barrier Systems, Volume III – Appendix B: Details of Full-Scale Crash Tests on Longitudinal Barriers," Federal Highway Administration, U.S. Department of Transportation, Washington, D.C. (prepared by Texas Transportation Institute, College Station, Texas), May 1985.

TTI Test 4798-13

Test Article:

- New Jersey concrete safety shape
- 250 ft (76.2 m) long
- Barrier height = 42.0 in (1067 mm)

Test Vehicle:

- 1974 International tractor
  - Wheel base from center of front axle to center of rear tandem axle was 147.5 in (374.7 cm)
- Fruehauf van-semitrailer
  - Distance from center of tandem axle assembly on tractor to center of tandem axle on trailer was 30.7 ft (9.36 m)
  - Trailer was loaded with sandbags

Impact Conditions:

Mass = 80,180 lb
Velocity = 52.1 mph
Angle = 16.5 degrees

Vehicle Instrumentation:

- The instrumentation details of the vehicle was not reported but the results presented in the report indicated that it included:
    - a triaxial accelerometer mounted on the tractor
    - angular rate transducers to measure roll, pitch, and yaw rates of the tractor
    - an instrumented dummy
- High-speed video
    - Overhead camera
    - Downstream camera aligned parallel to the barrier

A New Jersey profile concrete safety shape barrier was tested to determine if it would contain and redirect an 80,000 lb (36,300 kg) tractor/trailer. The vehicle remained upright and met all safety criteria of NCHRP Report 350.

The test vehicle was a **1974 International tractor** (a flat nose tractor) with a 40-ft (12-m) **Fruehauf van semitrailer** ballasted with sandbags. The sandbags were placed uniformly over the floor of the trailer and were restrained with plywood covering bolted to the floor of the trailer. Vertical dimensions of the ballast averaged 24 in (610 mm). The empty weight of the tractor/trailer was 29,600 lb (13,438 kg) and its test inertia weight was 80,180 lb (36,402 kg).

The center of gravity was estimated to be 55 inches (1400 mm) above ground. The center of gravity of the ballast was 67 inches (1700 mm) above ground. The composite center of gravity was computed to be 64.4 inches (1640 mm) above ground.

The impact speed and angle was 52.1 mph (83.8 km/hr) and 16.5 degrees. The impact point was 85 ft (26 m) from the upstream end of the barrier. The vehicle remained upright and met all safety criteria of NCHRP Report 350. The maximum roll angle of the trailer was 52 degrees.

The barrier was chipped and marred but there was no measurable deflection of the barrier during the test. There was extensive damage to the impact side of the tractor. No further details were provided in the report. The photograph in the report was too dark to discern any details of the damage.

1.4. Mak, King K., W.L. Beason, T.J. Hirsch, and W.L. Campise, "Oblique Angle Crash Tests of Loaded Heavy Trucks into an Instrumented Wall," Report No. DOT HS 807 256, National Highway Traffic Safety Administration, Washington, D.C., (prepared by Texas Transportation Institute, College Station, Texas), 1988.

Two tests were conducted involving 80,000-lb tractor/trailers impacting an instrumented wall at 55 mph and 15 degrees.

TTI Test No. 7046-3

Test Article:

- Instrumented wall
- Four independent reinforced concrete wall sections
    - Segment length = 10 ft (3.048 m)
    - Barrier Height = 90 in (228.6 cm)

Test Vehicle:

- 1973 White Freightliner tractor
    - Vin No. CA213H077608
    - Wheel base from center of front axle to center of rear tandem axle was 164.5 in (417.8 cm)
- 1966 Fruehauf van trailer
    - Distance from center of tandem axle assembly on tractor to center of tandem axle on trailer was 30.5 ft (9.32 m)
    - Trailer was ballasted with sandbags and secured with plywood boards and steel cables

Impact Conditions:

Mass = 80,080 lb
Velocity = 55 mph
Angle = 15.3 degrees

Vehicle Instrumentation:

- The vehicle was instrumented with four accelerometer groups:
    - one triaxial accelerometer block mounted on the rear tandem of the tractor;
    - one biaxial accelerometer block mounted toward the front of the tractor in front of the fuel tanks; and
    - two biaxial accelerometer blocks placed on the trailer.
- Three rate transducers were mounted near the vehicle center of gravity to measure yaw, pitch, and roll rates of the tractor.
- An Alderson Hybrid II anthropomorphic dummy was placed in the driver position and instrumented.
- The right impact side fuel tank was instrumented with a pressure transducer to measure the internal pressure of the tank during the test.

The test vehicle was a **1973 White Freightliner tractor** (flat nose tractor) with a **1966 Fruehauf van-trailer**. The test inertia weight was 80,080 lb (36324 kg). The impact speed and angle was 55 mph (88.5 km/hr) and 15.3 degrees. The vehicle was contained and redirected. As the vehicle left the barrier it pulled to the right due to damage to the right front suspension system and eventually rolled over onto its left side.

Damage to the vehicle was extensive. The entire right side of the vehicle was dented and scraped and the windshield popped out. Maximum crush occurred at the right front corner at bumper height of 10 inches and there was some occupant compartment intrusion. The frame, suspension, and wheel assembly of the vehicle was also damaged. The instrumented wall only received cosmetic damage.

The results from the instrumented wall showed three distinct peak loads in the 0.050 second average force-time history. The first peak load was approximately 66,000 lb and corresponded to initial impact of the tractor; the second peak load was approximately 176,000 lb and was associated with the rear tandem axles of the tractor and the front of the trailer; the third peak load was approximately 220,000 lb and was associated with the final impact of the trailer with the wall.

TTI Test No. 7046-4

Test Article:

- Instrumented wall
- Four independent reinforced concrete wall sections
    - Segment length = 10 ft (3.048 m)
- Barrier height = 90 in (228.6 cm)

Test Vehicle:

- 1971 Peterbilt tractor
    - Wheel base from center of front axle to center of rear tandem axle was 236 in (599 cm)
- 1968 Fruehauf tank-trailer
    - Distance from center of tandem axle assembly on tractor to center of tandem axle on trailer was 29.3 ft (8.94 m)
    - The tank-trailer was filled with water to ballast the vehicle's test inertia weight 79,900 lb (36,242 kg).

Impact Conditions:

Mass = 79,900 lb
Velocity = 54.8 mph
Angle = 16.0 degrees

Vehicle Instrumentation:

- The vehicle was instrumented with four accelerometer groups:
    - one triaxial accelerometer block mounted on the rear tandem of the tractor;
    - one biaxial accelerometer block mounted toward the front of the tractor in front of the fuel tanks; and
    - two biaxial accelerometer blocks placed on the trailer.

- Three rate transducers were mounted near the vehicle center of gravity to measure yaw, pitch, and roll rates of the tractor.
- An Alderson Hybrid II anthropomorphic dummy was placed in the driver position and instrumented.

The right impact side fuel tank was instrumented with a pressure transducer to measure the internal pressure of the tank during the test.

The test vehicle was a **1971 Peterbilt tractor** with a **1968 Fruehauf tank-trailer**. The tank-trailer was filled with water to ballast the vehicle's test inertia weight 79,900 lb (36,242 kg). The impact speed and angle was 54.8 mph (88.2 km/hr) and 16.0 degrees. During impact the entire front of the tractor came loose from the frame and began to shift to the left. The vehicle was contained and redirected.

Damage to the vehicle was extensive. The front axle of the tractor and both fuel tanks on the right side were torn away. The frame was damaged and the entire right side of the tractor was dented and scraped. There was some occupant compartment intrusion.

The instrumented wall received some marring and spalling but otherwise the damage was only cosmetic.

The results from the instrumented wall showed three distinct peak loads in the 0.050 second average force-time history. The first peak load was approximately 91,000 lb and corresponded to initial impact of the tractor; the second peak load was approximately 212,000 lb and was associated with the rear tandem axles of the tractor and the front of the trailer; the third peak load was approximately 408,000 lb and was associated with the final impact of the trailer with the wall.

1.5. Mak, King K., W.L. Campise, "Test and Evaluation of Ontario 'Tall Wall' Barrier with an 80,000-Pound Tractor-Trailer," Project No. 4221-9089-534, Ontario Ministry of Transportation, Ontario (prepared by Texas Transportation Institute, College Station, Texas), September 1990.

TTI Test No. 7162-1

Test Article:

- Ontario "Tall Wall" (unreinforced New Jersey Turnpike Authority "Tall Wall")
- 328 ft (100 m) long
- Barrier height = 41.3 in (1050 mm)
- Base width = 31.5 in (800 mm)
- Top width = 11.4 in (290 mm)

Test Vehicle:

- 1980 International tractor Model No. F2574
  - Wheel base from center of front axle to center of rear tandem axle was 171 in (434 cm)
- 1973 Trailmobile Model A11A-1SAV
  - Distance from center of tandem axle assembly on tractor to center of tandem axle on trailer was 35.8 ft (10.9 m)
  - Trailer was ballasted with sandbags and secured with plywood boards and steel cables

Impact Conditions:

Mass = 80,000 lb
Velocity = 49.6 mph (79.8 km/hr)
Angle = 15.1 degrees

Vehicle Instrumentation:

- The vehicle was instrumented with three rate transducers to measure roll, pitch, and yaw
- A triaxial accelerometer block mounted on the tractor near the fifth wheel
- A biaxial accelerometer block mounted toward the front of the tractor inside the cab
- A biaxial accelerometer block placed near the front of the trailer
- A biaxial accelerometer block placed at the rear tandem axles of the trailer

The test vehicle was a **1980 International tractor** with a **1973 Trailmobile van-trailer**. The test inertia weight was 80,000 lb (36,287 kg). The impact speed and angle was 49.6 mph (79.8 km/hr) and 15.1 degrees. The trailer rolled over the barrier during impact. The tractor remained attached to the trailer and came to rest with the tractor straddling the barrier 215 ft (65.5 m) downstream of impact. It was noted in the report that the rolling of the rear of the trailer box over the barrier was a direct result of the failure of the tandem axle assembly (which was poorly constructed). This same barrier with steel reinforcement passed an earlier test with the 80,000 lb truck (see Campise and Buth, 1985).

Damage to the vehicle was extensive. The front-left corner of the bumper was deformed and the left side of the tractor was damaged. The left front wheel was deformed and displaced rearward due to fractured U-bolts mounting the suspension to the axle. The tractor frame was bent and twisted. The front axle and steering arm were damaged and the fuel tank was bent. The left front and rear outer rims were bent.

The trailer received damage all along the lower left side and the left side under-frame. The right-side under-frame was damaged as the trailer rode over the barrier. The third seam in the left wall of the trailer separated and the wall came apart from the floor structure and the roof. The right wall was twisted and deformed due to induced damage. The trailer tandem axle assembly came loose from the frame and the left side of the frame was bent outward at the rear.

The barrier received minor damage and there was no lateral movement during impact.

1.6. Buth, C.E., T.J. Hirsch, and W.L. Menges, "Testing of New Bridge Rail and Transition Designs," Report No. FHWA-RD-93-068, Vol. XI Appendix J: 42-in (1.07-m) F-Shape Bridge Railing, Turner-Fairbank Highway Research Center, Federal Highway Administration, McLean, Virginia, (prepared by Texas Transportation Institute, College Station, Texas), 1993.

TTI Test No. 7069-10

Test Article:

- F-Shaped bridge railing
- 328 ft (100 m) long
- Barrier height = 42 in (1067 mm)
- Base width = 17.25 in (438 mm)
- Top width = 9 in (229 mm)

Test Vehicle:

- 1979 International TranStar 4200 tractor
  - Wheel base from center of front axle to center of rear tandem axle was 182 in (462 cm)
- 45 ft van trailer
  - Distance from center of tandem axle assembly on tractor to center of tandem axle on trailer was 36.2 ft (11 m)
  - Trailer was ballasted with sandbags and secured with plywood boards and steel cables

Impact Conditions:

Mass = 50,000 lb
Velocity = 52.2 mph (84 km/hr)
Angle = 14 degrees

Vehicle Instrumentation:

- A triaxial accelerometer mounted near the center of gravity
- A biaxial accelerometer mounted over the tandem axle
- A biaxial accelerometer mounted near the front of the trailer
- A biaxial accelerometer mounted near the rear of the trailer
- Three rate transducers mounted near the center of gravity of tractor to measure roll, pitch, and yaw
- Three rate transducers mounted near the center of gravity of trailer to measure roll, pitch, and yaw
- High speed cameras
  - Overhead
  - Downstream viewpoint parallel and aligned with the barrier

A 42 inch (1.07 m) tall F-shaped bridge railing was tested at the Texas Transportation Institute to performance Level 3 in *Guide Specifications for Bridge Railings* (i.e., 50,000 lb (22,799 kg) test vehicle impacting the length-of-need at a nominal speed and angle of 50 mph (80.5 km/hr) and 15 degrees). The vehicle was smoothly redirected and remained upright and stable.

The test article was a 42 inch (1.07 m) F-shaped concrete bridge rail, 17.3 inches (439 mm) thick at the base and tapers along its height to a thickness of 9 inches (230 mm) at the top.

The test vehicle was a **1979 International TranStar 4200 tractor** with a **45 ft van-trailer**. The empty weight of the tractor/trailer was 29,900 lb (13,574 kg) and its test inertia weight was 50,000 lb (22,700 kg). The impact point was 35 ft (10.1 m) from the upstream end of the bridge railing. The impact speed and angle was 52.2 mph (84.0 km/hr) and 14.0 degrees. The vehicle was contained and redirected. The brakes were applied when the vehicle reached the end of the parapet and came to rest approximately 300 ft (91 m) downstream from the impact point.

There was no lateral movement of the bridge rail during the test and no structural damage. The vehicle sustained significant damage on the impact side. Maximum crush at the front corner at bumper height was 18.0 inches (457 mm). Damage parts included front wheel assembly and suspension, rear outside wheel rims were bent and tires deflated, shock mounts were broken, tie rods were bent, steering rod was bent, springs were loose and impact side door was dented.

1.7. Buth, C.E., T.J. Hirsch, and W.L. Menges, "Testing of New Bridge Rail and Transition Designs," Report No. FHWA-RD-93-067, Vol. X Appendix I: 42-in (1.07-m) Concrete Parapet Bridge Railing, Turner-Fairbank Highway Research Center, Federal Highway Administration, McLean, Virginia, (prepared by Texas Transportation Institute, College Station, Texas), 1993.

TTI Test No. 7069-13

Test Article:

- Vertical concrete wall bridge railing
- 98.4 ft (30 m) long
- Barrier height = 42 in (1070 mm)

Test Vehicle:

- 1979 International TranStar 4200 tractor
    - Wheel base from center of front axle to center of rear tandem axle was 182 in (462.3 cm)
- 1977 Pullman Van Trailer
    - Distance from center of tandem axle assembly on tractor to center of tandem axle on trailer was 36.2 ft (11.02 m)
    - Trailer was ballasted with sandbags and secured with plywood boards and steel cables

Impact Conditions:

Mass = 50,050 lb
Velocity = 51.4 mph (82.7 km/hr)
Angle = 16.2 degrees

Vehicle Instrumentation:

- Triaxial accelerometer mounted near center of gravity
- A biaxial accelerometer mounted over the rear tandem on tractor
- A biaxial accelerometer mounted near the front of the trailer
- A biaxial accelerometer mounted toward the rear of the trailer
- Angular rate transducers were mounted on the tractor to measure roll, pitch, and yaw rates
- Three high-speed cameras
    - Overhead
    - Downstream viewpoint parallel and aligned with the barrier
    - Perpendicular to the parapet

A 98.4 ft (30 m) length of the 42 inch (1.07 m) vertical wall bridge railing was tested at the Texas Transportation Institute under impact conditions corresponding to *Guide Specifications for Bridge Railings* performance Level 3 (i.e., 50,000 lb (22,799 kg) test vehicle impacting the length-of-need at a nominal speed and angle of 50 mph (80.5 km/hr) and 15 degrees). The test resulted in the tractor/trailer steering around the end of the bridge rail system and rolling over on its side.

The test article was a 42 inch (1.07 m) concrete parapet, 10 in. (254 mm) thick with a thickened section 12 inches (305 mm) thick at the top.

The test vehicle was a **1979 International TranStar 4200 tractor** with a **1977 Pullman van-trailer**. The empty weight of the tractor/trailer was 27,690 lb (12,571 kg) and its test inertia weight was 50,050 lb (22,723 kg). The impact point was 24 ft (7.3 m) from the upstream end of the bridge railing. The impact speed and angle was 51.4 mph (82.7 km/hr) and 16.2 degrees. The vehicle was contained and redirected. The brakes were applied when the vehicle reached the end of the parapet and came to rest on its left side approximately 181 ft (55 m) downstream from the impact point.

There was no lateral movement of the parapet during the test and no structural damage. The vehicle sustained significant damage on the impact side. Maximum crush at the front corner at bumper height was 18.0 in (457 mm). Damage parts included front axle, Pittman arm, U-bolts, front leaf springs and bolts, front shock mounts, air brake lines, right fuel cell, left rear spring pin and clamp, and exhaust pipe. The cab and left door were bent.

1.8. Alberson, D.C., R.A. Zimmer, and W.L. Menges, "NCHRP Report 350 Compliance Test 5-12 of the 1.07-m Vertical Wall Bridge Railing," Report No. FHWA-RD-96-199, Office of Safety and Traffic Operations R&D, Federal Highway Administration, McLean, Virginia, May 1996.

TTI Test No. 405511-2

Test Article:

- Vertical wall bridge railing
- 131 ft (40 m) long
- Barrier height = 42 in (1067 mm)

Test Vehicle:

- 1983 Freightliner tractor
  - Wheel base from center of front axle to center of rear tandem axle was 185.5 in (471 cm)
- 1984 Great Dane van trailer
  - Distance from center of tandem axle assembly on tractor to center of tandem axle on trailer was 34.4 ft (10.5 m)
  - Trailer was ballasted with sandbags and secured with plywood boards and steel cables

Impact Conditions:

Mass = 79,366 lb
Velocity = 49.8 mph (80.1 km/hr)
Angle = 14.5 degrees

Vehicle Instrumentation:

- A triaxial accelerometer mounted near the center of gravity of tractor
- A triaxial accelerometer mounted near the fifth-wheel
- A triaxial accelerometer mounted near the center of gravity of the trailer
- Three rate transducers mounted near the center of gravity of tractor to measure roll, pitch, and yaw
- Two string potentiometers to measure longitudinal and vertical acceleration levels of the right front wheel
- Eleven uniaxial accelerometers mounted in the following locations:
  - Center top surface of the instrument panel
  - Inside end of the tractor's right front wheel spindle
  - Top of engine block
  - Inside end of the tractor's right wheel spindle
  - Inside end of the tractor's left wheel spindle
  - On the frame of the rear bogie of the trailer
  - On the rear axle of the trailer

- High speed cameras
    - Overhead field of view
    - Behind installation at an angle
    - Downstream viewpoint parallel and aligned with the barrier

In an earlier study (see Buth, et al. 1993), a 30 m length of the 1.07 m vertical wall bridge railing was tested under NCHRP Report 350 test Level 5 (i.e., 36,000V test vehicle impacting the length-of-need at a nominal speed and angle of 80 km/hr and 15 degrees) and resulted in the tractor/trailer steering around the end of the bridge rail system and rolling over on its side. This report contains the results of a 'repeat' test on the bridge rail extended to a 40 m length. The test was conducted at the Texas Transportation Institute under NCHRP Report 350 test Level 5 conditions to determine if the bridge railing would safely contain and redirect the vehicle without rolling the vehicle and also to assess the strength of the connection of the bridge railing to the bridge deck.

The test article was a 42 inch (1.07 m) concrete parapet, 10 inches (254 mm) thick with a thickened section 12 inches (305 mm) thick at the top.

The test vehicle was a **1983 Freightliner tractor** with a **1984 Great Dane van trailer**. The empty weight of the tractor/trailer was 30,628 lb (13,893 kg) and its test inertia weight was 79,366 lb (36,000 kg). The impact point was 17.4 ft (5.3 m) from the upstream end of the bridge railing. The impact speed and angle was 49.8 mph (80.1 km/hr) and 14.5 degrees. The vehicle remained upright and met all safety criteria of NCHRP Report 350.

There was no structural damage to the vertical wall. Most of the damage to the vehicle was to the impact side and included the right front springs, U-bolts, mounts, shocks, and steering linkages, the right rear springs and mounts, the front axle, the right side fuel tank and mounts, the right side tires and rims, the bumper, fan, radiator, hood, and cab. Damage to the trailer included the fifth-wheel frame, the dolly mounts, the rear axles, and the right side tires and rims. The right front corner was also torn open.

1.9. Marzougui, FOIL Test 03008, National Crash Analysis Center, Ashburn, VA, 2003

Test No. FOIL 03008

Test Article:

- F-shaped concrete safety shape
- Temporary barrier staked down and backfilled to minimize movement
- Barrier length = unknown
- Barrier height = 34 in (860 mm)

Test Vehicle:

- 1992 FLD120 Freightliner tractor
    - Wheel base from center of front axle to center of rear tandem axle was 214.5 in (545 cm)
    - Vin No. 1FUYDSYBINH480737
- Trailer was NOT used in the test

Impact Conditions:

Mass = 14,683 lb (6,660 kg)
Velocity = 31.25 mph (50.3 km/hr)
Angle = 25 degrees

Vehicle Instrumentation:

- Three rate transducers mounted near the center of gravity of tractor to measure roll, pitch, and yaw (plus three redundant rate transducers)
- Twenty-one uniaxial accelerometers were mounted in the following locations:
    - Center of gravity (x, y, and z-direction)
    - Center of gravity (redundant accelerometers in x, y, and z-direction)
    - Front rail, passenger side (z-direction)
    - Front axle, passenger side (z-direction)
    - Rear rail, passenger side (z-direction)
    - Front tandem axle, passenger side (z-direction)
    - Rear tandem axle, passenger side (z-direction)
    - Top of engine block (x, y, and z-direction)
    - Front rail, driver side (z-direction)
    - Front axle, driver side (z-direction)
    - Rear rail, driver side (z-direction)
    - Front tandem axle, driver side (z-direction)
    - Rear tandem axle, driver side (z-direction)
    - Cross member (x and y direction)
- High speed cameras
    - Overhead field of view
    - Downstream viewpoint parallel and aligned with the barrier
    - Upstream viewpoint parallel and aligned with the barrier
    - Viewpoint perpendicular to barrier on front side
    - Front onboard
    - Rear onboard

This test was conducted by NCAC at the Federal Outdoor Impact Facility in McLean, VA for the purpose of collecting crash performance/response data to use for validation of the NCAC tractor finite element model. The test involved a **1992 Freightliner FLD120 tractor** impacting into an F-shaped concrete safety barrier at an impact speed of 31.25 mph (50.3 km/hr) at an angle of 25 degrees. A crash report was not written but accelerometer data was collected at several locations throughout the tractor, rate gyros were mounted near the center of gravity, and high-speed video was captured from several view points.

1.10. Polivka, K.A., Faller, R.K., Holloway, J.C., Rohde, J.R., and Sicking, D.L., "Development, Testing, and Evaluation of NDOR's TL-5 Aesthetic Open Concrete Bridge Rail," Report No. TRP-03-148-05, Midwest Roadside Safety Facility, Lincoln, Nebraska, 2005

TTI Test No. ACBR-1

Test Article:

- TL-5 aesthetic open concrete bridge rail
- 121.4 ft (37 m) long
- Barrier height = 42 in (1067 mm)

Test Vehicle:

- 1989 GMC Brigadier T/S tractor
  - Wheel base from center of front axle to center of rear tandem axle was 170.6 in (433.4 cm)
- 1989 Great Dane van trailer
  - Distance from center of tandem axle assembly on tractor to center of tandem axle on trailer was 31.5 ft (9.6 m)
  - Trailer was ballasted with steel panels, concrete barriers, and foam

Impact Conditions:

Mass = 78,975 lb
Velocity = 49.4 mph (79.6 km/hr)
Angle = 16.3 degrees

Vehicle Instrumentation:

- A triaxial accelerometer mounted over the rear tandem axle of the tractor just below the frame-rail
- A triaxial accelerometer mounted near the center of gravity of the trailer, below the trailer floor
- A rate transducer mounted near the center of gravity of the vehicle to measure roll, pitch, and yaw rates
- High-speed cameras
  - Overhead field of view
  - Downstream viewpoint parallel and aligned with the barrier
  - Upstream viewpoint parallel and aligned with the barrier
  - Viewpoint perpendicular to barrier on front side

A 42 inch (1.07 m) tall aesthetic open concrete barrier was tested at Midwest Roadside Safety Facility to performance Level 5 in *National Cooperative Highway Research Program (NCHRP) Report 350, Recommended Procedures for the Safety Performance Evaluation of Highway Features* (i.e., 80,000 lb (36,000 kg) test vehicle impacting the length-of-need at a nominal speed

and angle of 50 mph (80 km/hr) and 15 degrees). The safety performance of the bridge rail was determined to be acceptable according to the TL-5 evaluation criteria specified in NCHRP Report 350.

The test article was 42 inches (1.07 m) tall and the installation length was 121.4 ft (37 m). The test vehicle was a **1989 GMC Brigadier T/S tractor** with a **1989 Great Dane van-trailer**. The empty weight of the tractor/trailer was 30,525 lb (13,846 kg) and its test inertia weight was 78,975 lb (35,822 kg). The impact point was 21.25 ft (6.48 m) from the upstream end of the bridge railing midway between posts 3 and 4. The impact speed and angle was 49.4 mph (79.6 km/hr) and 16.3 degrees. The vehicle was contained and redirected. At two seconds after initial impact, the vehicle exited the system at approximately 5 degrees. The vehicle came to rest 410.9 ft (125.25 m) downstream from the impact point and 173.25 ft (52.82 m) laterally behind a line projected parallel to the traffic side of the barrier.

Damage to the barrier was moderate and consisted of contact gouge marks, cracking of concrete bridge deck, concrete post cracks, concrete rail cracks, and spalling of the concrete. Some of the cracks on the concrete rail were reported as "major cracking." The maximum dynamic lateral deflection of the barrier was 11.22 inches (285 mm).

The vehicle sustained moderate damage on the impact side. The left (non-impact side) side of the floorboard opened up and the frame channel section was protruding into the occupant compartment. The hood was fractured and disengaged from the tractor. The front bumper was disengaged from the impact side frame rail. The fiberglass fuel tank cover was fractured at its midpoint. The fuel tank was crushed approximately 12 in and the lower corner was torn open. The left and right side fenders disengaged. The frame rail on the impact side sustained major deformations near the bumper attachment. The lower left side shock attachment and two of the three left side leaf springs disengaged. The bottom shock mount and the right-side axle disengaged. The inner left-side tie rod connection fractured at the ball joint. The outer left rear tandem tire was cut and the wheel rim was bent. Both right-side tandem tires and wheel rims were heavily damaged. The right-side front wheel assembly was pushed into the engine compartment. The right-front wheel rim was bent.

The trailer sustained scrape marks along the entire lower portion on the impact side. The support frame was also deformed. The trailer's rear tandem wheels on the impact side encountered significant damage.

Table 1. Summary of Vehicle Make and Model and Test Article Description for Tractor-Trailer Vehicle Crash Tests.

Test No.	Test Date	Test Agency	Vehicle			Barrier Description	Barrier Height (in.)
			Tractor Make	Tractor Type	Trailer Type		
6	1981	TTI	1978 Auto Car	Conventional	Van	Texas C202 Concrete Parapet w/ Texas C4 Steel Rail	54
2416-1	9/18/1984	TTI	1981 Kenworth	Conventional	Van	Texas T5 Concrete Bridge Railing (NJ Shape) w/ Texas C4 Steel Rail	50
4798-13	5/26/1983	TTI	1974 International	Cab-Over	Van	New Jersey Concrete Safety Shape	42
7046-3	4/7/1987	TTI	1973 White Freightliner	Cab-Over	Van	Vertical Instrumented Tall Wall	90
7046-4	5/8/1987	TTI	1971 Peterbilt	Conventional	Tanker	Vertical Instrumented Tall Wall	90
7046-9	5/27/1988	TTI	1979 International	Conventional	Van	Vertical Instrumented Tall Wall	90
7162-1	8/9/1990	TTI	1980 International	Conventional	Van	Ontario Un-Reinforced Concrete Median Barrier	42
7069-10	3/3/1988	TTI	1979 International TranStar 4200	Conventional	Van	F-Shape Concrete Bridge Railing	42
7069-13	7/11/1988	TTI	1979 International TranStar 4200	Conventional	Van	Vertical Concrete Bridge Railing	42
405511-2	12/12/1995	TTI	1983 Freightliner	Conventional	Van	Vertical Concrete Bridge Railing	42
03008	8/28/2003	FOIL	1992 Freightliner FLD120	Conventional	NA	F-Shape Concrete Safety Shape	32
ACBR-1	8/28/2003	MwRSF	1989 General Motors Brigadier	Conventional	Van	Aesthetic Open Concrete Bridge Rail	42

TTI – Texas Transportation Institute

FOIL – Federal Outdoor Impact Facility

MwRSF – Midwest Roadside Safety Facility

NA – Not Available

Table 2. Summary of Impact Conditions and Vehicle Parameters for Tractor-Trailer Vehicle Crash Tests.

Test No.	Impact Conditions			Individual Weights			Vehicle Dimensions			
	Impact Speed (mph)	Impact Angle (deg)	Test Inertial Weight (lbs)	Tractor Front Axle (lbs)	Tractor Rear Tandem Axle (lbs)	Trailer Rear Tandem Axle (lbs)	Tractor Wheelbase (in)	Trailer Wheelbase (ft)	Overall Tractor-Trailer Length (ft)	Nominal Trailer Length (ft)
6	49.1	15.0	79,770	11,490	33,760	34,520	162.0	29.25	53.9	40
2416-1	48.4	14.5	80,080	12,020	34,170	33,890	199.5	31.48	57.1	40
4798-13	52.1	16.5	80,180	12,150	34,010	34,020	147.5	30.71	50.2	40
7046-3	55.0	15.3	80,080	11,680	34,140	34,260	164.5	30.23	51.1	40
7046-4	54.8	16.0	79,900	11,840	33,570	34,490	236.0	29.17	55.4	36.5+
7046-9	50.4	14.6	50,000	8,540	19,790	21,670	169.0	35.88	58.6	45
7162-1	49.6	15.1	80,000	11,580	34,350	34,070	171.0	35.80	57.4	45
7069-10	52.2	14.0	50,000	9,400	21,760	18,840	182.0	36.17	59.2	45
7069-13	51.4	16.2	50,050	7,920	22,250	19,880	169.0	36.50	58.2	45
405511-2	49.8	14.5	79,366	11,210	34,249	33,907	186.0	34.42	58.3	NA
03008	31.3	25.0	14,683	3,744	2,916	NA	214.4	NA	NA	NA
ACBR-1	49.4	16.3	78,975	8,475	36,725	33,775	170.6	31.51	53.1	45

NA – Not Available

Table 3. Vehicle Properties for Test No. 6.

Date: 1981	**Test No.:** 6	
Tractor		
Year: 1978	**Make:** Auto Car	**Model:**
VIN NO.:		**Odometer:**
Trailer		
Year: 1978	**Make:** Auto Car	**Model:**
VIN NO.:		
Describe any damage to the vehicle prior to test		

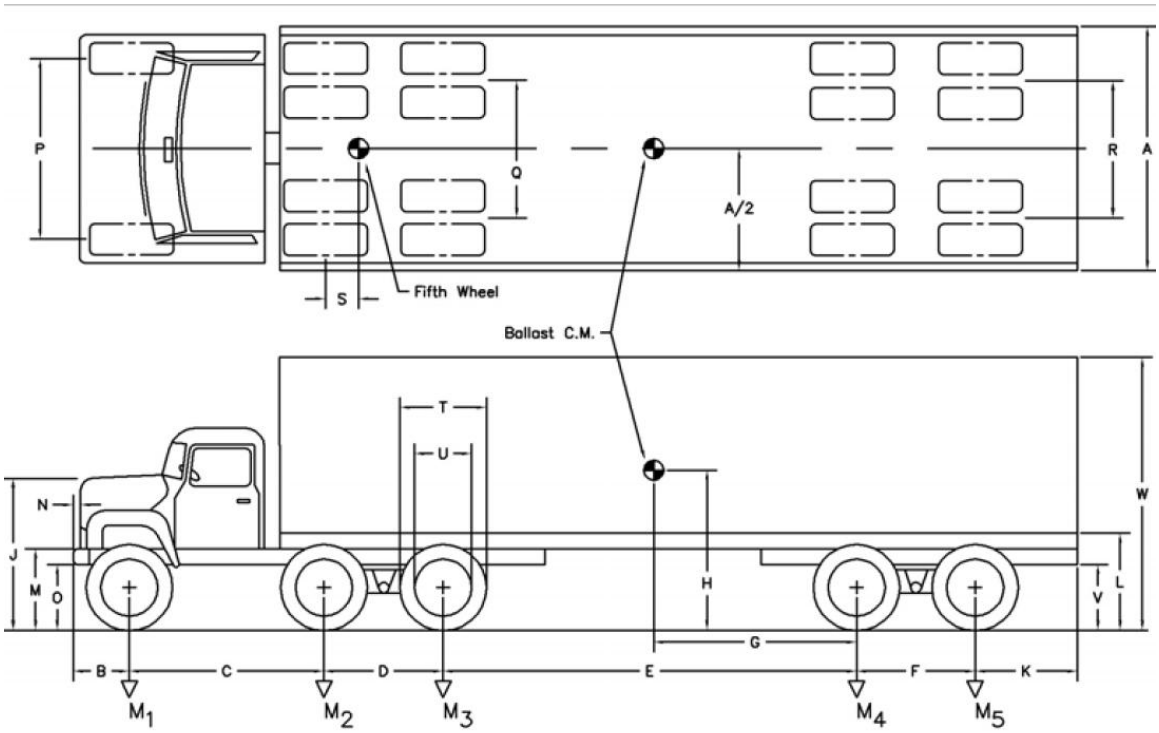

Geometry (in)

A		**G**		**N**		**T**	
B	**53.5**	**H**	70	**O**	28	**U**	
C+D/2	**162**	**J**	80.5	**P**		**V**	
D	**52**	**K+F/2**	80.5	**Q**		**W**	158
E+D/2+F/2	**351**	**(L+V)/2**	44.5	**R**			
F		**M**		**S**	14		

Mass (lb)	Curb	Test Inertial	Gross Static
M_1	10,720	11,490	
$M_2 + M_3$	13,070	33,760	
$M_4 + M_5$	8,880	34,520	
M_T	32,670	79,770	

Table 4. Vehicle Properties for Test No. 2416-1.

Date: 9-18-1984	**Test No.:** 2416-1	
Tractor		
Year: 1981	**Make:** Kenworth	**Model:**
VIN NO.:		**Odometer:**
Trailer – Van		
Year:	**Make:** Freuhauf	**Model:**
VIN NO.:		
Describe any damage to the vehicle prior to test		

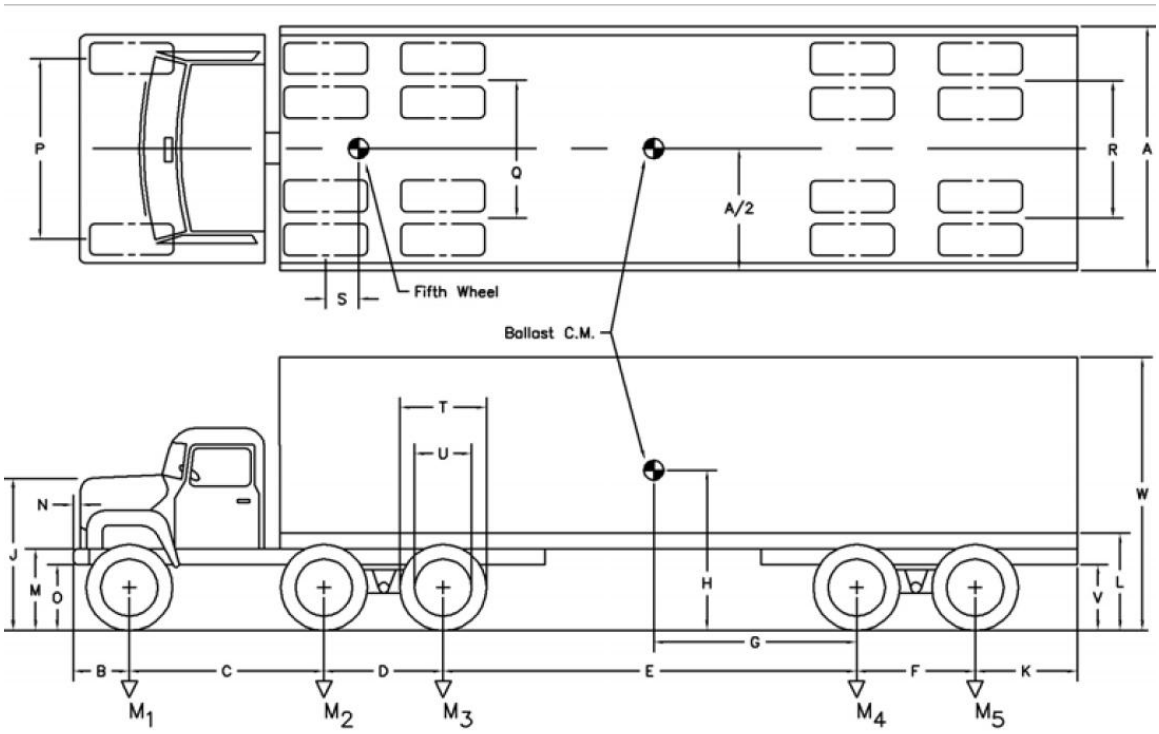

Geometry (in)

A		**G**		**N**		**T**	
B	51	**H**		**O**	28	**U**	
C+D/2	199.5	**J**	82.75	**P**		**V**	
D	53	**K+F/2**	56.4	**Q**		**W**	156
E+D/2+F/2	324.75	**(L+V)/2**	54	**R**			
F		**M**		**S**			

Mass (lb)	Curb	Test Inertial	Gross Static
M_1		12,020	
$M_2 + M_3$		34,170	
$M_4 + M_5$		33,890	
M_T	32,080	80,080	

Table 5. Vehicle Properties for Test No. 4798-13.

Date: 5-26-1983	**Test No.:** 4798-13	
Tractor – Cabover		
Year: 1974	**Make:** International	**Model:**
VIN NO.:		**Odometer:**
Trailer - Van		
Year:	**Make:** Freuhauf	**Model:**
VIN NO.:		
Describe any damage to the vehicle prior to test		

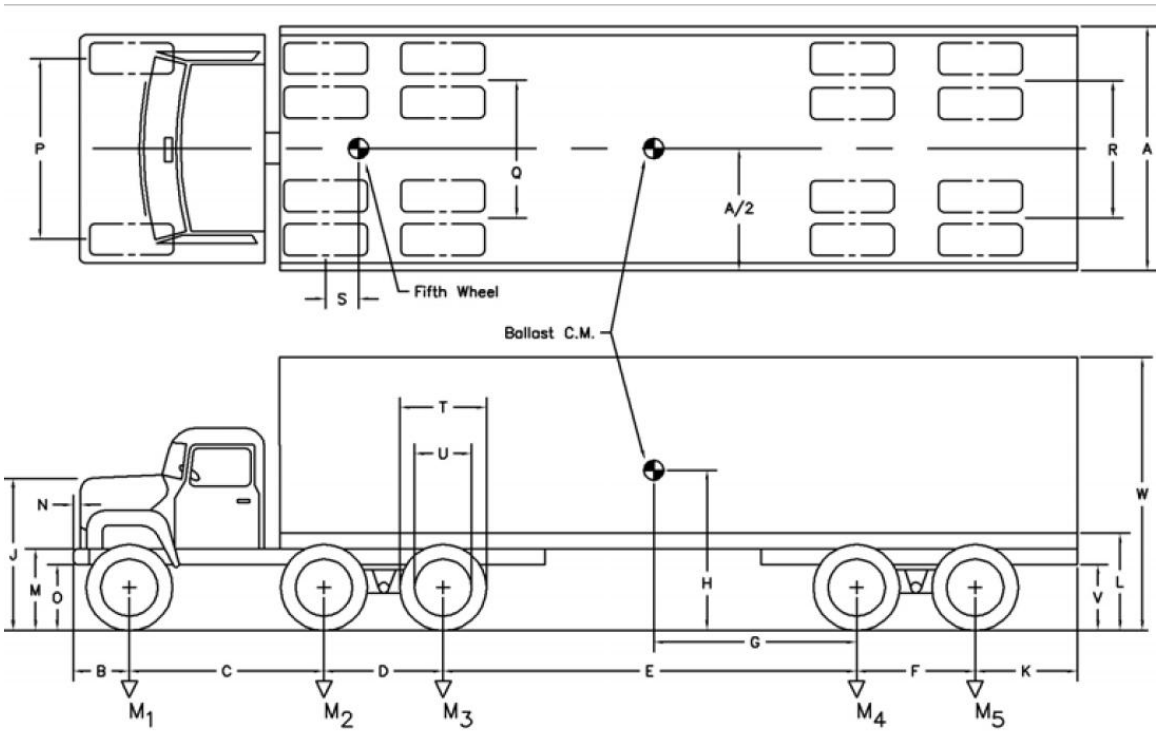

Geometry (in)

A		**G**		**N**		**T**	
B	31	**H**	67	**O**		**U**	
C + D/2	147.5	**J**	N.A.	**P**		**V**	
D		**K+F/2**	55.5	**Q**		**W**	144
E+D/2+F/2	368.5	**L**	55	**R**			
F		**M**		**S**			

Mass (lb)	Curb	Test Inertial	Gross Static
M_1		12,150	
$M_2 + M_3$		34,010	
$M_4 + M_5$		34,020	
M_T	29,600	80,180	

Table 6. Vehicle Properties for Test No. 7046-3.

Date: 4-07-1987	**Test No.:** 7046-3	
Tractor – Cabover		
Year: 1973	**Make:** White Freightliner	**Model:** WFT 8664T
VIN NO.: CA213H077608		**Odometer:**
Trailer - Van		
Year: 1966	**Make:** Freuhauf	**Model:**
Serial No. FWG647909		
Describe any damage to the vehicle prior to test		

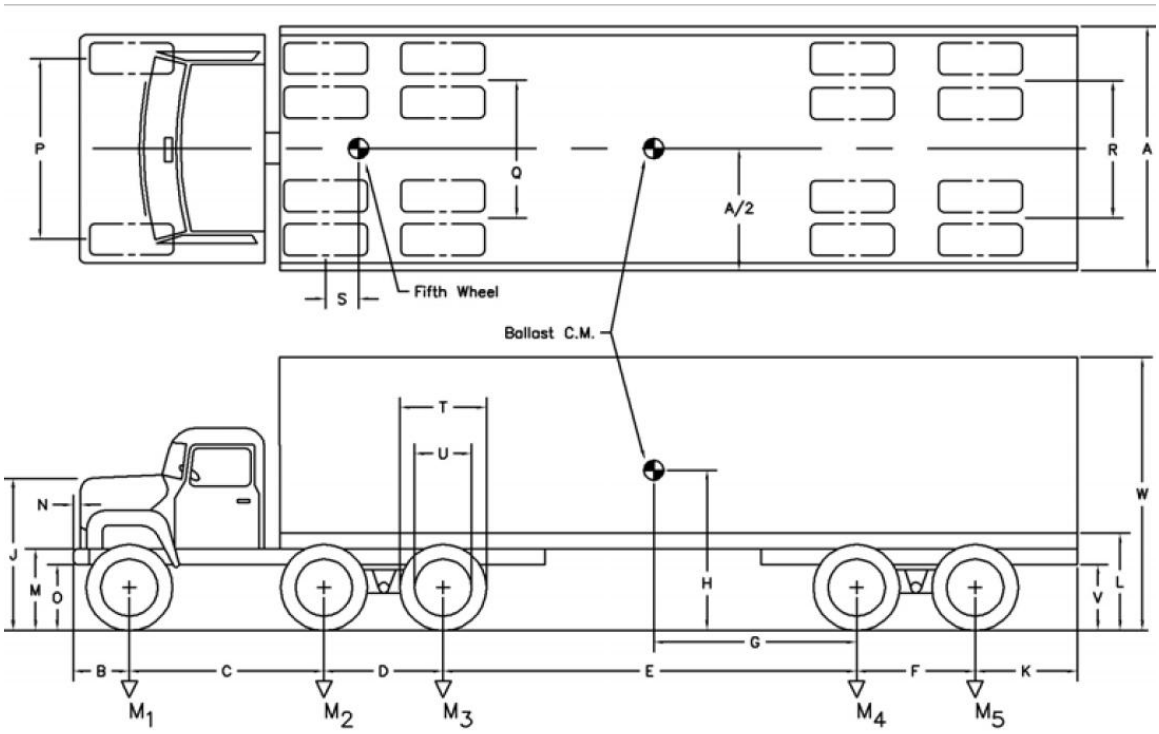

Geometry (in)

A		**G**		**N**		**T**	
B	29.25	**H**		**O**		**U**	
C + D/2	164.5	**J**	N.A.	**P**		**V**	
D		**K+F/2**	56.25	**Q**		**W**	147
E+D/2+F/2	367	**(L+V)/2**	43	**R**			
F		**M**		**S**			

Mass (lb)	Curb	Test Inertial	Gross Static
M_1		11,680	
M_2		17,380	
M_3		16,760	
M_4		16,540	
M_5		17,720	
M_T		80,080	

Table 7. Vehicle Properties for Test No. 7046-4.

Date: 5-08-1987	**Test No.:** 7046-4	
Tractor – Cabover		
Year: 1971	**Make:** Peterbilt	**Model:**
VIN NO.:		**Odometer:**
Trailer - Tank		
Year: 1968	**Make:** Freuhauf	**Model:**
Serial No.		
Describe any damage to the vehicle prior to test		

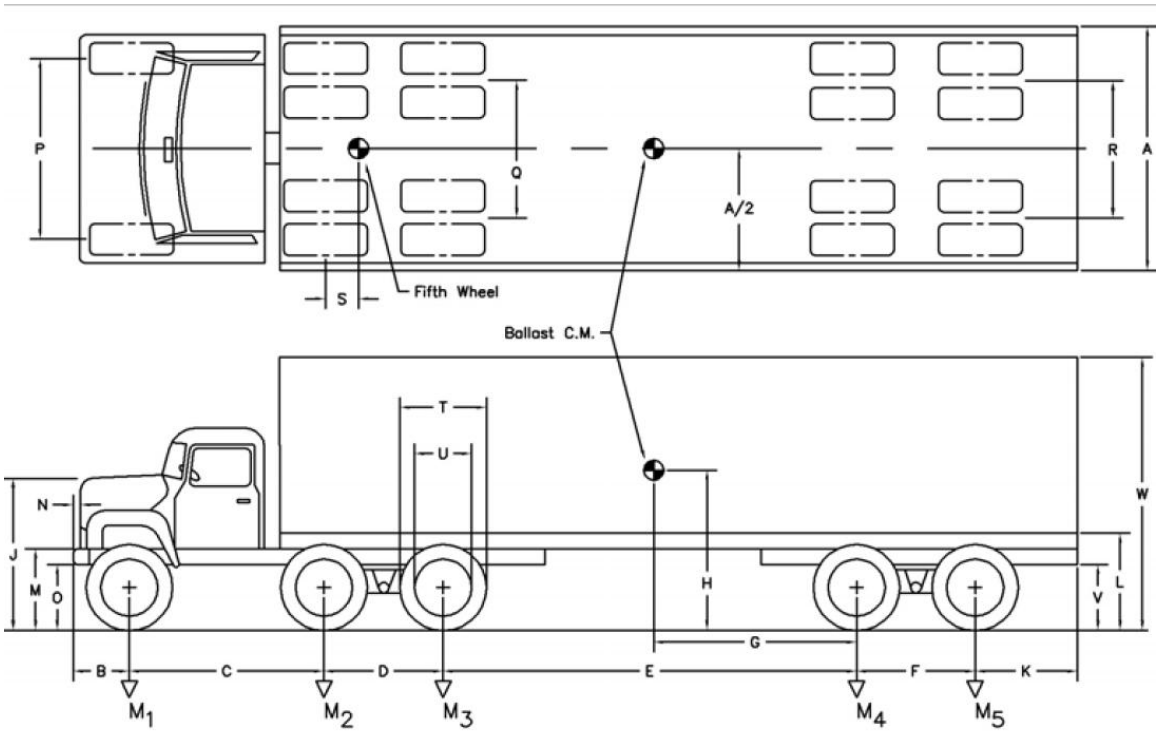

Geometry (in)

A		**G**		**N**		**T**	
B	29	**H**		**O**	18.5	**U**	
C + D/2	236	**J**		**P**		**V**	
D		**K**	25.5	**Q**		**W**	113
E	301	**L**		**R**			
F	49	**M**	30.5	**S**			

Mass (lb)	Curb	Test Inertial	Gross Static
M_1	8,410	11,840	
M_2	5,580	16,960	
M_3	5,520	16,610	
M_4	4,460	16,810	
M_5	2,840	17,680	
M_T	26,810	79,900	

Table 8. Vehicle Properties for Test No. 7162-1.

Date: 8-09-1990	**Test No.:** 7162-1	
Tractor		
Year: 1980	**Make:** International	**Model:**
VIN NO.:		**Odometer:**
Trailer - Van		
Year: 1973	**Make:** Trailmobile	**Model:**
Serial No.		
Describe any damage to the vehicle prior to test		

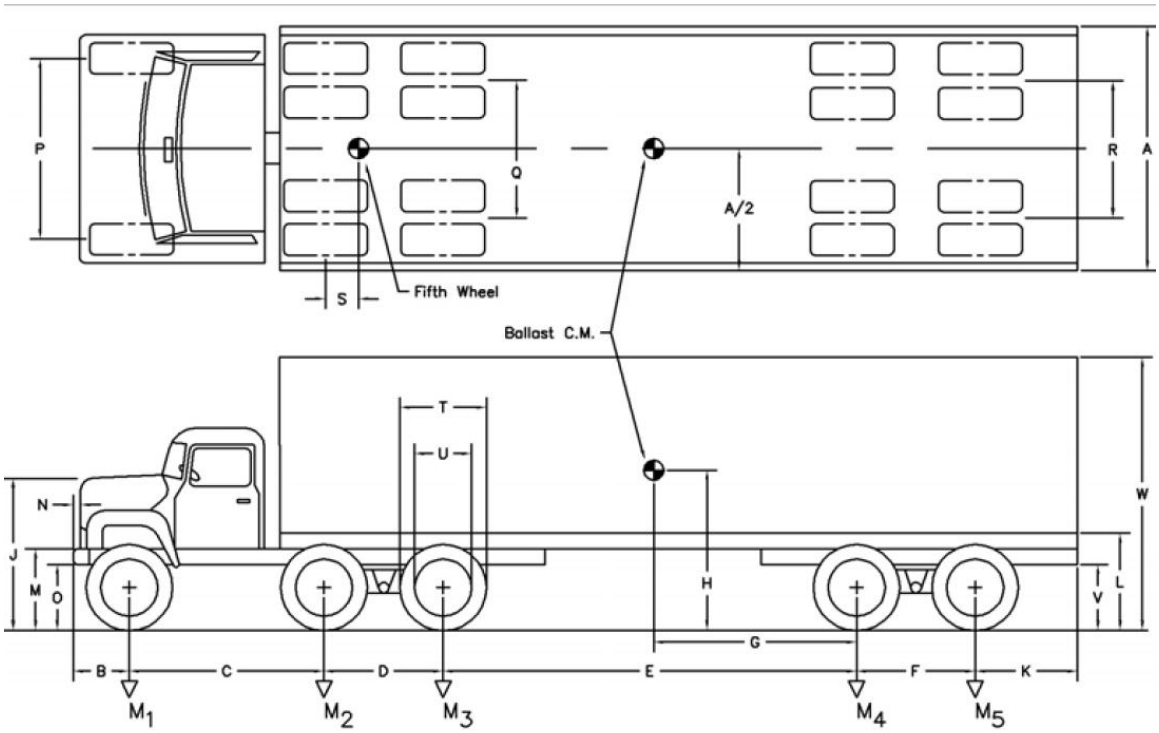

Geometry (in)

A		**G**		**N**		**T**	
B	34.5	**H**		**O**	26.8	**U**	
C + D/2	171	**J**		**P**		**V**	
D	54	**K+F/2**	54	**Q**		**W**	154.3
E+D/2+F/2	429.6	**L**	52	**R**			
F		**M**	38.8	**S**	8.5		

Mass (lb)	Curb	Test Inertial	Gross Static
M_1	8,840	11,580	
M_2+ M_3	12,470	34,350	
M_4+ M_5	8,400	34,070	
M_T	29,710	80,000	

Table 9. Vehicle Properties for Test No. 7069-10.

Date: 3-3-1988	**Test No.:** 7069-10	
Tractor		
Year: 1979	**Make:** International	**Model:** TranStar 4200
VIN NO.:		**Odometer:**
Trailer - Van		
Year:	**Make:**	**Model:**
Serial No.		
Describe any damage to the vehicle prior to test		

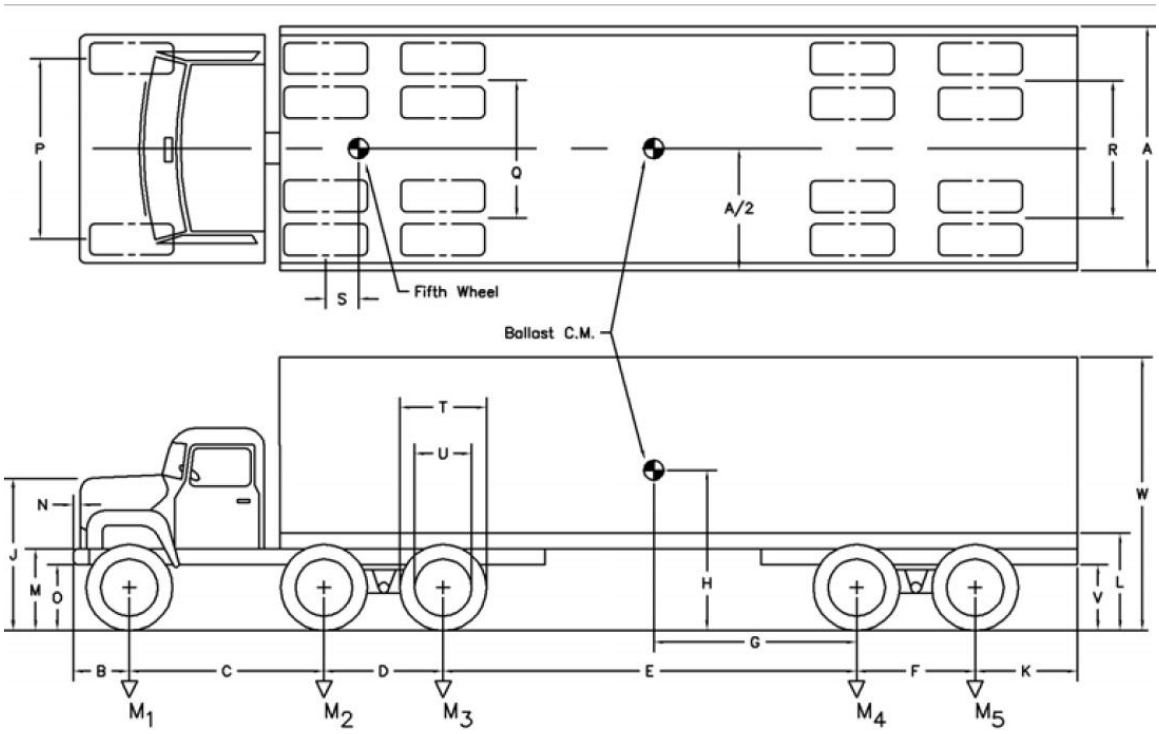

Geometry (in)

A		**G**		**N**		**T**	
B	31	**H**		**O**	20.5	**U**	
C + D/2	182	**J**		**P**		**V**	
D		**K+F/2**	61	**Q**		**W**	156
E+D/2+F/2	434	**(L+V)/2**	53.5	**R**			
F		**M**	30.5	**S**	11		

Mass (lb)	Curb	Test Inertial	Gross Static
M_1		9,400	
M_2+ M_3		21,760	
M_4+ M_5		18,840	
M_T	29,900	50,000	

Table 10. Vehicle Properties for Test No. 7069-13.

Date: 7-11-1988	**Test No.:** 7069-13	
Tractor		
Year: 1979	**Make:** International	**Model:** TranStar 4200
VIN NO.:		**Odometer:**
Trailer – Van		
Year: 1977	**Make:** Pullman	**Model:**
Serial No.		
Describe any damage to the vehicle prior to test		

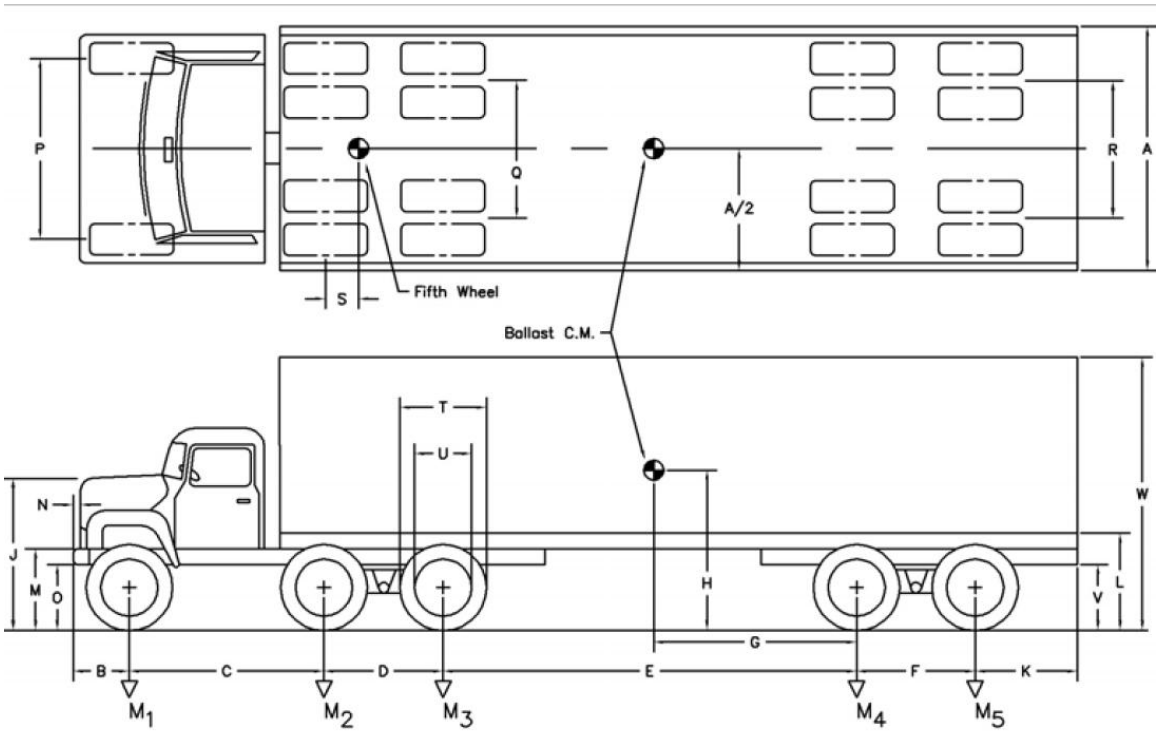

Geometry (in)

A		**G**		**N**		**T**	
B	31	**H**		**O**	20.5	**U**	
C + D/2	169	**J**		**P**		**V**	
D	50.25	**K+F/2**	60	**Q**		**W**	162
E+D/2+F/2	438	**(L+V)/2**	48	**R**			
F		**M**	30.5	**S**			

Mass (lb)	Curb	Test Inertial	Gross Static
M_1	7,380	7,900	
M_2+ M_3	11,890	22,250	
M_4+ M_5	8,420	19,880	
M_T	27,690	50,050	

Table 11. Vehicle Properties for Test No. 405511-2.

Date: 12-12-95	**Test No.:** 405511-2	
Tractor		
Year: 1983	**Make:** Freightliner	**Model:**
VIN NO.: 1FUPYB4DP223978		**Odometer:** 328144
Trailer		
Year: 1984	**Make:** Great Dane	**Model:** 7310TL45
VIN NO.: 1GRFA9024FS068401		
Describe any damage to the vehicle prior to test		

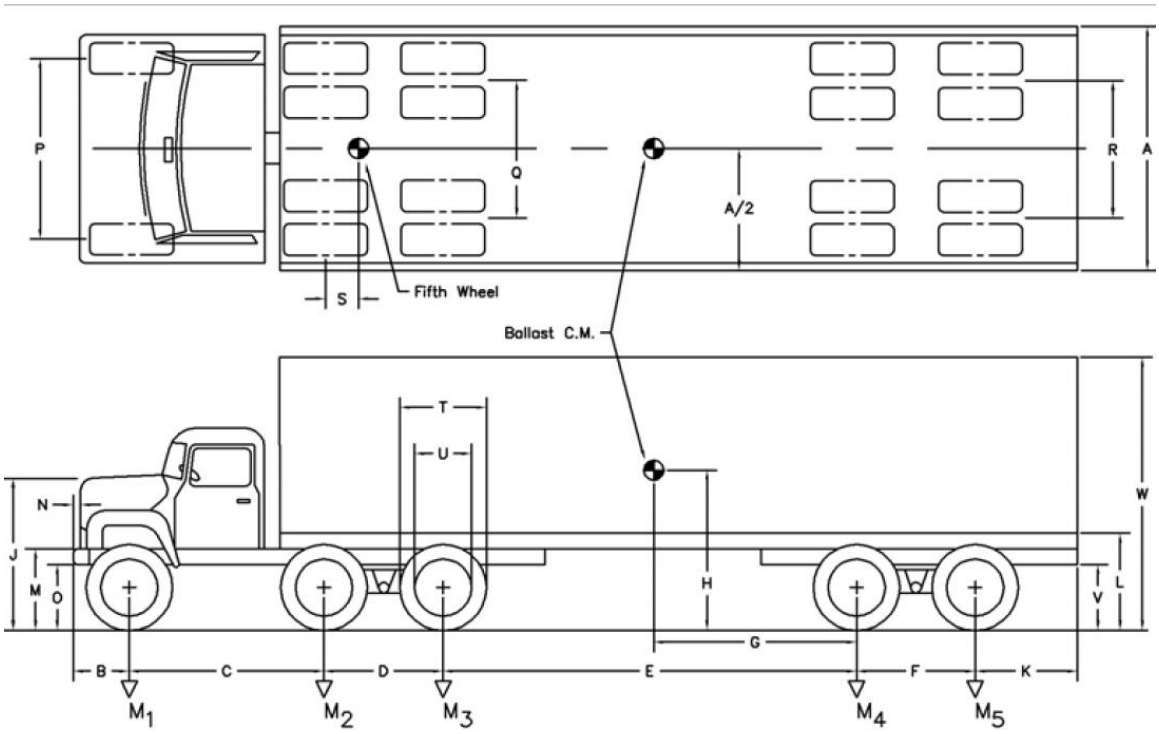

Geometry (in)

A	102	**G**	239	**N**	0	**T**	44
B	26	**H**	72	**O**	16	**U**	25.2
C	159	**J**	75	**P**	79	**V**	37.4
D	53	**K**	50.5	**Q**	75	**W**	157.5
E	362.5	**L**	52	**R**	79		
F	47.6	**M**	31.5	**S**	10.6		

Mass (lb)	Curb	Test Inertial	Gross Static
M_1	8,651	11,211	
M_2	5,809	17,670	
M_3	6,610	16,579	
M_4	3,770	16,206	
M_5	5,789	17,701	
M_T	30,629	79,366	

Table 12. Vehicle Properties for Test No. 03008.

Date: 8-28-2003	**Test No.:** 03008	
Tractor		
Year: 1992	**Make:** Freightliner	**Model:** FLD120
VIN NO.: 1FUYDSYBINH480737		**Odometer:** 754,596
Trailer (Van)		
Year: N.A.	**Make:** N.A.	**Model:** N.A.
VIN NO.:		
Describe any damage to the vehicle prior to test		

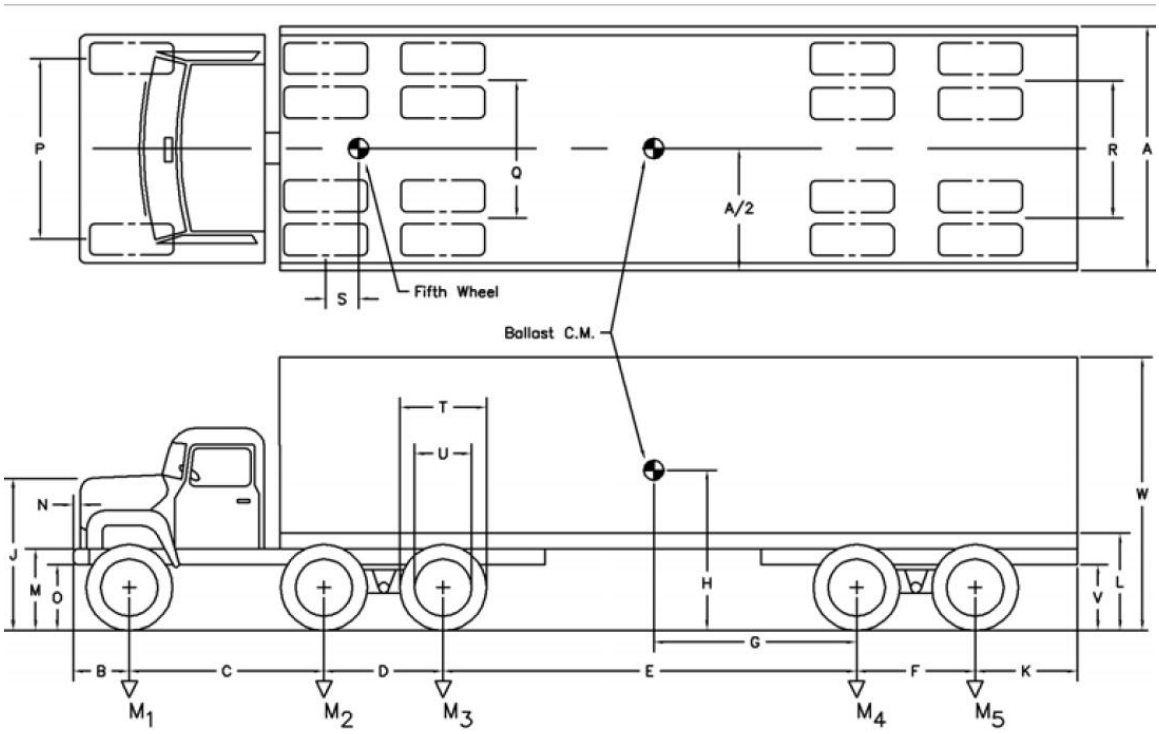

Geometry (in)

A	30.23	**G**		**N**	6.65	**T**	40.8
B	43.5	**H**		**O**	73.0	**U**	25.7
C	188.8	**J**	69.2	**P**	79.5	**V**	
D	51.25	**K**		**Q**		**W**	
E		**L**		**R**			
F		**M**	40.1	**S**			

Mass (lb)	Curb	Test Inertial	Gross Static
M_1	9,691		
M_2	3,104		
M_3	4,057		
M_T	16,852	14,683	

Table 13. Vehicle Properties for Test No. ACBR-1.

Date: 8-28-2003	**Test No.:** ACBR-1	
Tractor		
Year: 1989	**Make:** General Motors	**Model:** Brigadier
VIN NO.: 4GTT9C4C3KV800398		**Odometer:** 754,596
Trailer (Van)		
Year: 1989	**Make:** Great Dane	**Model:** Brigadier
VIN NO.: 1GAA9623LB056236		
Describe any damage to the vehicle prior to test		

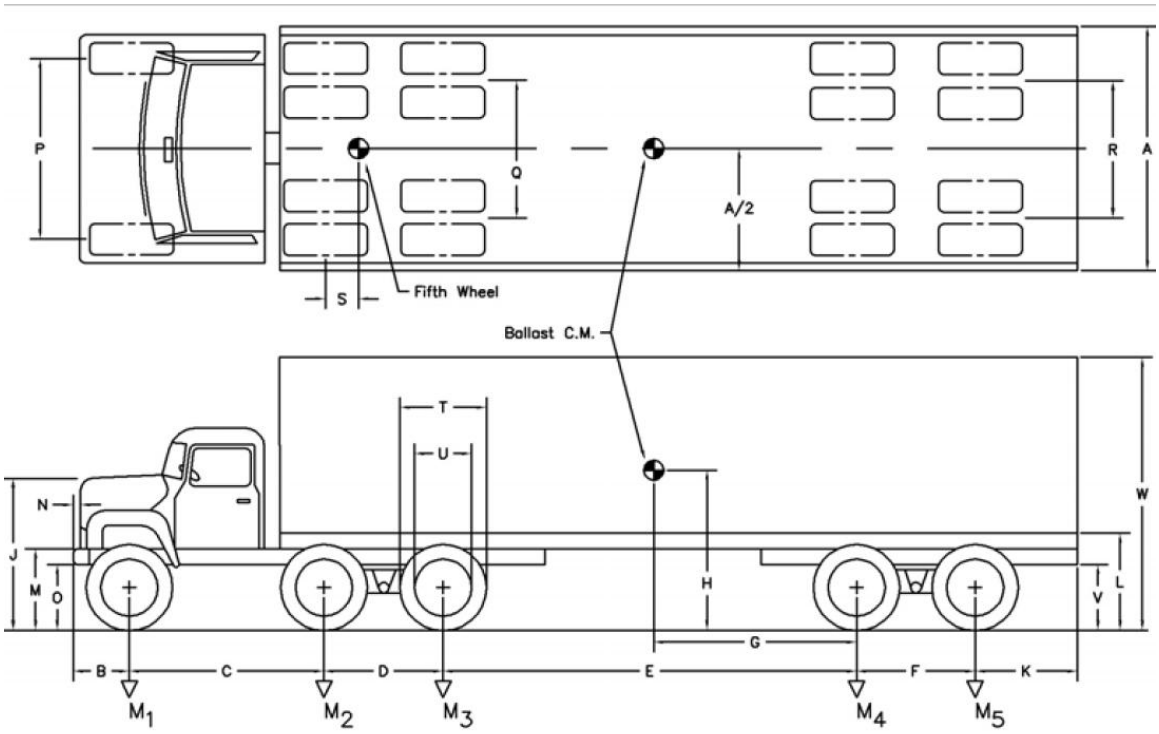

Geometry (in)

A	102.4	**G**	217.5	**N**	3.25	**T**	42.5
B	28	**H**	73	**O**	21.9	**U**	25.5
C	145	**J**	70.75	**P**	79.5	**V**	37
D	51.25	**K**	36.5	**Q**	71.75	**W**	157.75
E	328	**L**	48.5	**R**	77.4		
F	49	**M**	38.75	**S**	24		

Mass (lb)	Curb	Test Inertial	Gross Static
$\mathbf{M_1}$	8,050	8,475	
$\mathbf{M_2}$	7,425	18,950	
$\mathbf{M_3}$	5,500	17,775	
$\mathbf{M_4}$	4,925	16,025	
$\mathbf{M_5}$	4,625	17,750	
$\mathbf{M_T}$	30,525	78,975	

CHAPTER 3. TRACTOR-TRAILER FINITE ELEMENT MODEL EVALUATION AND ENHANCEMENT

The NTRCI Finite Element Analysis Team has evaluated a finite element (FE) model of a tractor-trailer developed by the National Crash Analysis Center (NCAC) and is currently making necessary modifications to the model to enhance its fidelity. This model was developed for the purpose of simulating tractor-trailer crash events with particular emphasis on those crash events involving roadside safety hardware (e.g., bridge rails, median barriers, etc.). In the first part of this study, Battelle led the Team in conducting a basic evaluation of the NCAC tractor model to identify critical model features that warranted improvement regarding the model's ability to accurately simulate vehicle response in impacts with roadside safety hardware. This chapter of the Phase A Report summarizes the modifications that have been made to the tractor FE model and provides discussion on the results.

The intended application of the model is not to examine the crashworthiness of the tractor vehicle but rather to evaluate the crash performance of roadside safety features being struck by a tractor based on National Cooperative Highway Research Program (NCHRP) Report 350 evaluation parameters [1]. In such applications, the tractor serves as a "bullet" vehicle, so model performance is judged by accuracy of load transfer of the vehicle to the barrier as well as accuracy in simulating the kinematic behavior of the tractor during and after impact. The intended use of the model must be considered in determining what constitutes "good enough" regarding the fidelity of the model. Reduced-element ("bullet") models such as this are not considered valid for general applications due to the lack of geometric detail of components and connections, and/or omission of various components. These simplifications will have a cumulative affect on the accuracy of the results produced by the model; so the intended application of the model must be considered in its development.

The latest version of the tractor FE model (tractor_V01b) was obtained from the NCAC and an evaluation of the model was conducted. The evaluation involved a basic assessment of several features of the model including:

- Overall mass distribution and inertial properties
    - Point mass assignments vs. increased densities of neighboring components representing un-modeled parts (e.g., missing components inside cab).
- Material assignments and characterization
    - Comparison of actual material types used in the various components of the vehicle vs. those used in the finite element model.
- Assessment of geometric accuracy of the major structural components such as truck frame-rails.
- Component thickness assignments for shell elements.
- Beam property assignments.
- Component connections (spotwelds, nodal rigid bodies, joints, merged nodes, weld elements, etc.).

- Assessment of suspension components and their connections to the vehicle body (including possible failure modes)
    - Air-ride suspension characterization
    - Shock/damper characterization
    - Failure of suspension components: U-bolts, shear pin, suspension mounts, etc.
- Tire model fidelity.
- Detailed *CONTACT survey
    - Contact assignments
    - "Robustness" (numerical stability)
    - Initial penetration of components, etc.

Based on this assessment, deficiencies in the model that were deemed critical for accurately simulating vehicle response in impacts with roadside safety hardware were identified and corresponding modifications were made to the model.

MODEL IMPROVEMENTS

Finite Element Mesh

The original version of the tractor model had 50,344 nodes, 46,470 elements, and 361 part definitions. Typical element sizes for non-structural components in the model, such as the hood and doors, were 25 – 150 mm and typical element sizes for structural components, such as main frame rails, were 30 – 50 mm. There were some elements in the model that were smaller that caused a relatively small critical time-step for the analysis. For example, there were approximately 75 elements with a critical time step less than a microsecond. "Mass scaling" was used to add mass to these small elements to achieve the desired time step. Most of these elements were in non-critical areas of the model – e.g., the door handle on the storage compartment of the sleeper. These parts were remeshed to improve element quality and computational performance.

The original model used the least computationally expensive element formulations and default options on hourglass stabilization. Stiffness-based hourglass control is better suited for parts that experience large deformations and does not significantly increase computational time. For all types of elements in the original vehicle model, the number of integration points is set at the default value. In light of the model's purpose, such decision is prudent because the number of integration points tend to linearly increase the simulation time. However, for the important structural parts, such as the main-frame and the parts that are expected to bear the brunt of the impact force, five integration points through thickness is the currently accepted minimum because default two points may make the shell too soft and deform too abruptly.

The target minimum time-step for the *modified* mesh was 1.4 microseconds. There are approximately 100 elements with a minimum time-step less than the target minimum. Using mass scaling to enforce the 1.4 microsecond time-step resulted in a total of 7 lb added to the model – which was distributed over those 100 elements.

Overall Mass Distribution and Inertial Properties

An initial assessment of the overall mass distribution in the tractor FE model was made based on a comparison to the Freightliner FLD120 tractor used in Test 03008 performed at the Federal Outdoor Impact Laboratory (FOIL). Table 14 shows a comparison of the wheel loads from the FE model to those measured on the test vehicle. Table 14 includes both the curb mass and the test inertial mass of the test vehicle. For purposes of this comparison, only the curb (as-received) mass is of interest since the test inertial mass is the mass of the vehicle after it was modified for the test (e.g., removal of several parts and addition of test instrumentation).

The total mass of the tractor model was 7,485 kg and the total curb mass of the actual tractor was 7,644 kg. The model was 159 kg (350 lb) too light, which is only a 2% error. The error in mass distribution in the FE model resulted in an error in the center of gravity of 210 mm (9% error) rearward and 26 mm (2.5% error) to the right of the center of gravity measured from the test vehicle (refer to table 15).
Because the model was developed as a "bullet" model, many components of the vehicle were not included. The developers were careful to ensure that all structural members were accounted for in the model, but many non-structural members were excluded. Although these components may not contribute significantly to the overall stiffness of the vehicle, they do affect the local and global inertial properties. These masses and their locations must be accounted for in the model.

This is typically done in one of three ways: 1) discrete mass elements added to the nodes at the location of the missing components; 2) increase material density for parts in the vicinity of the missing components; or 3) modify the geometry of the parts (e.g., increased thickness of shell elements) in the vicinity of the missing components. The preferred method would be to add mass to the nodes at exactly the location of the missing components. Modifying the material density would be the second choice because this would likely result in distribution of the mass over a much larger area and it would affect the dynamic response. To avoid over stiffening the model, increasing the element thickness should not be used as a method to increase mass unless the component is non-structural and is not expected to deform significantly during analysis.

Table 14. Wheel Loads Measured on a Freightliner FLD120 Tractor Vehicle Compared to those Measured in the Finite Element Model.

Position	Measured Curb Mass (kg)[1]	Test Inertial Mass (kg)[1]	Original FE Model Inertial Mass (kg)	Difference / %Error
Left Front	2,176	1,914	1,925	-251 kg / 11.5%
Right Front	2,220	1,830	1,900	-320 kg / 14.4%
Left-Middle Rear	920	654	1,230	+160 kg / 9.4%
Left-Rear	790	808	640	
Right-Middle Rear	488	604	1,390	+252 kg / 16.4%
Right Rear	1,050	850	400	
Total Mass	**7,644**	**6,660**	**7,485**	**-159 kg / 2%**

[1] FOIL Test 03008

Table 15. Location of Vehicle Center of Gravity – Test Vehicle and Finite Element Model.

Location of Vehicle C.G. Relative to Left, Front Wheel	Test Vehicle (based on curb weight)	Finite Element Model	Difference / %Error
Longitudinal – c.g.	2,354 mm	2,564 mm	210 mm / 9%
Lateral – c.g.	1,019 mm	1,045 mm	26 mm / 2.5%

The FE model did not include any discrete nodal masses. The mass of the missing components were accounted for by increasing material densities or increasing thickness of structural elements. Figure 1 shows the parts of the vehicle for which the material densities were increased to account for missing mass.

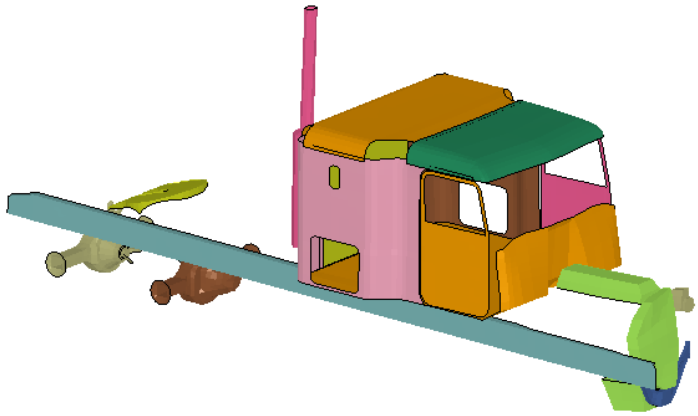

Figure 1. Illustration. Parts of the Vehicle for which the Material Densities were Increased to Account for Missing Mass.

There are other parts that appear to have material density values that are too low, which would lower the mass of those parts. Figure 2 shows all the parts that were modeled with a value for Young's modulus of steel (~200,000 MPa), but have material densities less than that of steel. Chapter 4 of this report, Tractor-Trailer Material and Inertial Properties Evaluation, conducted by ORNL, it was found that many of those parts were not actually made from steel and the properties of those components have been corrected in the *modified model.*

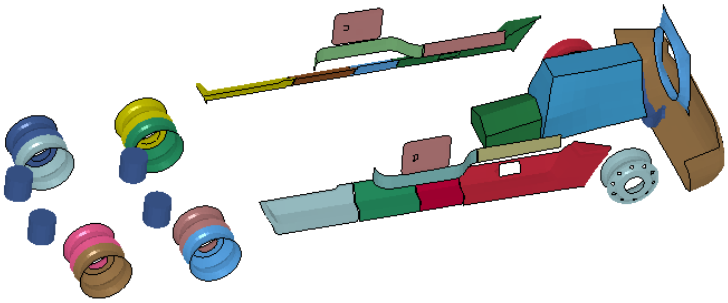

Figure 2. Illustration. Parts that were Modeled with a Value for Young's Modulus Consistent with Steel, but have Material Densities Less than that of Steel.

A more detailed discussion of the evaluation and improvements to the inertial properties of the tractor is provided in Chapter 4 Tractor-Trailer Material and Inertial Properties Evaluation.

Material Assignments and Characterization

Regardless of the amount of geometric detail and mesh refinement of a FE model, realistic results can not be obtained without proper characterization of material properties of the various model components. Metals, such as steel and aluminum, are relatively easy to characterize using standard material models available in most commercial FE codes. LS-DYNA, for example, has several material models appropriate for simulating the behavior (including thermal and strain-rate effects) of metals.

Since the tractor test vehicle was disposed of prior to the start of this project, it was not possible to extract test coupons from the vehicle. However, ORNL has a library of detailed material properties corresponding to a wide range of different types of materials, especially steels. Once the material classifications of the components were identified, this database was used for assigning properties to the steel components of the model.

The *materials assignment and characterization* task is discussed in more detail in Chapter 4 of this report.

Assessment of Geometric Accuracy of the Major Structural Components

The initial shape, thickness, and geometric detail of major tractor structural components will directly affect overall vehicle stiffness, mass, and deformation modes during crash simulation. Research team staff visited a Freightliner dealership to survey tractors of similar make and model to the FE model. Measurements were taken of several components of the vehicle and compared to the model. In almost all cases involving structural members, such as frame rails and frame rail cross bracing, the thickness of the components measured on the physical vehicle was consistent with the thickness of the corresponding component in the model. For many of the non-structural components such as the truck cabin, fenders, hood, fuel tank, etc., the thickness was different from the actual component's thickness. In some cases, the exact thickness could not be measured due to restricted access to the part or because the part was a composite of several

layers of sheet metal riveted together (see figure 3) and it was not clear what value should be used.

Figure 3. Photograph. Freightliner FLD120 Tractor Cabin Illustrating Component Material and Connections.

The geometry of the structural components in the model corresponded reasonably well with the physical geometry; however, all radii in the physical geometry are represented as straight corners in the FE model due to the size of the elements for the FE mesh (figure 4). In the process of improving the model, refinements of the mesh were made in many regions of the model, but improvements to the geometry of most of these components were not. Increased geometric fidelity was not possible without access to the CAD geometry. Detailed reverse-engineering of parts was out of scope of the project.

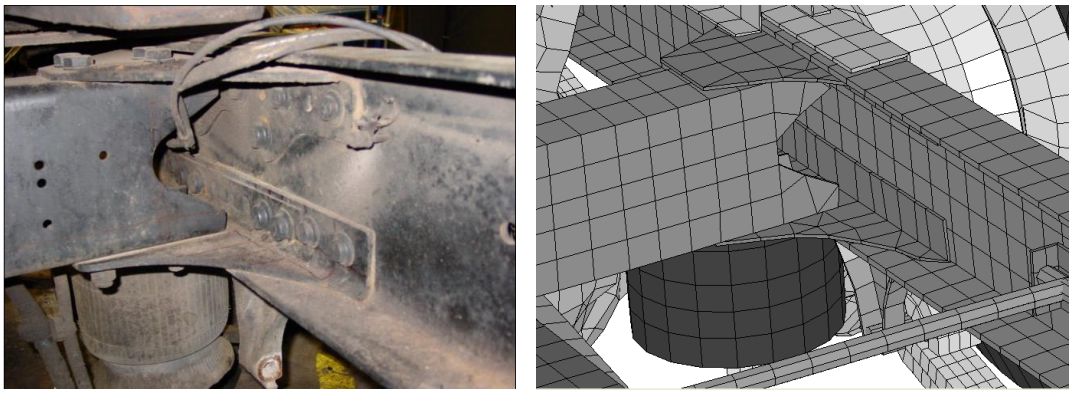

Figure 4. Photograph and Illustration. Finite Element Model of Frame Rail and Cross Bracing Compared with those Components on the Physical Vehicle.

Assessment of Suspension Components, Connections, and Failure Modes

An important aspect of a bullet vehicle model is its ability to simulate the overall kinematics of the vehicle in an impact event, which implies the existence of accurate models for mass

distribution, global bending stiffness, torsion stiffness, and response of wheels and suspension components. For example, when a vehicle impacts a concrete safety shape barrier (e.g., F-shape and New Jersey shape barriers) at oblique angles, the spinning wheels of the vehicle tend to climb the barrier, which can significantly affect the dynamic behavior of the vehicle and, consequently, affect the loading on the barrier. If such capability is missing in the model, the simulation results can not be expected to provide reliable information regarding performance of the roadside safety barrier.

Front Leaf Spring Suspension

One of the primary uses of the tractor model will be to simulate NCHRP Report 350 Test Level 5 impacts into longitudinal barriers. These impact scenarios involve an 80,000-lb (36,000 kg) tractor-trailer impacting the barrier at 50 mph (80 km/hr) at an impact angle of 15 degrees. In such an impact scenario, the front tires and front axle are the first to experience the brunt of the impact force, thus these components must be modeled in sufficient geometric and material detail.

A basic assessment of the front suspension model of the tractor revealed several areas that could be corrected to enhance the crash performance of the vehicle. The areas of concern are related to:

- Geometric and mesh discretization of the geometry of the leaf springs
- Over-constraint of the leaf springs, limiting their range of motion
- Material property definition of the leaf spring steel
- Missing critical components in the linkage of the leaf spring system to the frame rail of the tractor
- Preload of suspension under gravity loading
- Geometric and stiffness representation of the suspension-stop
- Inability of the wheels to steer
- Missing steering linkage between left and right wheels.

No failure criteria were defined for U-bolts, shear pins, suspension mounts, etc., in the original tractor model. Failure of one or more of these components is always observed in actual crash tests, which directly influences tractor kinematics and post-impact behavior.

The tractor model's front suspension uses shell elements to model the leaf springs. The individual leaves are modeled with a uniform thickness of 12 mm, whereas the physical components taper from a thickness of 16 mm at the center to approximately 7-9 mm at the end. Also, several nodal rigid body constraints are used that prevent the leaves from sliding against one another and prevent the leaf spring system from rotating at the pinned connections to the frame rail. The leaf spring material is characterized as a relatively mild steel with yield strength of 50,750 psi (350 MPa), whereas the physical components are expected to have a yield strength much higher - approximately 181,297 psi (1,250 MPa).

The suspension geometry in the tractor model was based on its equilibrium position under the weight of the sprung mass of the truck; however, the model did not account for any preload in the suspension components. Consequently, the sprung mass of the truck displaced significantly downward when gravity was applied to the model. A study was performed to investigate a better method of modeling the suspension system. A methodology was identified, which involves pre-stressing the leaves in the leaf-spring assembly to account for the gravity load of the tractor. This method provided very promising results and was relatively easy to implement. Researchers at Midwest Roadside Safety Research Facility (MwRSF) recently applied this same methodology to modeling the leaf springs on the rear of the NCAC C2500 model with good results [2].

Leaf Spring Suspension Characterization

A leaf spring assembly for a 1992 Freightliner FLD120 tractor was purchased from a local Freightliner dealer. A laboratory test was conducted to measure the force/velocity response of the leaf spring assembly. The test and test setup is shown in figure 5.

Figure 5. Photograph. Laboratory Test of a 1992 Freightliner FLD120 Leaf-spring Suspension.

The leaf-spring purchased from the local Freightliner dealer was digitized by Research team staff. A 3-D geometric rendering of the part was produced using Pro-Engineer™ CAD software and HyperMesh™ was used to create the FE mesh of the component (see figure 6). Two modeling approaches were investigated:

- Thick shell element approach
- Thin shell element approach.

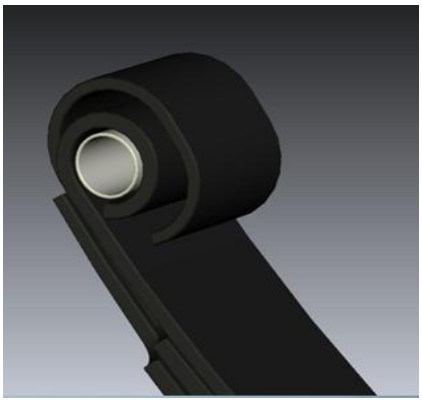

Figure 6. Photograph. Digitized 3-Dimensional Geometry of the 1992 Freightliner FLD120 suspension.

Thick Shell Model

The advantages of modeling the part with *thick shell* elements are apparent: the taper of the leaves are accounted for exactly and explicitly in the mesh, initial penetration between leaves is easier to control (since the geometry is exact), and the thickness of the leaves suggests that they would be better characterized using *thick shell* theory. The analysis, however, resulted in an overly stiff response of the leaf-spring. It was also determined that the *thick shell* elements were not sufficiently 'robust' under large deformations. Suspension components often experience significant deformation during impact with roadside safety barriers; so the computational model of these components must remain stable under high deformations in order for the model to be useful to practitioners.

Thin Shell Model

The leaf spring was also modeled using *thin shell* elements. This model was a little more tedious to develop since the thickness of the elements were defined as a line in the input file rather than explicitly defined by the geometry of the mesh. The taper of the leaves was accounted for in the model in a piecewise manner, as shown in the exploded view in figure 7. Each colored segment was defined as a separate part in the model and a representative thickness was assigned to each segment based on the average thickness of the segment (measured from the physical component).

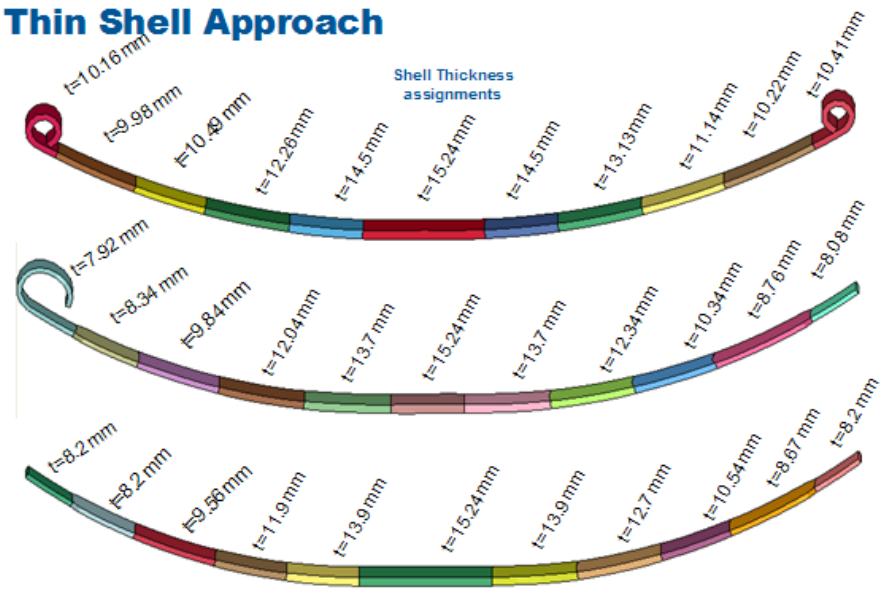

Figure 7. Illustration. Exploded View of Leaf-spring Thin Shell Model

A paper published in the ASM International Journal documents the results of a study where the failure of a leaf-spring in a sport utility vehicle was investigated [3]. The study reported that fracture of the leaf-spring material occurred at the pin connection at a stress of 211,755 psi (1460 MPa).

The leaves of the leaf-spring model were meshed with full-integrated shell elements (type 16 in LS-Dyna) with warping stiffness turned on (hourglass control type 8). The material was modeled with yield stress of 181,300 psi (1,250 MPa) and failure strain set to 0.182 (corresponding to an ultimate stress of 211,755 psi). The typical element size used in the model was 20 mm long x 20 mm wide and the total number of elements was 1,380. The smallest time-step for an element in the mesh was 1.4 microseconds in an element located at the end of the leaf spring at the pin connection.

An analysis was conducted to evaluate the stiffness of the leaf-spring model based on a comparison with the laboratory test results. The boundary and loading conditions were modeled based on the test fixture used in the laboratory test as shown in figures 5 and 8.

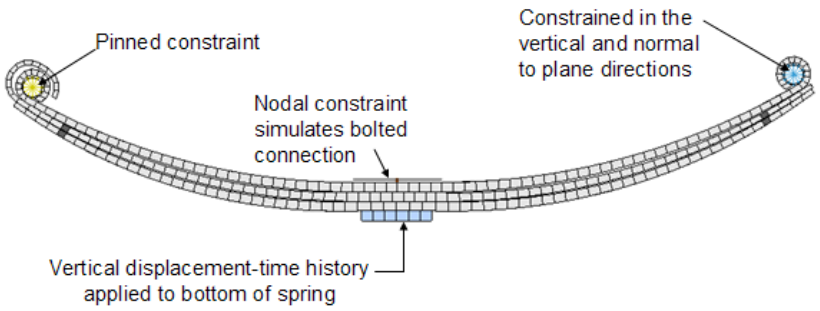

Figure 8. Illustration. Finite Element Model for Validating Stiffness Response.

A comparison of the model results are shown in figure 9. The response of the model resulted in a constant stiffness of 1,313 lb/in (230 N/mm) which compared relatively well with the response measured in the test (206 N/mm). As a further check of the model, the mesh was refined such that the typical element size was 10 mm x 10 mm. The refined mesh resulted in a stiffness of 1,265 lb/in (221 N/mm). It is expected that the response would continue to approach that of the test with further mesh refinement; however, the coarser mesh will be used for application in the tractor model to maintain a reasonable time-step for the analysis.

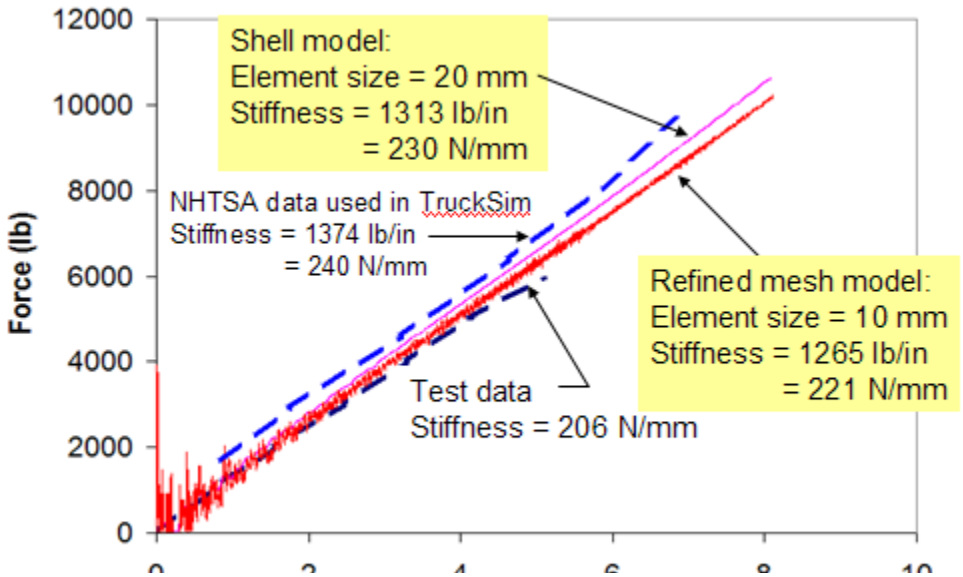

Figure 9. Chart. Force-displacement Response of Leaf Spring from Test and FEA.

Gravity Preload of Leaf-Spring

The geometry of the tractor model is based on its equilibrium position under gravity loading. It is necessary then to properly position the leaf spring in the vehicle model in its *preloaded* state

and accurately account for the *pre-stress* in the suspension components. The suspension is supporting approximately 4,845 lb (21,550 N) under gravity load.

An analysis was conducted to compress the leaf-spring model into its proper equilibrium position. The nodal coordinates of the suspension in this deformed state were extracted and put back into the leaf-spring model. The element stresses at this position were also obtained from the analysis (via *interface_springback option in LS-Dyna) and were used to apply pre-stress to the leaf-spring elements (via the *initial_stress_shell card in LS-Dyna). Figure 10 shows the equilibrium position of the tractor model under gravity load with the pre-stressed leaf-spring model.

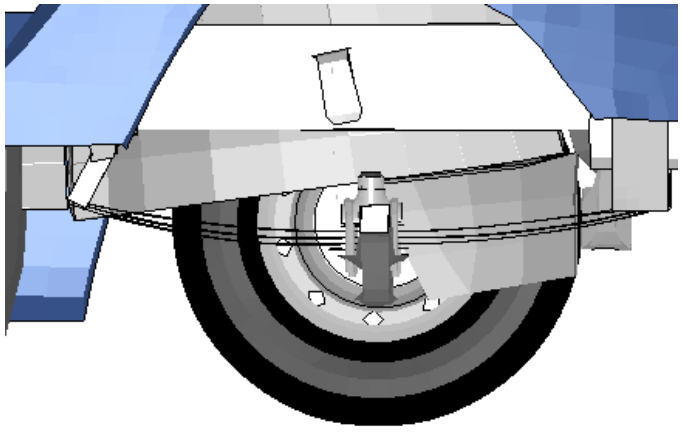

Figure 10. Illustration. Equilibrium Position of the Tractor Model with Pre-stressed Leaf-spring Model.

Suspension Displacement Limiter (Suspension Stop)

The *suspension stop* component, shown in figure 11, limits the displacement of the leaf spring during compression. This component is made of cast aluminum and is positioned on top of the leaf spring directly over the axle. It is fastened to the leaf spring using two 0.825-inch diameter U-bolts. When the suspension is fully compressed the *suspension stop* will impact against the bottom of the truck frame rail. The *suspension stop* includes a rubber cylinder that is approximately 1.5 inches long inserted into the top of the *suspension stop*. This rubber cylinder extends slightly above the tip of the *suspension stop* to soften the impact against the frame rail.

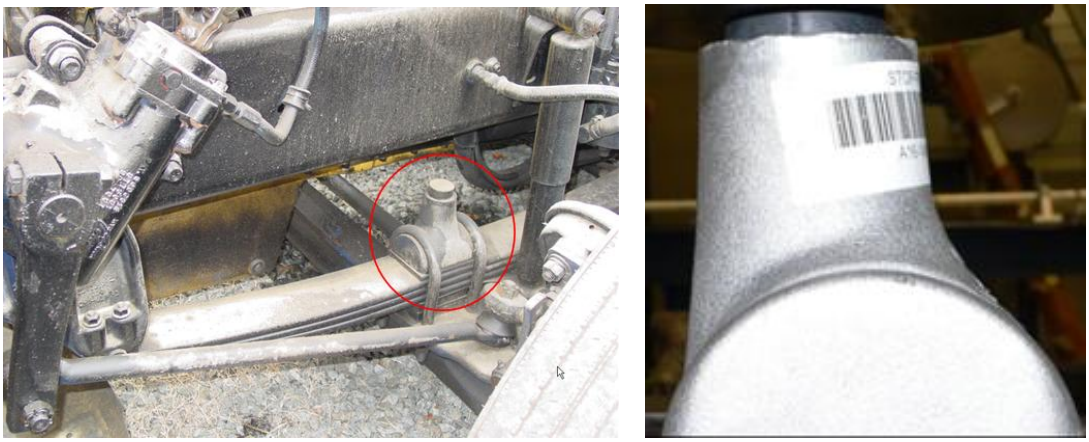

Figure 11. Photograph. Suspension Displacement Limiter for a 1992 Freightliner FLD120 Tractor.

The load-deflection response of the rubber tip was measured in the laboratory using displacement control on a uniaxial load machine. The displacement was ramped at a constant velocity from 0 to 0.417 inches in 447 seconds. The results are shown in figure 12. The response of the rubber tip was characterized in the model using *mat_simplified_rubber_with_damage in LS-Dyna and the model response is compared to the test in figure 12.

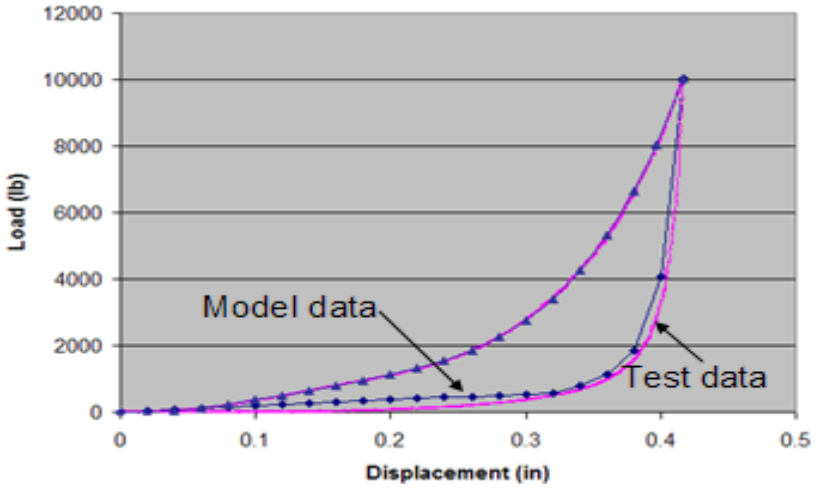

Figure 12. Chart. Load-displacement Response of Rubber Tip on *Suspension Stop*.

The geometry of the *suspension stop* is also important. The U-bolts that fasten the leaf spring to the front axle are also used to fasten the *suspension stop* to the leaf spring. The U-bolts are seated into a 'saddled' groove on either side of the *suspension stop*. Without the proper geometry and proper contact defined between these components, their connection can not be properly modeled. The U-bolts were tightened using a pseudo-temperature to shrink a single element on each side of the U-bolts. This was done by defining a coefficient of thermal expansion on those elements and defining a temperature drop at the start of the analysis. The elements shrink due to the temperature change and 'clamp' all the suspension components together. As the components compress together, the gaps between components close and a tensile force is generated in the U-bolts. This process was accomplished by iteratively decreasing the temperature until a pre-load of approximately 4,000 lb (17,793 N) was achieved.

The aluminum housing part of the *suspension stop* was modeled with tetrahedral elements with rigid material properties. The expected deformation of this part during impact was considered to be insignificant, e.g., the impact energy is absorbed primarily through deformation of the rubber cylinder. The geometry, on the other hand, was considered very important since achieving an accurate model of the connection of the leaf spring to the axle depends on having an accurate geometric model of the *suspension stop* and its contact with the U-bolt.

The model of this component was discretized with a very refined mesh in order to sufficiently capture the geometry. Note, however, that the number and size of these elements do not enter into computations (except for contact) since the material is characterized with rigid material properties. Figure 13 shows the FE model for the *suspension stop*.

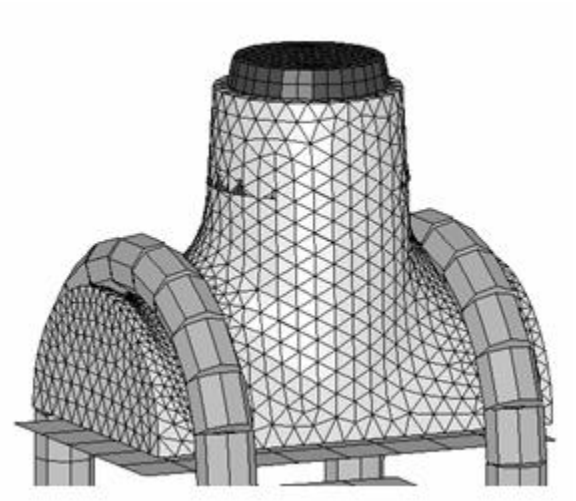

Figure 13. Illustrtation. FE Model of Suspension Stop.

The strength and failure of the U-bolts is also critical for accurately predicting and simulating failure of the connection. The material properties of the U-bolts are defined in the enhanced model based on properties of a grade 8 bolt, where the yield stress is assumed to be 129,920 psi (896 MPa). The failure strain was estimated to be 0.18. The U-bolt component should be tested in the laboratory to better define its properties.

Shock Absorbers

Shock absorbers have a significant influence on suspension response. Generally, these components have nonlinear and unsymmetrical behavior – i.e., different extension and compression response. The shock absorber in the original tractor model was modeled as a linear damper with damping constants that respond the same in compression and in extension.

Front and rear shock absorbers were purchased and tested to determine their force-velocity response. The shock absorbers (Monroe Gas-Magnum) were tested in a uniaxial loading machine using sinusoidal displacement input with +-0.5 inch maximum displacement. Load-velocity data were collected for loading rates of 0.5, 1, 2, 4, and 8 Hz. The results of the tests for the front shock absorber are shown in figure 14. The tests showed that the response of the shock absorber is effectively linear and symmetric for displacement rates less than 3 in/s, i.e., force increases linearly with displacement rate and the response is the same in extension and compression. At displacement rates higher than 3 in/s, however, the response is both nonlinear and non-symmetric with the response in extension being approximately 2 times higher in magnitude than the response in compression. Also, the shock absorber responds differently in compression for increasing velocity than it does for decreasing velocity (note the 'hysteretic' shaped response in compression in figure 14). Similar tests were conducted on the rear shock absorber and the general response was very similar to that of the front shock absorber.

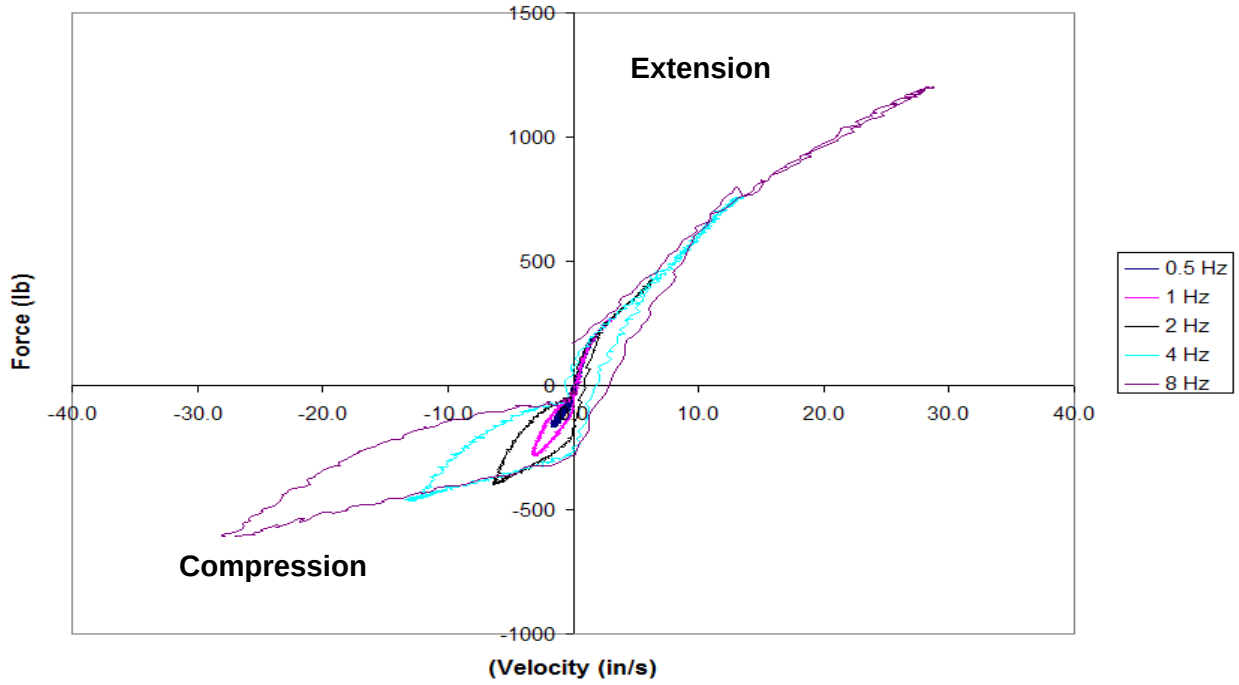

Figure 14. Chart. Force-velocity Response of Front Shock Absorber for the 1992 Freightliner FLD120 Tractor.

The shock absorbers are modeled in the enhanced model as discrete elements with response characterized using *mat_damper_nonlinear in LS-Dyna. The test data was processed to generate a force-velocity curve for input into the material model that 'best defined' the response of the shock absorbers. The force-velocity characterization curve for the front and rear shock absorbers are shown in figures 15 and 16, respectively.

Velocity	Force
-38	-726
-33	-618
-13	-251
-6.5	-121
-3.2	-62.3
-1.7	-48.3
0	0
1.7	63.3
3.2	201
6.4	434
13	714
34	1325
40	1465

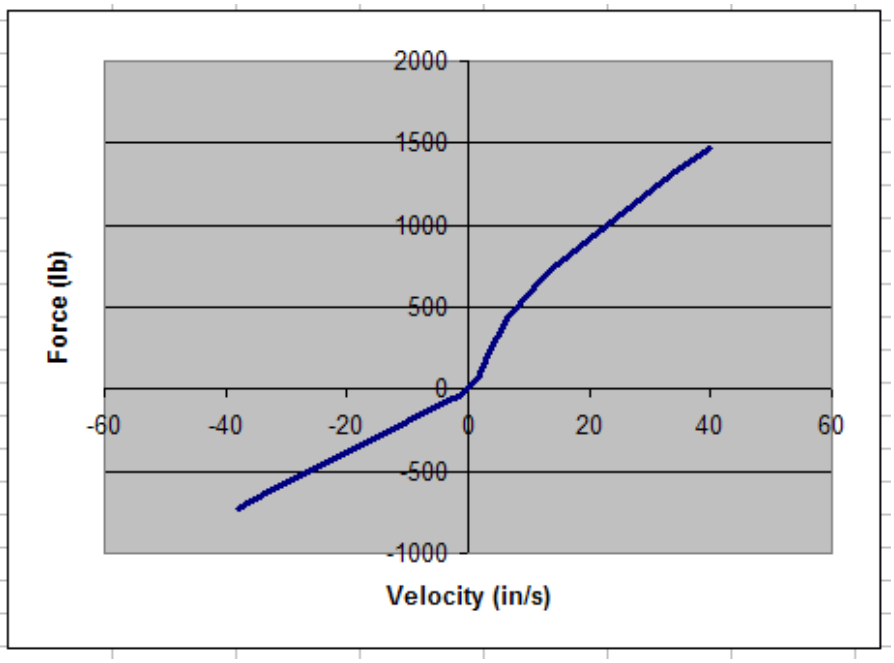

Figure 15. Chart. Force-velocity Curve used to Characterize the Front Shock Absorber in the Tractor Model.

Velocity	Force
-28.9	-629
-13	-455
-6	-380
-3.5	-266
-1.89	-150
0	0
1.6	206
13.3	748
28.25	1196

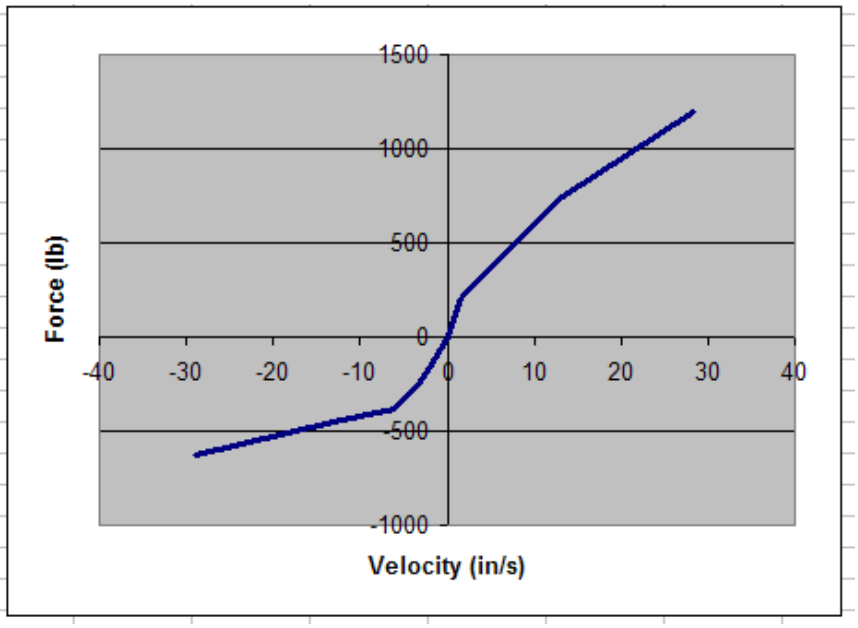

Figure 16. Chart. Force-velocity Curve used to Characterize the Rear Shock Absorber in the Tractor Model.

Rear Suspension

A cursory inspection of an actual Freightliner tractor rear suspension revealed that the leaf spring component of the rear suspension was very stiff – essentially rigid, and could be modeled as such – and the suspension response is primarily governed by the Airide suspension component. The rear suspension of the tractor model was modeled with a 2-leaf spring and a non-physical "place-holder" representation of an Airide suspension bag, as shown in figure 17. The model of the rear tandem axles, the rear suspension, and their connection to the frame rails through the "place holder" of the Airide suspension effectively stiffened the truck structure and also affected the sprung mass response of the vehicle (e.g., the axles and the frame move as a single component).

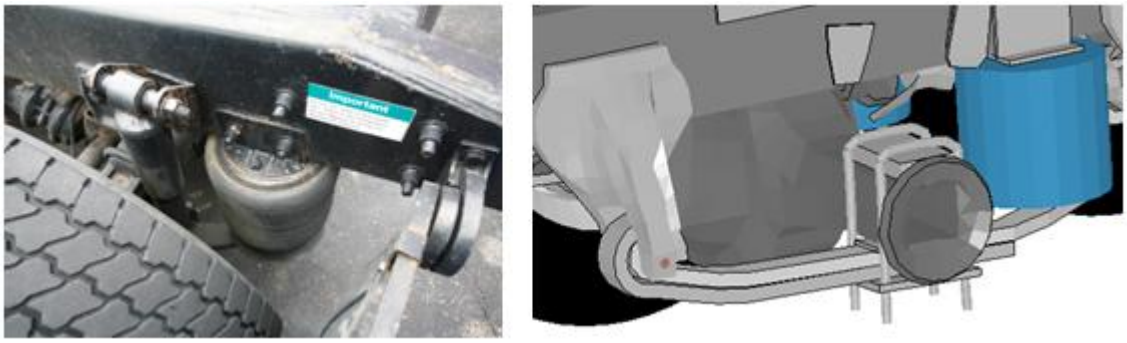

Figure 17. Photograph / Illustration. Airide Suspension Component on Freightliner FLD Tractor and Finite Element Model.

The modifications to the rear suspension are summarized below:

- Removed all nodal rigid body constraints
- Made pin material rigid
- Made pin-bracket material rigid
- Connected pin to pin-bracket using spherical joints
- Connected suspension to pin using extra nodes for rigid bodies
- Connected bracket to frame rail using extra nodes for rigid bodies
- Modified thickness of air-ride suspension part from 10 mm to 4 mm
- Changed material of air-ride suspension part from steel properties to "rubber like" properties (for visual effects only)
- Added discrete elements to the suspension model to model response of Airide component (see following discussion for details).

The rear suspension the 1992 Freightliner FLD120 tractor incorporates a Firestone Airide suspension, Part No. 1T15ZR6, as shown in figure 17. Because of the complexity of modeling the Airide suspension component in geometric detail, an idealized characterization of the component was used in the enhanced model via discrete spring and damper elements. The

suspension component was purchased from a local Freightliner dealer and a test program was developed and carried out in the Battelle labs to characterize the load response of the component for inclusion into the FE model. The response of this component is a function of internal pressure, deflection, and deflection rate. The test program was designed to collect necessary data for properly characterizing the response of the component for each of these factors. Tests were conducted at 'bag pressures' of 20 psig, 40 psig, 60 psig, and 80 psig and deflection rates of 0.01 in/s, 1.2 in/s, and 6 in/s. The test matrix is shown in table 16.

Table 16. Test Matrix for the Airide Suspension Component.

Pressure	Deflection Rate		
	0.01 in/sec	1.2 in/sec	6 in/sec
20 psig	X	X	X
40 psig		X	
60 psig	X	X	X
80 psig		X	

For each test, the "zero position" of the Airide component was set to mid-stroke, corresponding to a spring height of 12.5 inches, and held at this position while the internal air pressure in the component was set to the desired value. The tests were conducted under displacement control. Starting from the zero position, the displacement was ramped up 3 inches to a spring height of 15.5 inches, and the displacement was held at this position for a period of time (typically 10 seconds) to allow for relaxation/recovery of the load. The displacement was then ramped down 6 inches to a spring height of 9.5 inches, and again held for a period of time. The displacement was then ramped back up 6 inches to a spring height of 15.5 inches and again held. This process was repeated for two additional cycles. Test photos are shown in figure 18 and the displacement-time history for each deflection rate is shown below in figures 19 to 21. A representative force-time history plot from a test is shown in figure 22.

Zero position
Spring height = 12.5 in

First ramp
Spring height = 15 in

Second ramp
Spring height = 9.5 in

Third ramp
Spring height = 15 in

Figure 18. Photograph. Sequential Views of Airide Suspension Component in Laboratory Test.

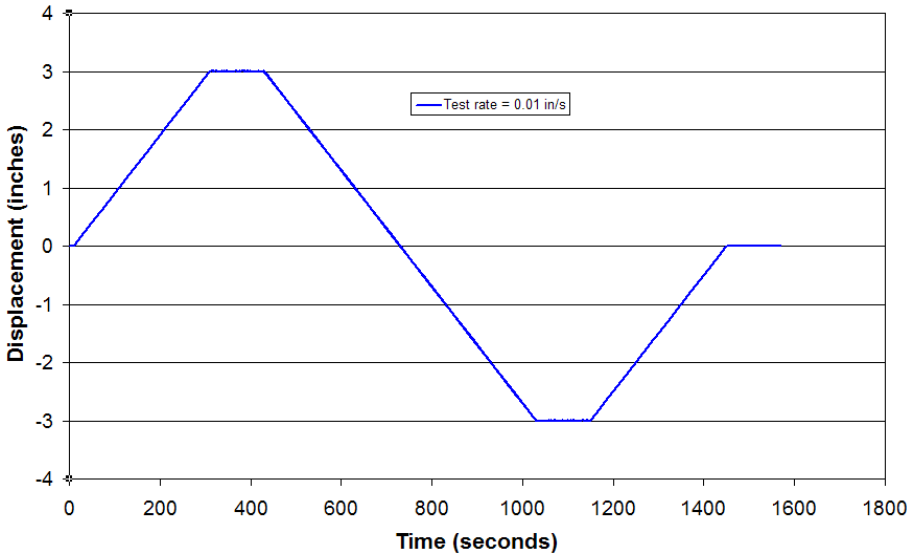

Figure 19. Chart. Displacement-time History of Hydraulic Ram for Load Rate of 0.01 in/sec.

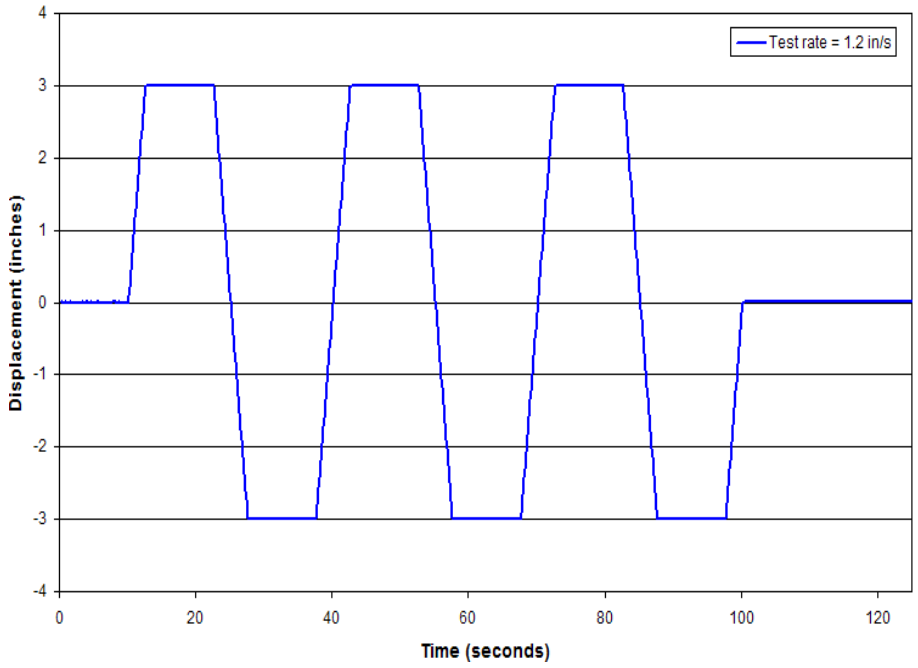

Figure 20. Chart. Displacement-time History of Hydraulic Ram for Load Rate of 1.2 in/sec.

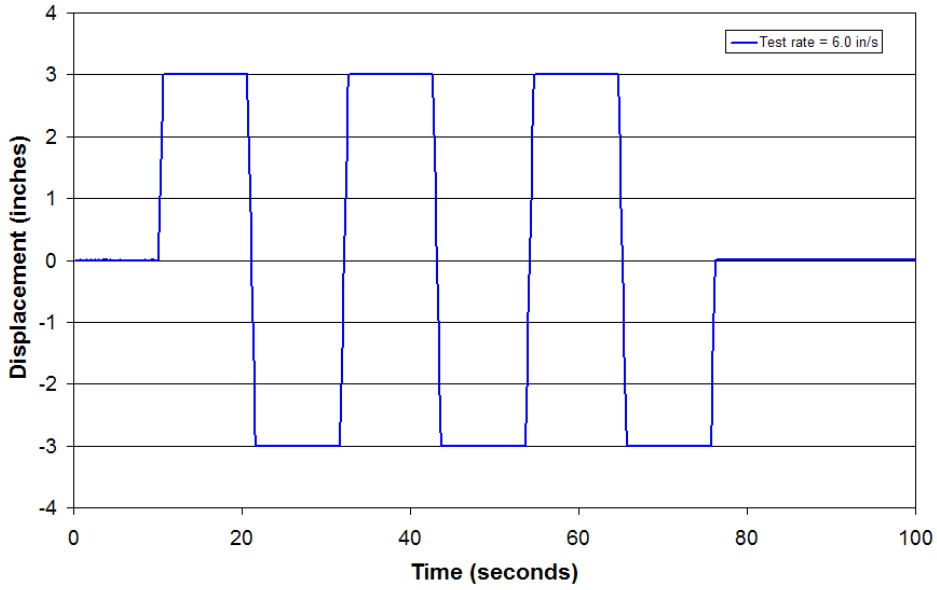

Figure 21. Chart. Displacement-time History of Hydraulic Ram for Load Rate of 6.0 in/sec.

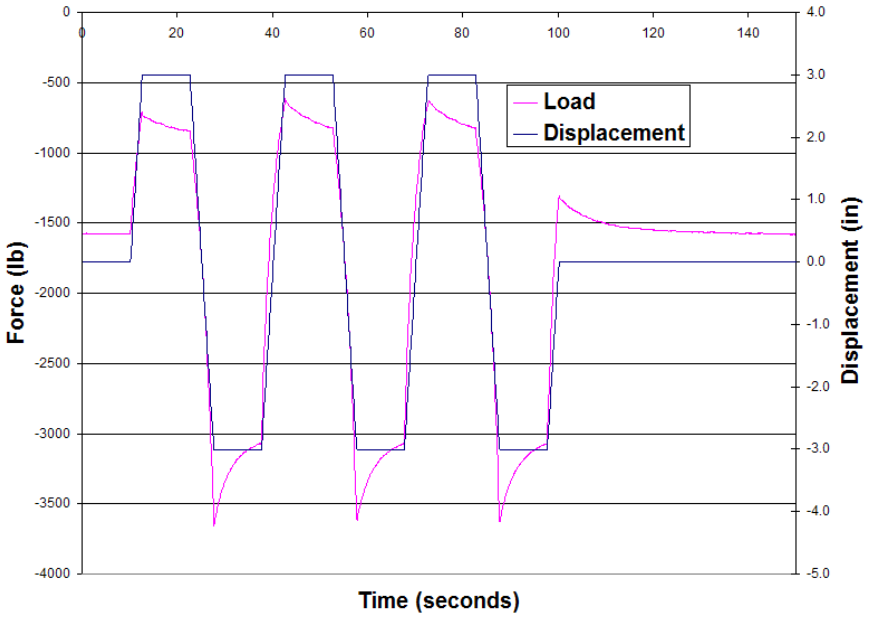

Figure 22. Chart. Force-time History and Displacement-time History of Airide Component at Bag Pressure of 20 psig at Displacement Rate 1.2 in/s.

Quasi-static load-deflection data from the laboratory tests conducted at 20 psig and 60 psig bag pressures are shown in figure 23. The 20 psig and 60 psig bag pressures are significant since they correspond to the bag pressures for an unloaded tractor and an 80,000-lb tractor-trailer combination, respectively.

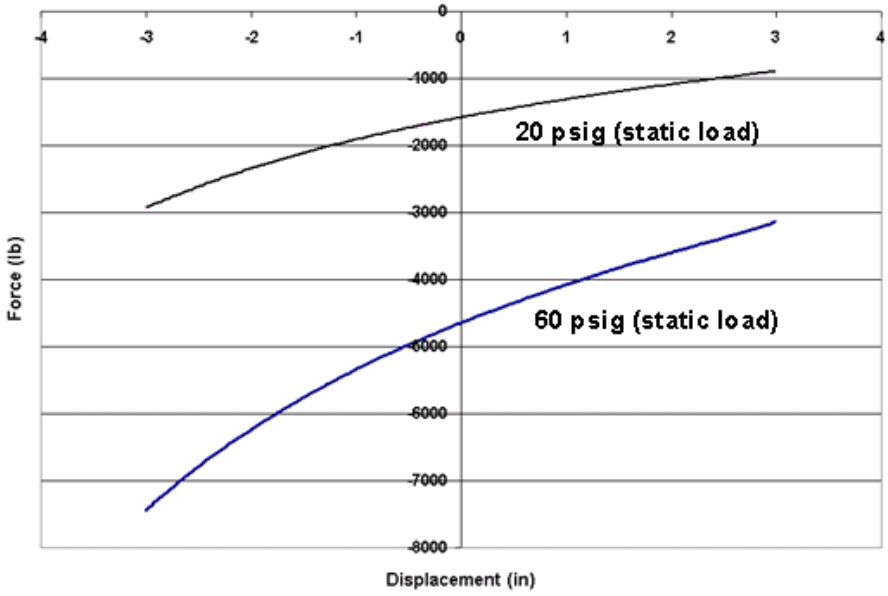

Figure 23. Chart. Quasi-static Load-deflection Data for Airide Component at 20 and 60 psig.

Figure 24 shows a comparison of the Airide component response at 60 psig under quasi-static loading and the 6 in/s load rate case, which clearly shows that for a given 'bag pressure' the response is nonlinear and rate dependent. It also shows that the response is considerably different in compression than it is in extension.

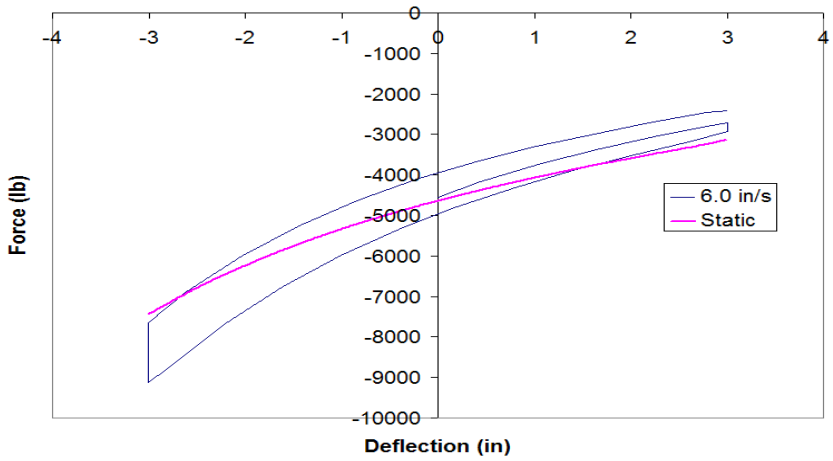

Figure 24. Chart. Load-deflection Data for Airide Component at 60 psig Pressure.

From the test results, it was determined that the Airide suspension response could be approximated by a three-parameter Maxwell model, as illustrated in figure 25.

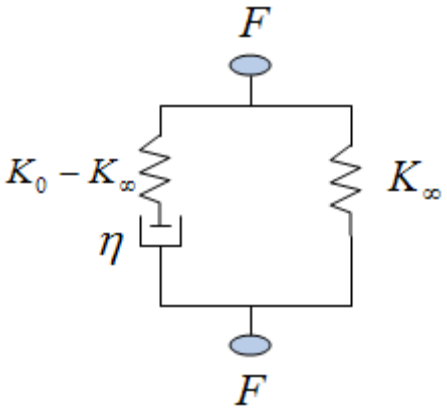

Figure 25. Illustration. Three Parameter Maxwell Model.

The behavior of this model can be described by:

$$F = F_{\infty} + (F_0 - F_{\infty})e^{-\beta t}$$

Figure 26. Equation. Three Parameter Maxwell Model.

When the component is given a prescribed displacement, d, and held at that position, the immediate load response is defined by $F_0 = K_0 * d$ and the long-term equilibrium response is defined by $F_\infty = K_\infty * d$. The parameter $\beta = K_0/\eta$ corresponds to a time decay constant that governs the rate of force relaxation.

The material model library in LS-Dyna includes a three-parameter Maxwell model called *MAT_SPRING_MAXWELL. The input parameters for this model are given as constant coefficients for K_0, K_∞, β. To partially account for the nonlinear response, the Airide component was modeled using two discrete elements, as shown in a sketch in figure 27. One of the elements is characterized by the *MAT_SPRING_MAXWELL material model and the other is characterized with *MAT_SPRING_NONLINEAR_ELASTIC. The parameter, K_∞, in the Maxwell model was set to zero and the quasi-static (e.g., long-term) response was modeled using a non-linear elastic spring (K_{ne} in figure 27) characterized by a force-deflection curve obtained from laboratory tests on the Airide suspension at a "quasi-static" rate (0.01 in/s).

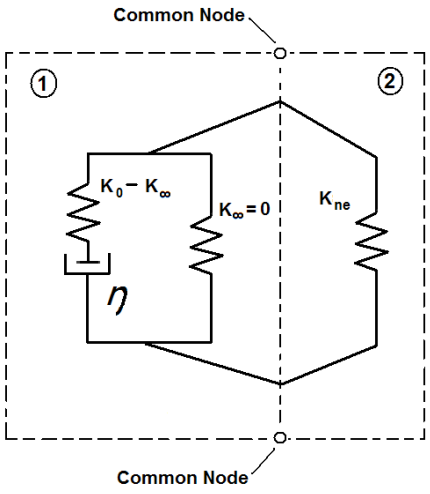

Figure 27. Illustration. Sketch of the Two-element Model used for Modeling the Airide Suspension Component in the Enhanced Tractor Model.

With the K_∞ in the Maxwell model set to zero, the *MAT_SPRING_MAXWELL model simplifies to a linear spring and damper in series. A portion of the force-time plot corresponding to creep of the component under fixed displacement (see figure 22) was used to define the spring and damper constants for the *MAT_SPRING_MAXWELL model. As seen in figure 22, the creep response is different for extension and compression; the compression response was used to calibrate the model.

A summary of the Airide suspension model material parameter input is shown in table 17. Figures 28 and 29 show the model's response compared with the test data for verification that the model was calibrated properly. The model replicates the test response very well in compression (which is the data used to calibrate the model), but does not accurately capture the rate behavior in extension. This is because the *MAT_SPRING_MAXWELL model in LS-Dyna is symmetric in extension and compression. Considering the application of the tractor model (e.g., crash analysis), it was concluded that the compression behavior of the suspension was more important than the extension and thus the model response was considered acceptable.

Table 17. Summary of the Airide Suspension Model Material Input.

Unloaded Tractor (20 psig bag pressure)				
Discrete Element	**Material Model**	**Material Parameters**		
		K_0 (N/mm)	**K_∞ (N/mm)**	**B (s^{-1})**
Element 1	*MAT_SPRING_MAXWELL	36.24	1.0E-4	0.29 s^{-1}
Element 2	*MAT_SPRING_NONLINEAR	Load curve (see figure 23)		
80,000-lb tractor-trailer Combination (60 psig bag pressure)				
Discrete Element	**Material Model**	**Material Parameters**		
		K_0	**K_∞**	**η**
Element 1	*MAT_SPRING_MAXWELL	54.0	1.0E-4	0.219
Element 2	*MAT_SPRING_NONLINEAR	Load curve (see figure 23)		

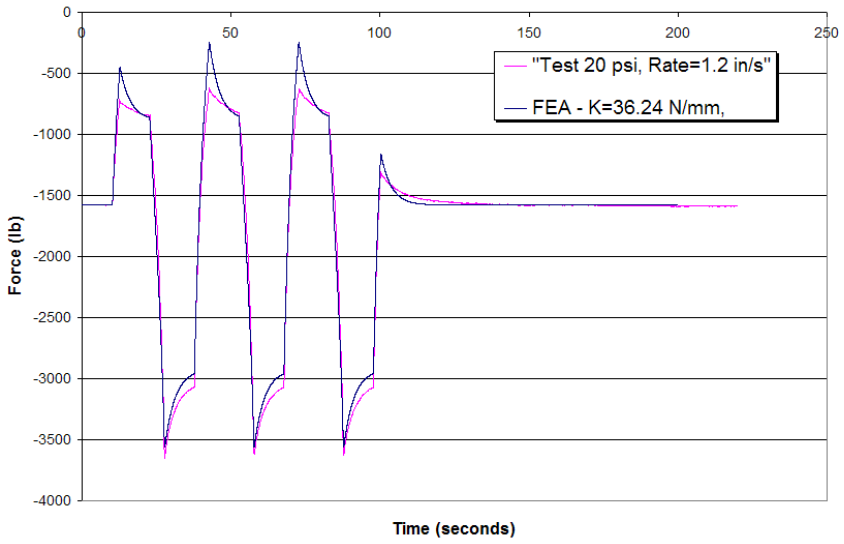

Figure 28. Chart. Finite Element Model's Response Compared with the Test Data for Bag Pressure of 20 psig and Displacement Rate of 1.2 in/s.

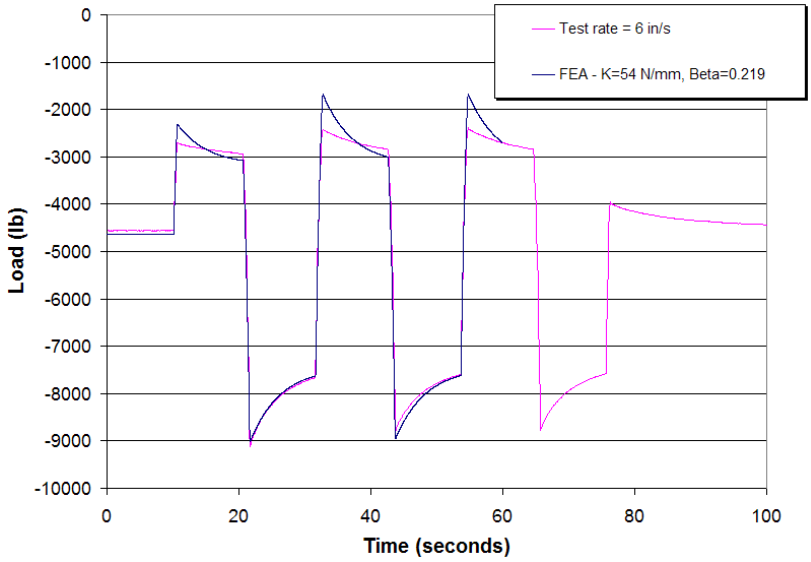

Figure 29. Chart. Finite Element Model's Response Compared with the Test Data for Bat Pressure of 60 psig and Displacement Rate of 6 in/s.

Component Connections

Component connector elements such as spotwelds, nodal rigid bodies, joints, weld elements, etc., in the tractor model need to be reviewed in some detail for appropriateness and compatibility with local mesh density and functional intent. As stated above, some areas of the tractor model were observed to be potentially over-constrained due to placement of nodal rigid bodies vs. local mesh refinement. The final choice and type of connector elements used will be determined after the final FE mesh is established, and will be dictated by larger functional requirements.

Tire Model

When a vehicle impacts an object such as a roadside safety barrier, one or more of its tires may deflate or "blowout" as the tire(s) interact with the object. Tire deflation affects the dynamics of a vehicle during impact because it alters the magnitude of forces and the mechanism of how those forces are transferred between various vehicle components. For example, during full-scale, low-angle impacts with longitudinal concrete barriers, the front, impact side tire of a vehicle often gets pushed back into the wheel housing. If the tire remains inflated during this event, the wheel will stack against adjacent parts and impose significant forces on its surroundings. The magnitude of these forces may be sufficient to cause deformation or failure of critical components (e.g., frame-rail or suspension), which will affect subsequent kinematic behavior of the vehicle.

The tires of the tractor model are modeled using a single part constructed of isotropic thin shell elements with constant thickness representing all regions of the tire, including side wall and tread. The air pressure inside the tire is simulated using the simple airbag option in LS-Dyna and cannot accurately simulate proper tire response. This method of modeling tires has been shown to produce unrealistic deformation and response of the tire during impact [4].

The development of a computationally efficient tire model that incorporates the critical parts of a tire structure such as the bead coils, radial fibers, rubber sidewall, under-belt radial fibers, steel belt, and tire tread simulation is considered important to model accuracy, but was beyond the scope of work in this project. Therefore, the tire model in the enhanced vehicle model remains unchanged.

Detailed *Contact Survey

The tractor model has a fairly rudimentary contact definition. The current contact is defined mostly by self-contact of large parts sets. Initial simulations run with the current tractor model have shown instances of initial penetration between components. To better simulate overall tractor behavior, each component-to-component contact needs to be evaluated for appropriate friction coefficient, "node" or "surface" definition, effect of edge contact, and numerical stability. Since the number of contact definitions tends to decrease the scalability of the speed of the solution on multiple processors when running LS-DYNA, an effort will be made to limit the number of contact definitions while properly accounting for all contact between the various components of the model.

There are 5 contact cards defined in the enhanced model. A summary of the contact definitions are provided in table 18. There were no initial contact penetrations reported in the LS-Dyna message file.

Table 18. Summary of Contacts Defined in the Model.

Contact No.	Contact Type	Description
1	*contact_automatic_single_surface	Contact between all parts
2	*contact_automatic_general	Contact between all suspension parts
3	*contact_automatic_surface_to_surface	Contact between *suspension stop* rubber tip and frame-rail
4	*contact_automatic_surface_to_surface	Contact between *suspension stop* aluminum housing and frame-rail
5	*contact_automatic_surface_to_surface	Contact between front tires and components in the wheel housing

ASSESSMENT OF *ENHANCED-MODEL* PERFORMANCE – COMPARISON WITH FULL-SCALE CRASH TEST

The accuracy of the enhanced model was assessed by comparing simulation results to a full-scale crash test of a Freightliner FLD120 tractor impacting a 42-inch tall F-shape concrete barrier. The test (Test No. 03008) was conducted by the NCAC at the FOIL in McLean, Virginia on August 28, 2003[5].

The impact speed of the tractor was 31.25 mph (50.3 km/hr) at an impact angle of 25 degrees. The purpose of the test was to collect data to be used for validation of the NCAC FE model of the tractor. The tractor was instrumented with 18 accelerometers and a rate gyro, as well as three redundant accelerometers and a redundant rate gyro at the center of gravity of the vehicle. The placement of the instrumentation is illustrated in figure 30 taken from the test setup report.

The barrier was composed of seven segments of 12-ft (3.658 m) long concrete F-shape barriers. The barrier segments were staked to the ground with five 1-1/4 inch diameter steel rods equally spaced at 2-ft intervals. The ground surface material was not reported, but communication with NCAC staff confirmed it to be soil. In order to minimize deflection of the barrier during impact, two rows of concrete barriers were placed behind the first and a soil backfill was added for additional support (figure 31).

The test vehicle was a 1992 Freightliner FLD120 tractor with a curb mass of 16,852 lb (7,644 kg). The test inertial mass was 14,683 lb (6,660 kg) with the addition of test instrumentation and the removal of several nonstructural components, including: hood, sleeper, stairs, mud flaps, exhaust, seats, battery box, batteries, fluids, gear shift, and other miscellaneous components.

Figure 31 shows the initial impact point of the test vehicle, which was approximately 36 inches downstream of the joint between barrier segments 2 and 3.

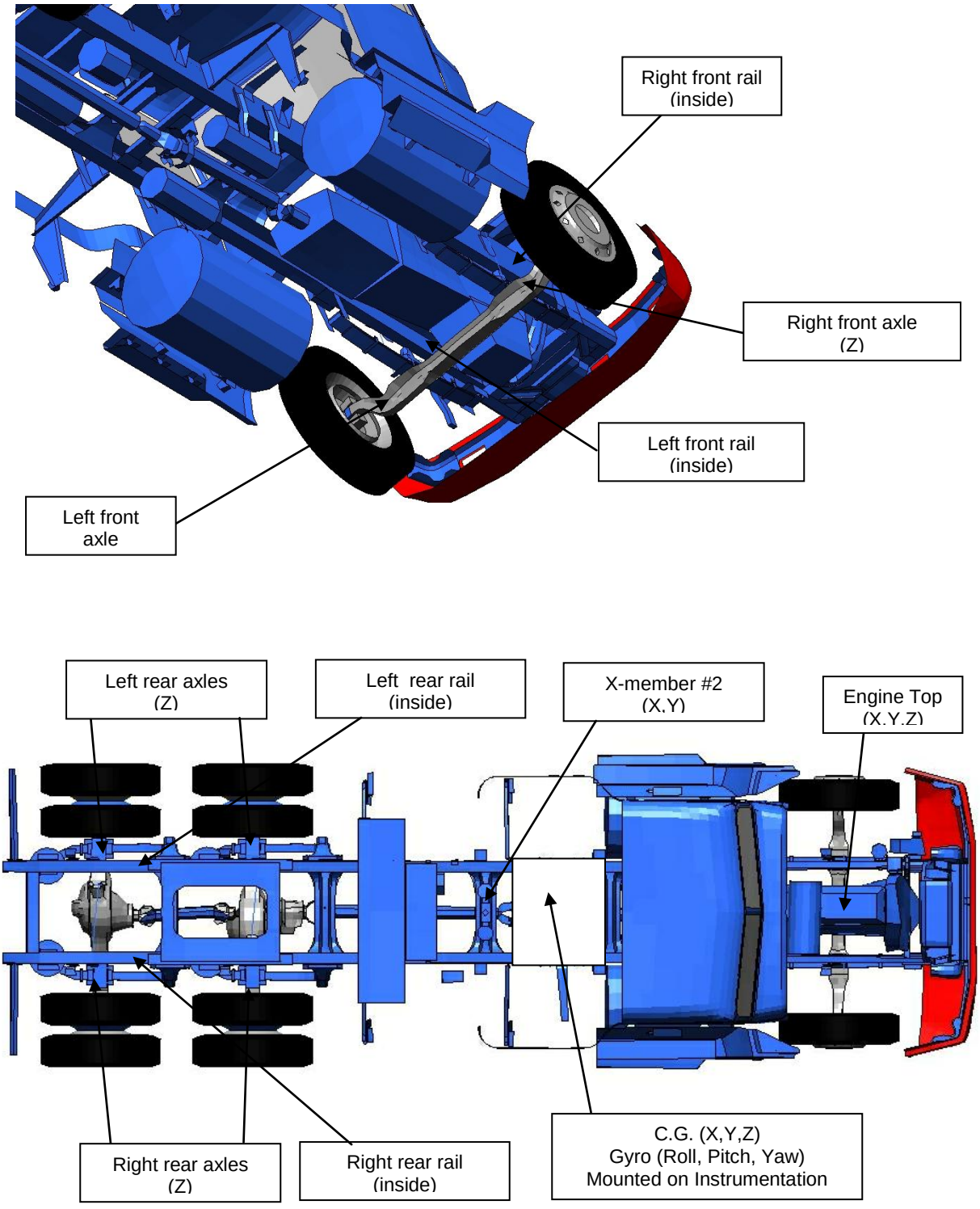

Figure 30. Illustration. Schematic of Tractor Test Vehicle used in FOIL Test 03008 Identifying Locations of Accelerometer Instrumentation [2].

Figure 31. Photograph. Photos of Test Vehicle and Barrier used in FOIL Test No. 03008 [2].

Finite Element Simulation using Enhanced Tractor Model

An FE simulation of FOIL Test No. 03008 was conducted using the *enhanced tractor model* (version 07-1226b). The tractor model was slightly modified for this simulation by removing the exhaust and a section of the sleeper. There were many other components removed from the test vehicle that were not removed from the FE model for this simulation. A significant effort would be required to modify the tractor model to correspond exactly to the modifications made to the test vehicle. It was considered premature to make those modifications at the time of this analysis because ORNL was still in the process of correcting the inertial properties.

The FE model was based on a tractor with an integral cabin and sleeper, as shown in figure 32(a). This sleeper/cabin is connected to the truck frame at six locations: two at the front of the cabin, two just behind the seats, and two at the back of the sleeper compared to only four constraints connecting the cabin to the frame on the test vehicle. These connections are modeled using nodal rigid body constraints. As a result of these connections, the stiffness of the cabin (which is basically a steel box) adds significantly to the overall stiffness of the tractor and, consequently, its kinematic response. The removal of the sleeper from the model was therefore considered to be of significant influence to the response of the tractor during impact and was removed accordingly, as shown in figure 32(b).

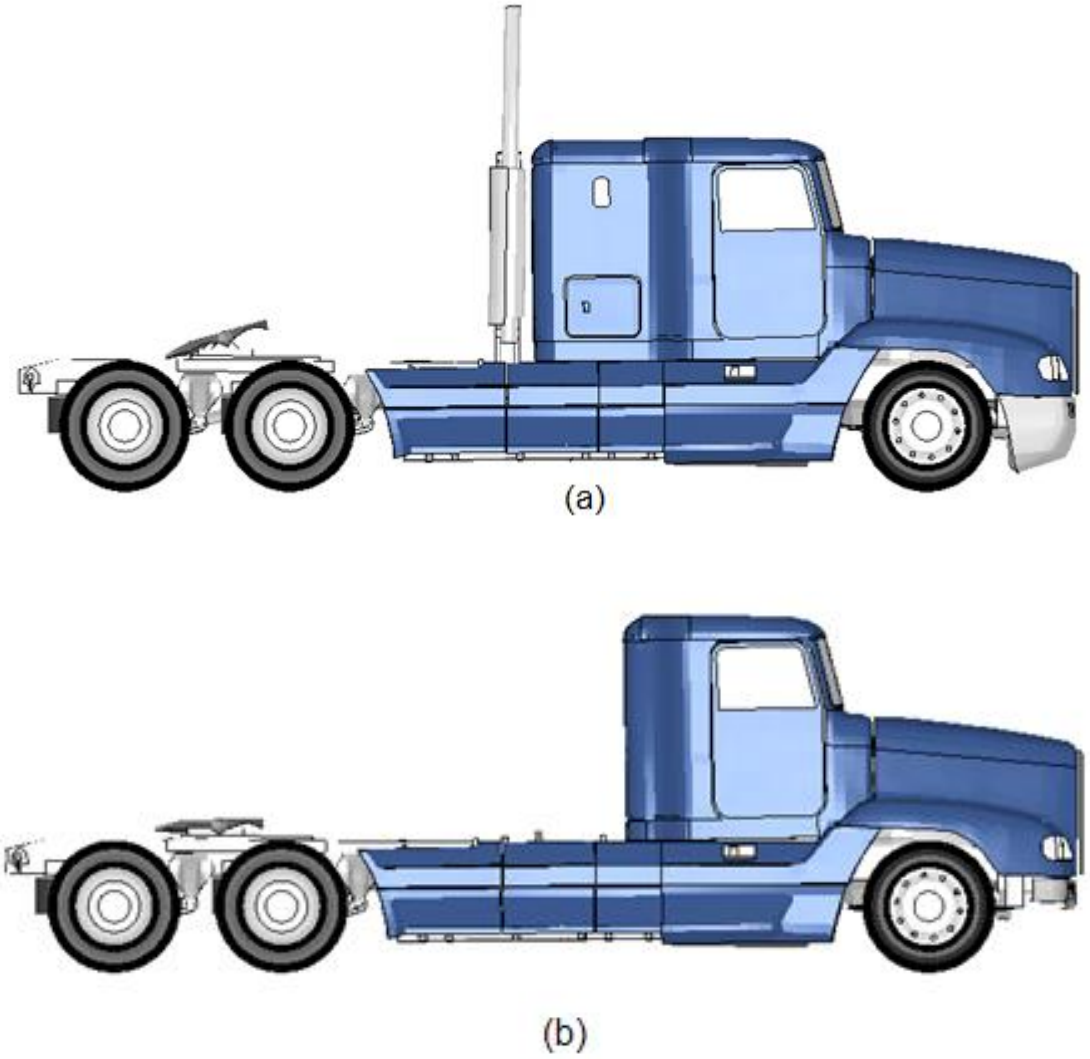

Figure 32. Illustration. (a) FE Model of Freightliner FLD120 tractor (b) Modified FE Model of Tractor with Exhaust and Section of Sleeper Removed.

Table 19 shows a summary of the wheel loads from the FE model compared with the curb mass and the test inertial mass measured on the test vehicle. Although the total mass of the enhanced model compares very well with that of the physical vehicle, the mass of the modified model used in the simulation was 10.5% too heavy compared to the test inertial mass of the physical vehicle.

The center of gravity of the test vehicle was 2,354 mm in the longitudinal direction and 1,019 mm in the lateral direction measured relative to the front, left wheel hub. The center of gravity of the FE model was 2,541 mm and 1,142.8 mm in the longitudinal and lateral directions, respectively.

Table 19. Wheel Loads Measured on a Freightliner FLD120 Tractor Vehicle Compared to those Measured in the Finite Element Model.

Position	Physical Vehicle Curb Mass (kg)[1]	Enhanced FE Model Inertial Mass (kg)	Difference / %Error	Physical Vehicle Test Inertial Mass (kg)[1]	Modified FE Model Inertial Mass (kg)	Difference / %Error
Left Front	2,176	2,015	-161 kg / 7.4%	1,914	~1890	-24 kg / 1.3%
Right Front	2,220	2,063	-320 kg / 7.1%	1,830	~1890	-60 kg / 3.3%
Left-Middle Rear	920	~1820	+110 kg / 6.4%	654	~1696	+234 kg / 16.0%
Left-Rear	790			808		
Right-Middle Rear	488	~1820	+282 kg / 18.3%	604	~1696	+242 kg / 16.6%
Right Rear	1,050			850		
Total Mass	**7,644**	**7,718**	**+74 kg / 1.0%**	**6,660**	**7,373**	**-713 kg / 10.7%**

The impact conditions for the FE simulation were consistent with those reported in the full-scale crash test – e.g., 31.25 mph at an impact angle of 25 degrees. The friction between the tractor and barrier was set to 0.2 and the friction between the tires and the barrier was set to 0.8. The barrier model in the simulation consisted of seven 12-ft (3.658 m) long F-shape barrier segments with rigid material properties and rigid fixity to the ground. This was not an accurate characterization of the barrier based on the results from the full-scale test. For the full-scale test, efforts were made to make the barrier as 'rigid' as possible (refer to figure 31), but there was still significant movement of the barrier segments during impact as shown in figure 33. It was beyond the scope of this project to develop a valid model of the barrier which included the concrete safety shapes, their connections to each other, the soil foundation, the barrier stakes and their interaction with the ground, and the soil backfill.

The movement of the barrier during impact caused two things to happen: 1) reduced the impact force between the vehicle and barrier and 2) caused a slight separation between one of the barrier segments and its downstream neighbor, exposing the edge of the downstream barrier segment for the vehicle to snag on (refer to figure 33). To partially account for this latter phenomenon, the barrier segment immediately downstream of the initial impact point was offset 0.78 inches (20 mm) toward the traffic side to create a slight snag point for the vehicle model during the simulation.

Figure 33. Photograph. Top View of FOIL Test 03008 Illustrating Barrier Movement during Impact

A qualitative assessment was made by comparing sequential snapshots of the impact event from the results of the simulation and crash test to verify sequence and timing of key phenomenological events during impact. Acceleration and angular velocity-time history data was collected at the center of gravity of the tractor model and a qualitative assessment of simulation results was made based on comparison with test data. Occupant risk factors (i.e., occupant impact velocities, maximum ride-down accelerations, maximum 50-ms average accelerations, as well as vehicle roll, pitch, yaw displacements) were also calculated using the computer software, TRAP, with the acceleration and angular-time history data collected in the analysis as input. A summary of these data are provided in table 20.

Figures 34, 35, and 36 show sequential snapshots of the impact event at specific times comparing the results of the simulation to the full-scale test from a downstream viewpoint, overhead viewpoint, and side viewpoint, respectively. The hood and fenders were removed from view in the FE model in figure 35 to better compare the simulation to the test.

Note: The camera speed was reported as 500 fps in the test setup report, but from reviewing the videos and comparing them to the roll, pitch, and yaw time-history data it appears that the camera speed was approximately 800 fps. Since the test video did not include a time stamp, figures 34, 35, and 36 show the position of the tractor in the test based on a camera speed of 800 fps.

Table 20. Comparison of Performance Measures from FEA Predictions and Full-scale Test (measurements taken over the first 1.0 second of impact).

	Test	FE Simulation
Vehicle Information		
Make and Model	1992 Freightliner FLD120	Modified FE tractor model
Total Mass	6,660 kg	7,373 kg
Mass Distribution		
Front axle	3,744 kg	3,981 kg
Rear tandem	2,916 kg	3,392 kg
C.G. longitudinal	2.35 m	2.54 m
Impact Conditions		
Speed (km/h)	50.3	50.3
Angle (deg)	25	25
Occupant Risk Values		
Impact Velocity (m/s)		
x-direction	3.7	3.4
y-direction	2.1	2.9
Max Ridedown Acceleration g's)		
x-direction	-1.7	-4.2
y-direction	-3.9	-6.2
Max 50-ms Average Acceleration		
x-direction	-3.4	-4.2
y-direction	-4.0	-5.7
European Com. for Standardization (CEN) Values		
THIV (km/hr)	15.3	14.8
PHD (g's)	9.9	34.0
ASI	0.54	0.69
Post Impact Vehicle Behavior (deg)		
Max. roll angle	7.6	10.0
Max. pitch angle	3.6	3.6
Max. yaw angle	-28.5	-29.3

Time = 0.170 seconds

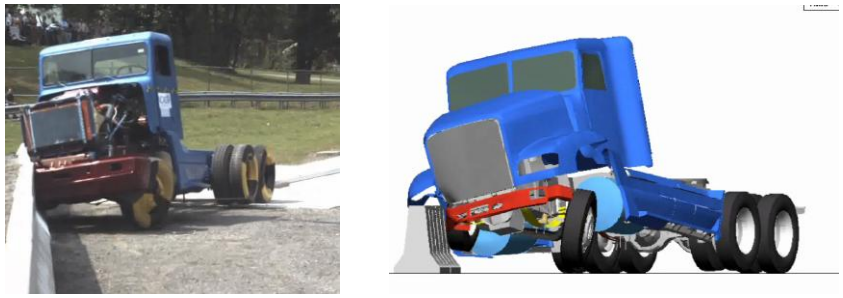

Time = 0.370 seconds

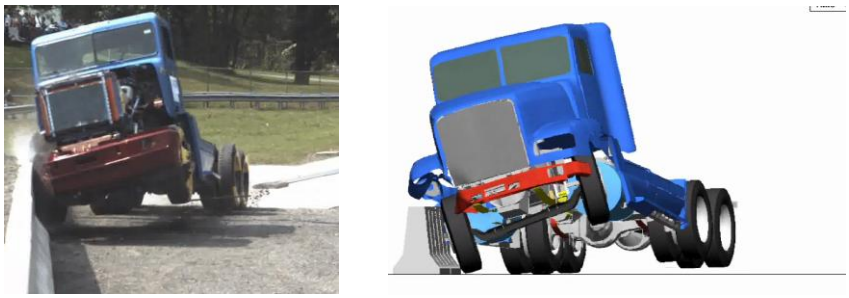

Time = 0.670 seconds

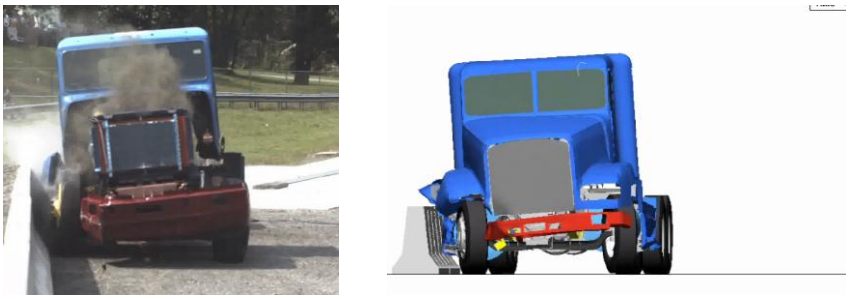

Time = 0.750 seconds

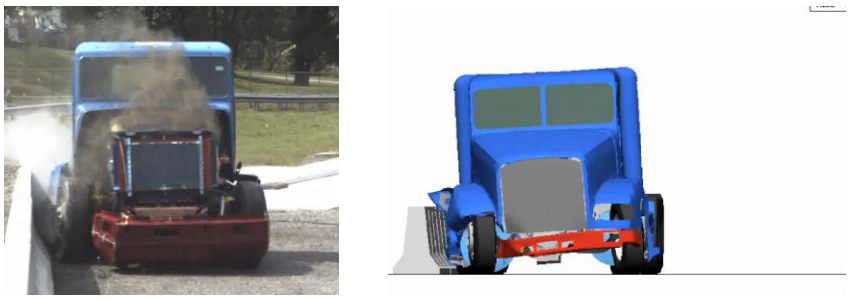

Figure 34. Photograph / Illustration. Sequential Views of FOIL Test No. 03008 and FE Simulation from a Downstream View Point.

Time = 0.170 seconds

Time = 0.370 seconds

Time = 0.670 seconds

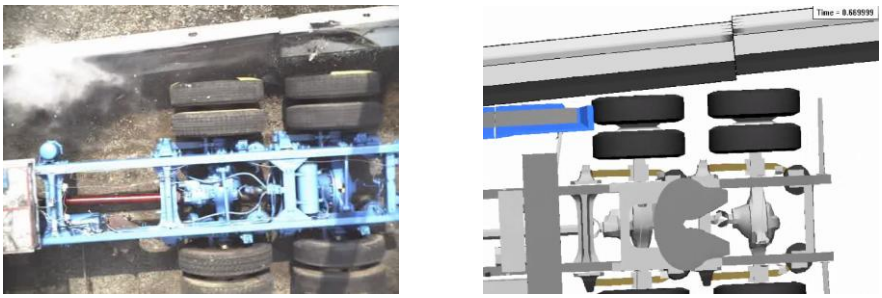

Time = 0.750 seconds

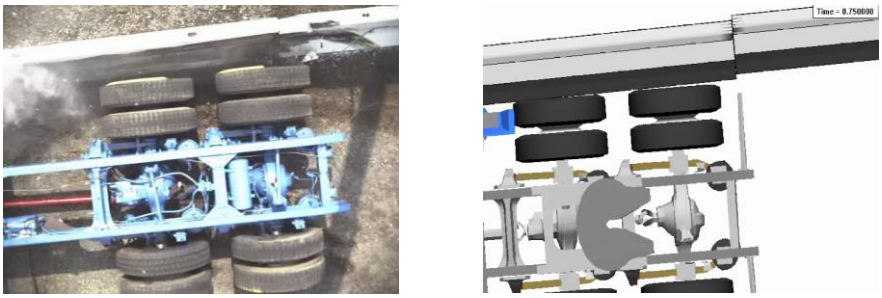

Figure 35. Photograph / Illustration. Sequential Views of FOIL Test No. 03008 and FE Simulation from an Overhead View Point.

Time = 0.170 seconds

Time = 0.370 seconds

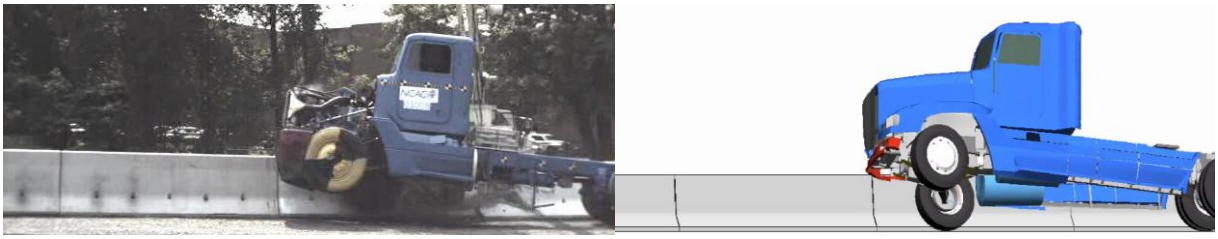

Time = 0.670 seconds

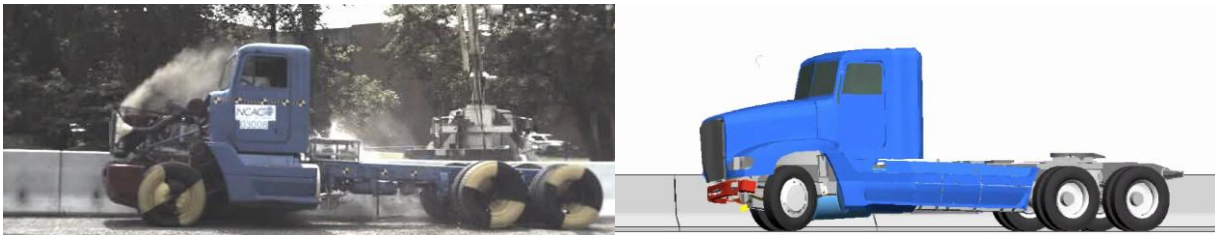

Time = 0.750 seconds

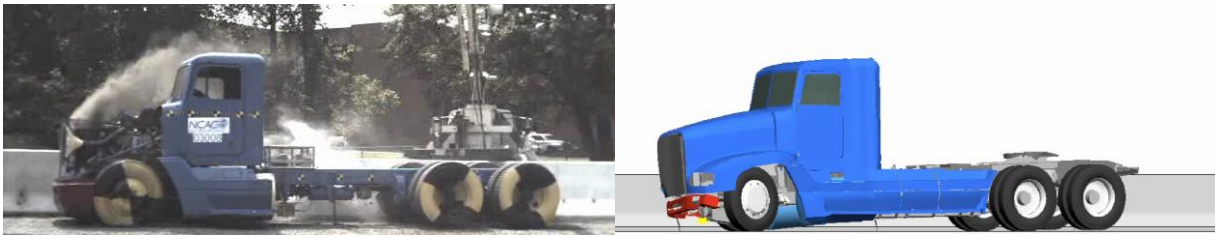

Figure 36. Photograph / Illustration. Sequential Views of FOIL Test No. 03008 and FE Simulation from a Side View Point.

Figure 37 shows the longitudinal acceleration time history at the center of gravity of the tractor measured in the full-scale test and computed in the simulation. Figures 38, 39 and 40 show the roll, pitch and yaw angular displacements, respectively, measured at the truck center of gravity for the crash test and simulation.

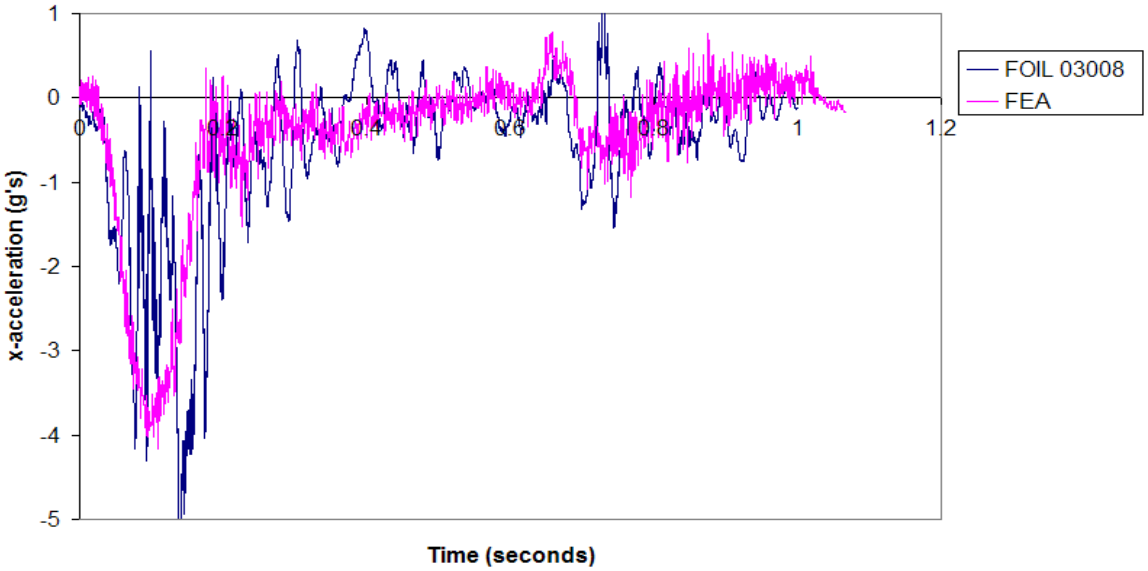

Figure 37. Chart. Longitudinal Acceleration Measured at the Center of Gravity of the Tractor for Test and REA.

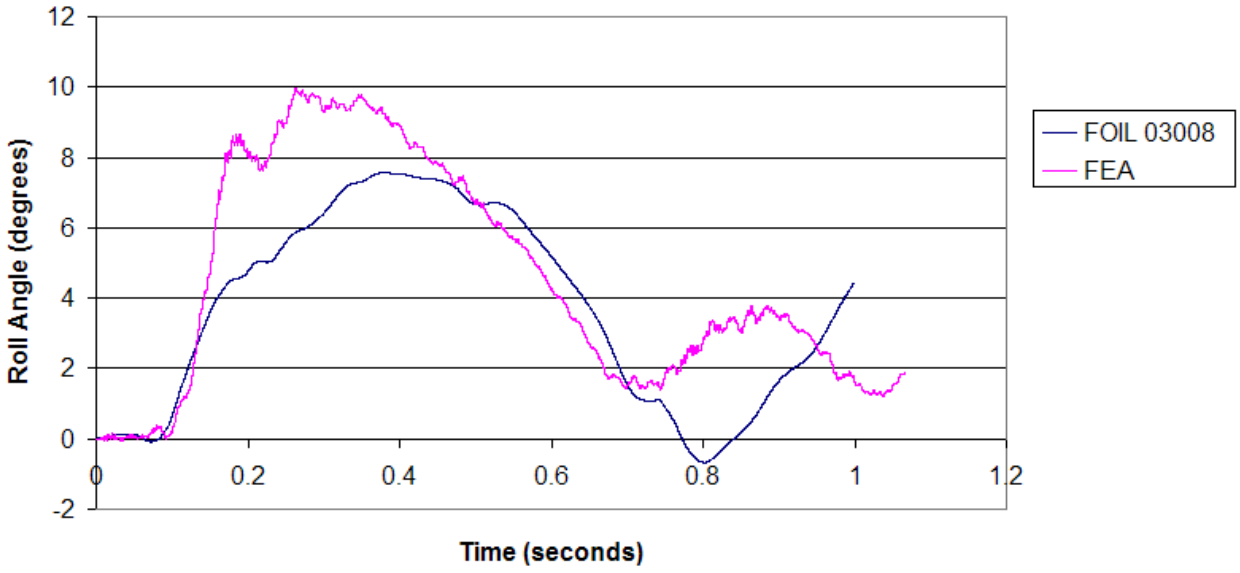

Figure 38. Chart. Roll Angle Measured at the Center of Gravity of the Tractor for Test and FEA.

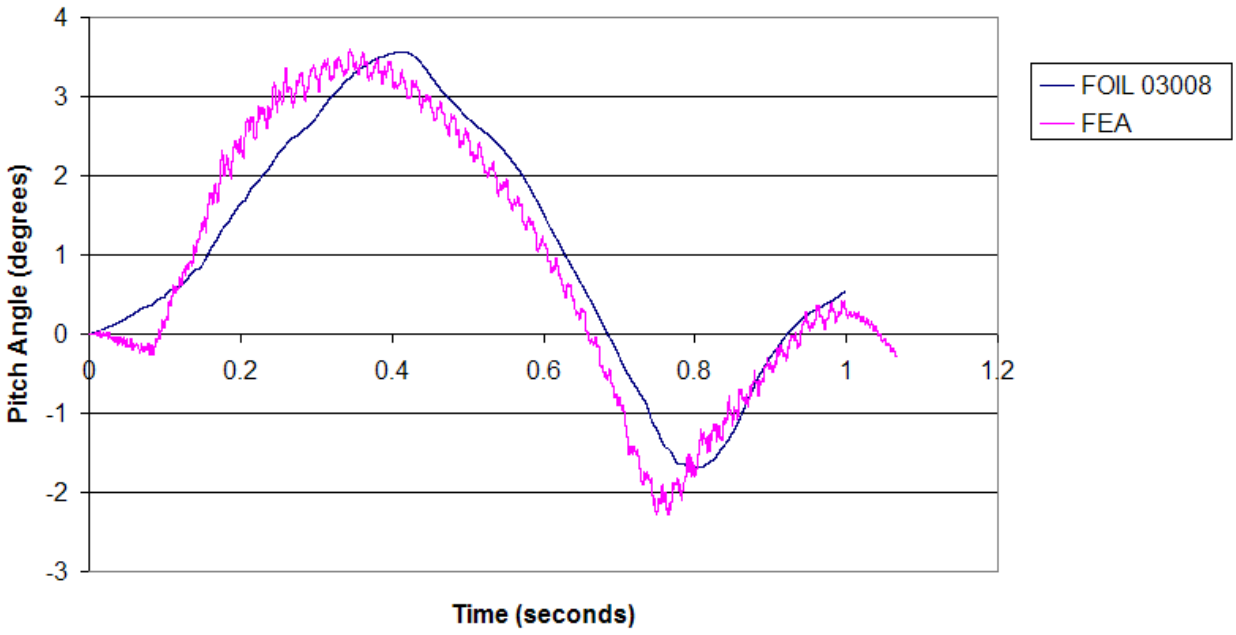

Figure 39. Chart. Pitch Angle Measured at the Center of Gravity of the Tractor for Test and FEA.

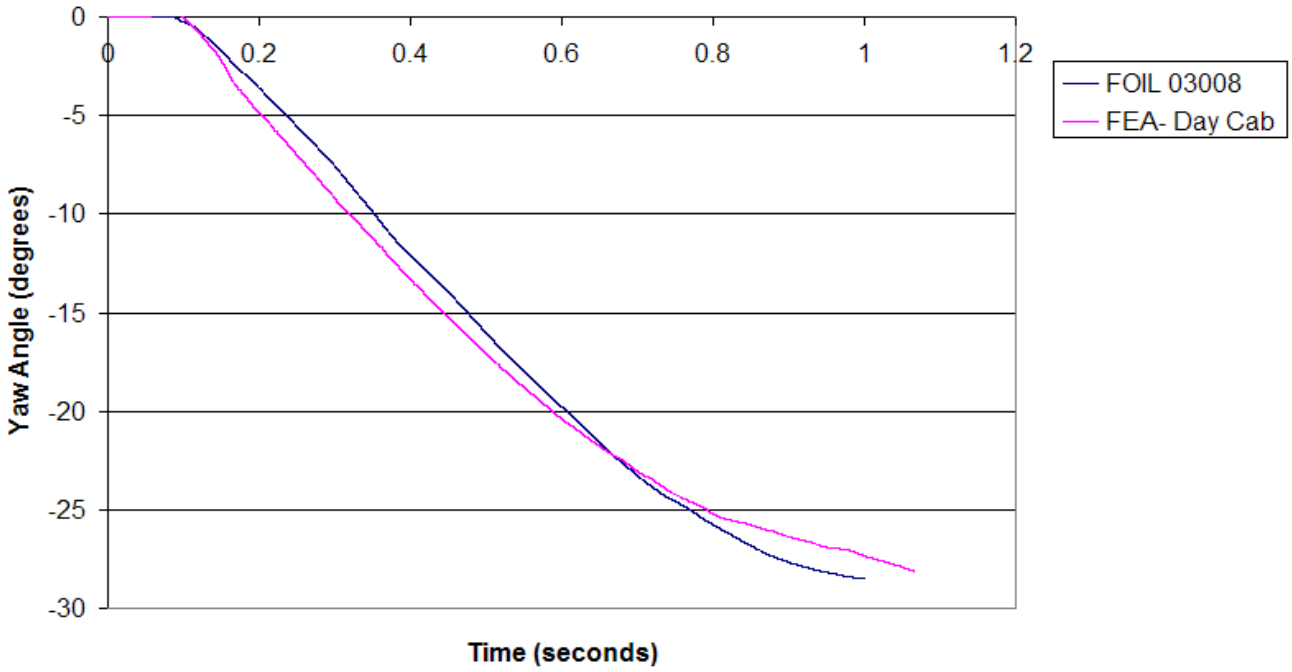

Figure 40. Chart. Yaw Angle Measured at the Center of Gravity of the Tractor for Test and FEA.

Discussion of Simulation and Test Results

As discussed in the previous chapter, the simulation model did not correspond exactly to the test setup. For example,

- The test vehicle was stripped of several components prior to the test which altered its mass and inertial properties. In the FE model, only the exhaust and a section of the sleeper were removed.
- The test barrier was not 'rigid' as it was intended; it experienced significant movement during impact. The barrier in the FE model was modeled as completely rigid with fixed constraints.

Even with these discrepancies, the simulation results corresponded very well to the test results based on a global response of the tractor. From the acceleration plots shown in figure 37 it can be seen that the vehicle experiences the highest accelerations between 0.1 and 0.2 seconds of the impact event. During this time range the maximum acceleration computed at the center of gravity of the tractor model was approximately 4 g's compared to approximately 5 g's in the full-scale test. After this time the accelerations drop to less than 1 g until approximately 0.67 seconds. This time corresponds to when the driver-side wheel impacts the ground and accelerations increase to slightly above 1 g in both the simulation and test.

From the sequential views of the impact event in figures 34, 35, and 36, the kinematics of the tractor model correspond very well to the test vehicle regarding both magnitude and timing of events. This is also verified in the angular-time history plots in figures 38, 39, and 40. The maximum roll angle of the tractor model measured at the tractor's center of gravity was higher in the simulation than the test (i.e., 10 degrees and 7.6 degrees respectively). This is hardly noticeable from the front view shown in figure 34, where the roll angle of the cabin is approximately 12.0 and 11.5 degrees for the simulation model and the test vehicle, respectively (roll angles measured directly from the figure).

The most notable discrepancy regarding the roll-time history occurs at approximately 0.75 seconds, as illustrated in the annotated plot in figure 41. At around 0.7 seconds the roll-time history curve is flat for a short period of time corresponding to when the *suspension stop* engages the frame rail on the driver side. When the *suspension stop* is engaged, the load on the tire increases. The tire model is very stiff in the simulation and the tractor model immediately begins to rebound at 0.75 seconds. In the test, the tire compresses (flattens) considerably after the *suspension stop* has been engaged resulting in continued negative roll rate of the tractor until it starts to rebound at 0.8 seconds.

Figure 41. Chart. Roll Angle Measured at the Center of Gravity of the Tractor Showing Annotations from the Tire of the Test Vehicle.

The deformations of the tractor during impact were isolated to the front, impact side of the vehicle in both the simulation and test. The FE model showed significant damage to some non-structural members such as the "steps" and fuel tank, which were not present on the test vehicle. There was no noticeable damage to the frame rail in either the simulation or the test. The primary transfer of forces between the barrier and the vehicle appear to go through the front bumper and wheel assembly (figure 42) and it is these components that receive the majority of damage in the test and simulation. The response of the wheel assembly, in particular, has a significant affect on the kinematic behavior of the vehicle.

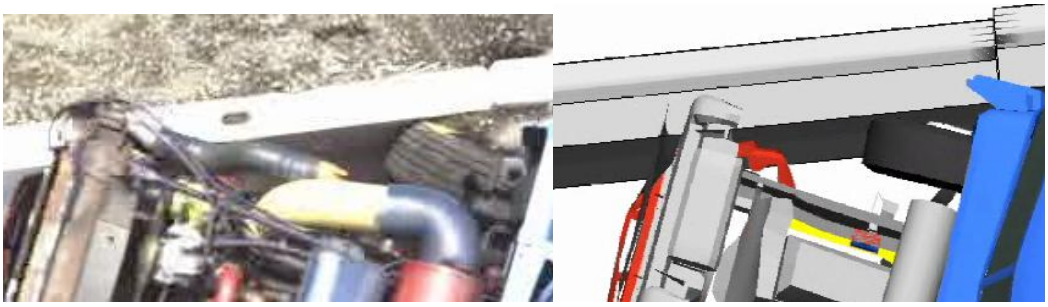

Figure 42. Photograph / Illustration. Snapshot of Test and Simulation Illustrating Primary Load Path between Barrier and Vehicle is through the Bumper and Wheel.

Suspension Damage

The damage to the suspension in the full-scale test was limited to the fracture of the top leaf spring at the pinned connection at the front mounting bracket on the impact side and the fracture of one U-bolt on the non-impact side, as shown in figure 43. In the FE simulation, the top leaf spring on the impact side and the front U-bolt fractured at approximately 0.21 seconds. Although one of the U-bolts failed, the connection of the suspension to the axle remained intact until the second U-bolt fractured at 0.8 seconds, as shown in figure 45. The fracture of the second U-bolt coincided with the suspension being fully compressed during tire interaction with the ground after the vehicle had redirected from the barrier (refer to figures 34, 35, and 36).

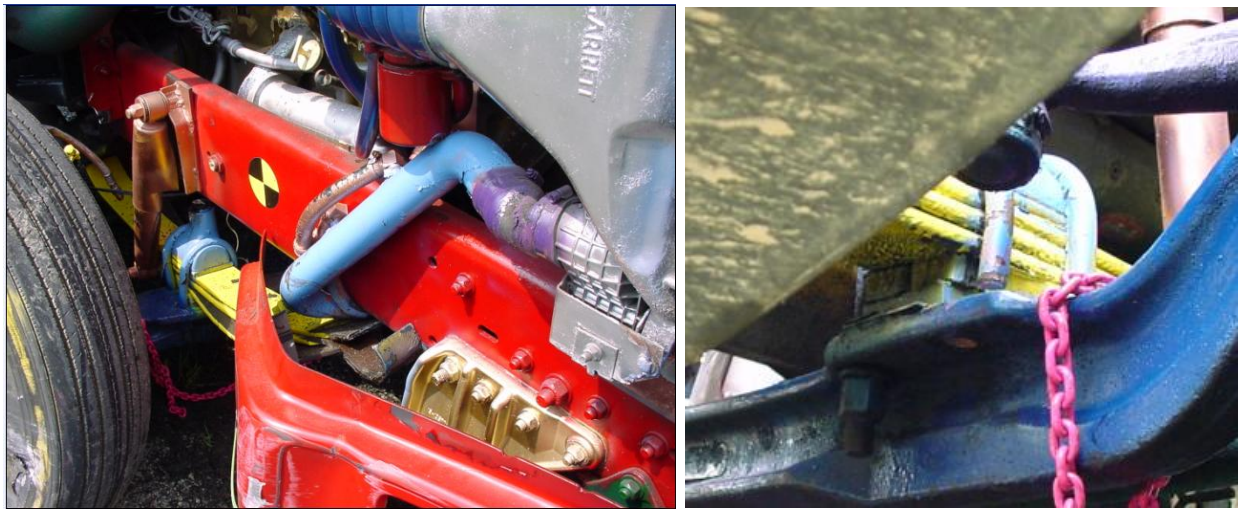

Figure 43. Photograph. Post Test Photos Showing Damage to Suspension Components .

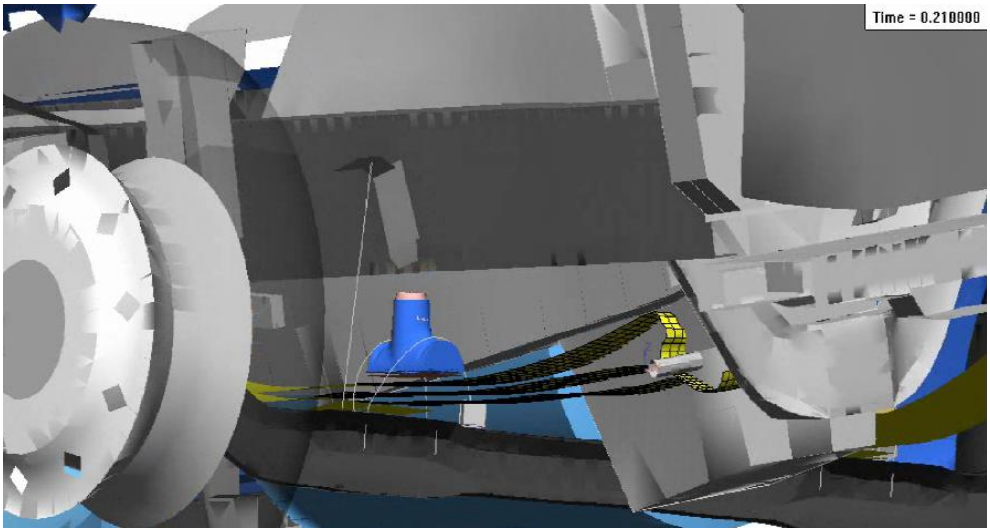

Figure 44. Illustration. Results of FEA Showing Fracture of Leaf Spring and Front U-bolt During Analysis.

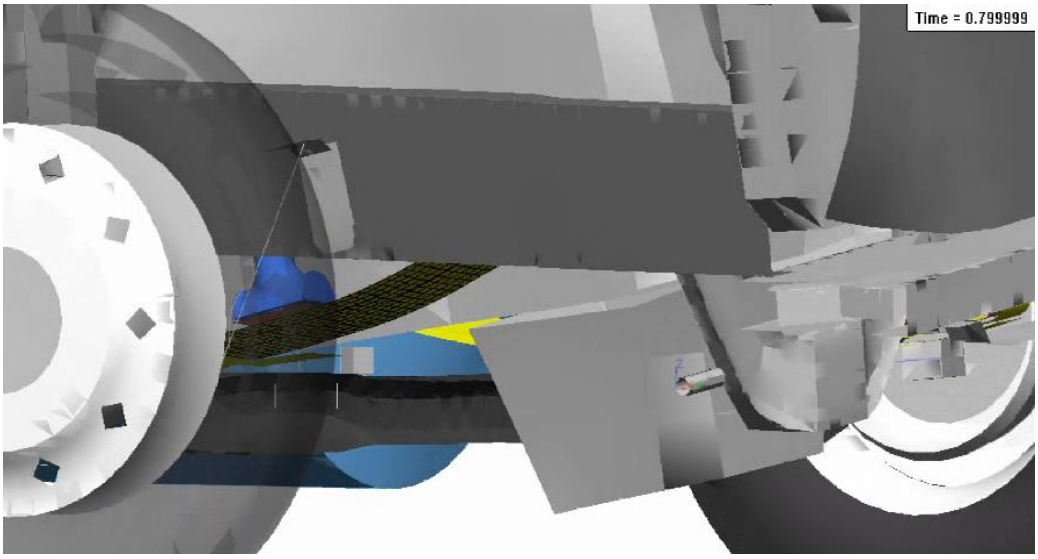

Figure 45. Illustration. Results of FEA Showing Fracture of Failure of Second U-bolt During Analysis.

Summary of *Enhanced-Model* Performance Assessment

The accuracy of the enhanced model was assessed by comparing simulation results to a full-scale crash test of a Freightliner FLD120 tractor impacting a 42-inch tall F-shape concrete barrier. The impact speed of the tractor was 31.25 mph (50.3 km/hr) at an impact angle of 25 degrees. The barrier was composed of seven segments of 12-ft (3.658 m) long concrete F-shape barriers. In order to minimize deflection of the barrier during impact, the barrier was staked to the ground with five 1-1/4 inch diameter steel rods equally spaced at 2-ft intervals and an additional two rows of concrete barriers were placed behind the first and a soil backfill was added.

The FE tractor model geometry and inertial properties did not match exactly to those in the full-scale test. The test vehicle was stripped of several components prior to the test which altered its mass and inertial properties, whereas, only the exhaust and a section of the sleeper were removed in the FE model. The model of the barrier was also idealized to be rigid, whereas, test barrier experienced significant movement during impact.

Even with these discrepancies, the FE model was able to effectively capture all the important phenomenological events during the impact related to vehicle kinematics. For a more direct comparison, all the components removed from the test vehicle will need to be removed from the model and a more accurate representation of the barrier will need to be modeled.

TRAILER MODEL

The tractor model did not include a trailer. The ultimate usefulness of the tractor FE model, particularly for simulating NCHRP Report 350 Test Level 5 impacts, obviously depends upon the capability to simulate the entire tractor-trailer vehicle. Development of the tractor FE model was started before the trailer FE model because the tractor is much more complex.

Trailer Model Development

Some very preliminary work was done at NCAC on creating a FE model of a trailer. Figure 46 shows an overall view of this trailer model. After a quick survey of this FE model and taking some measurements, it was determined that this trailer model was not representative of trailers used in TL-5 tests nor was it representative of typical trailers seen in service. The NCHRP Report 350 specifies that the overall length of the tractor-trailer not exceed 50 ft (15.24 m), the maximum overhang of the trailer not exceed 86.6 inches (2.2 m), the cargo bed height must fall within 50-54 inches (1.27 – 1.37 m), and the center of gravity must fall within 70.9-74.8 inches (1.8 – 1.9 m). Figure 47 shows some dimensions on overall views of a typical over-the-road trailer that was used in a full-scale crash test conducted at MwRSF compared with the initial trailer model [6]. Note that the basic dimensions of this trailer model do not agree with those of the trailer used in the full-scale test. Also, many structural components were missing and no element thicknesses or material properties were provided.

Based on the fact that the initial trailer model was far from complete and that its geometry did not correspond to that of typical trailers, a decision was made to create a new trailer model. It was determined that creating a new FE model of a trailer from 'scratch' would require no more effort than would be required to modify the original trailer model to make it more representative of typical trailers – especially if the CAD geometry could be obtained for a new trailer model.

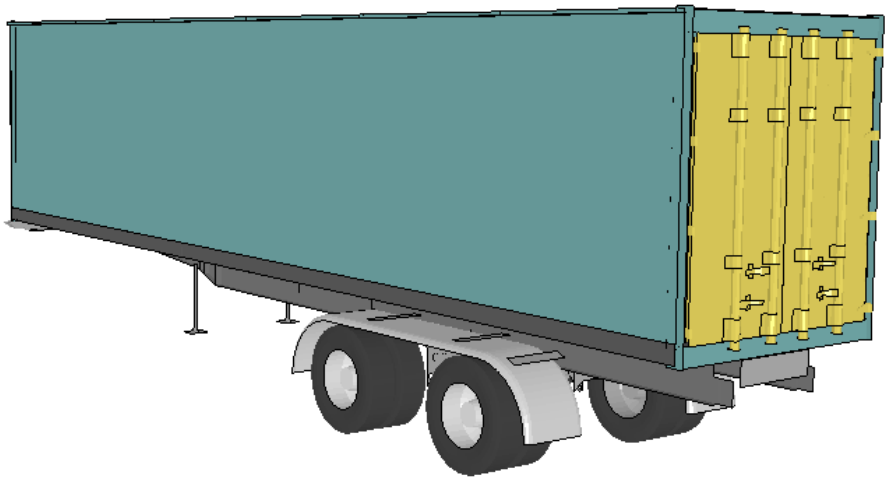

Figure 46. Illustration. Early Version Trailer Model.

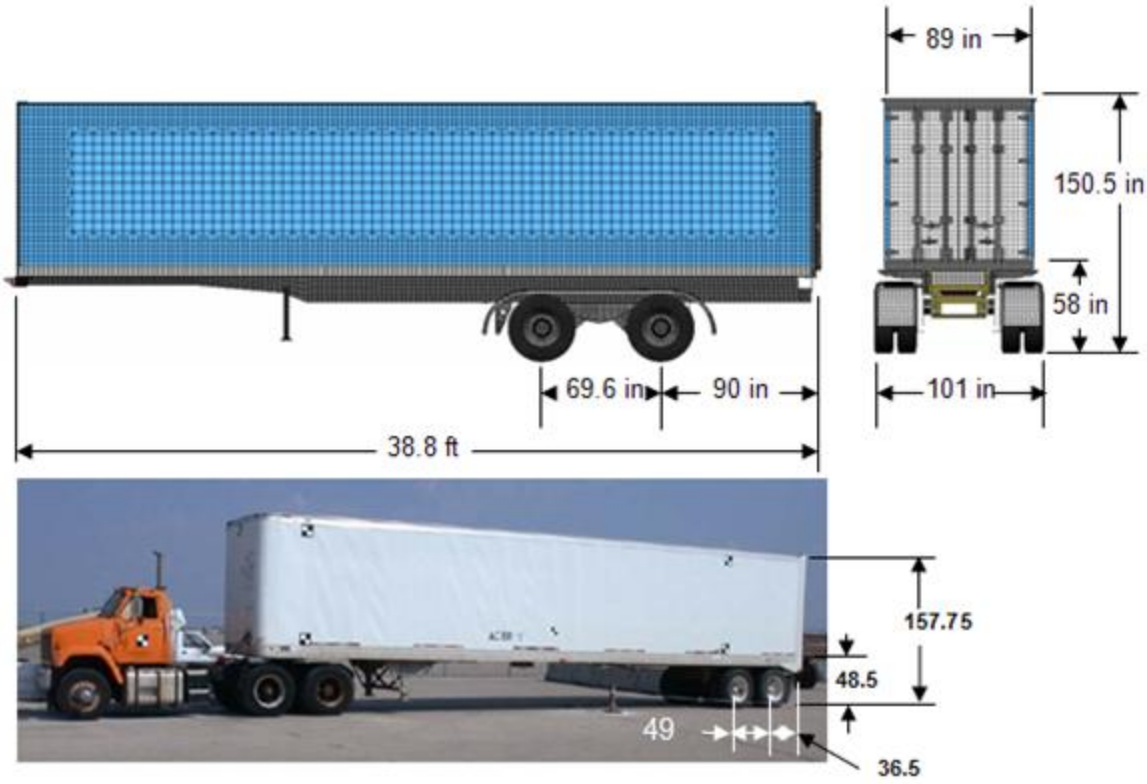

Figure 47. Illustration. Overall View of Initial Trailer Model and Typical Over-the-Road Trailer.

There are several companies that offer CAD geometry of a variety of vehicles, aircraft, people, animals, etc., primarily for the film and animation industry. After a brief web-search, Research team staff contacted one such company – Digimation, Inc. in St. Rose, Louisiana (www.digimation.com). Digimation had several CAD models of semi-tractor-trailers "in-stock", but none of those met our specific requirements, namely:

- More detail in the bogey/suspension/wheels area
- Less detail elsewhere
- All major components defined as separate parts.

Digimation was willing to create a "custom" CAD model of a 50' semi-trailer for us that met our requirements at an attractive price.

Creating this semi-trailer CAD geometry model was a collaborative effort between the Research team and Digimation. Before Digimation started work on the CAD geometry model, Research team staff visited the local Freightliner dealer and surveyed a 53' Stoughton trailer that they had on their lot. Research team staff took photographs and measurements which were ultimately provided to Digimation to help them more accurately create the structural details in the model. Research team staff created a large portion of the geometry of the main bogey frame rails and cross-channels directly from measurements and sketches. The tires and wheels were copied from the tractor rear wheel set.

Digimation delivered the completed trailer CAD model in STEP format which was directly readable by the HyperMesh® FE meshing package. Digimation's CAD geometry was merged with the parts that Research team created. This provided an excellent starting point for meshing the FE model of the trailer. Figure 48 shows an overall view of the CAD geometry as-received from Digimation.

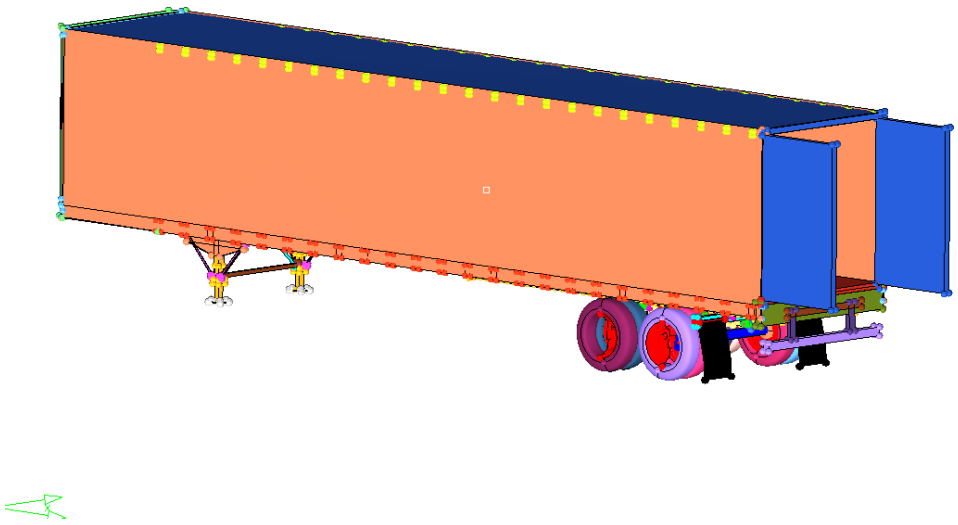

Figure 48. Illustration. Trailer CAD Geometry Model from Digimation, Inc.

The trailer FE model should reflect a "typical/generic" semi-trailer. To get an idea as to the basic design of a typical semi-trailer, Research team staff visited a two local Columbus companies. One – as mentioned previously – was FYDA Freightliner who specializes in semi-tractor sales, parts, and service, but has numerous trailers on their lot. The other company that was visited was National Semi Trailer who specializes in trailer rental and leasing. At both these companies Research team staff measured, photographed, and observed Great Dane and Stoughton trailers. Figure 49 shows a 53' Stoughton trailer at FYDA Freightliner. Figures 50 and 51 show the undercarriages of a typical Stoughton and Great Dane trailer.

Figure 49. Photograph. Stoughton 53' Trailer at FYDA Freightliner Dealer.

Figure 50. Photograph. Undercarriage of Stoughton Trailer.

Figure 51. Photograph. Undercarriage of Stoughton Trailer.

In general, for current semi-trailers there are more similarities than differences. The trailers observed had the following general characteristics:

- Mostly Air-Ride suspensions
- Moveable bogey (wheelset fore-aft adjustment)
- 53-foot length very common
- Wooden flooring and sides
- Lateral I-beams under wooden flooring
- Two parallel longitudinal Z-channels under lateral beams
- Two large C-channels - sliding connection to Z-channels.

During these visits, component thicknesses were directly measured in areas that were accessible. Beam and channel dimensions were directly measured in areas that were accessible. In areas that were not accessible or would require disassembly, thicknesses and dimension were estimated.

The FE model was made with (mostly) hexahedral solid and quadrilateral shell elements using HyperMesh®. The procedure was generally to auto-mesh the CAD geometry as much as possible, and "hand-mesh" certain areas that required additional geometric detail or features that were not accounted for in the CAD geometry. Contacts, connections, joints, etc. were mostly done "manually" also. An effort was made to create the part-to-part connections that were joined/welded/bolted by using "common-nodes" directly or by using constrained nodal rigid bodies rather than simply specifying "tied" contact wherever possible because tied contact is more computationally expensive and less reliable.

The trailer model currently has 74 parts, 9 materials, 115,371 nodes, 103,962 deformable elements (37,337 elastic, 61,685 elastic-plastic), 3,500 rigid elements, and 1,440 nodal rigid bodies and connectors. Figure 52 shows an overall view of the Trailer FE Model. Figure 53 shows a detailed view of the undercarriage of the trailer FE Model.

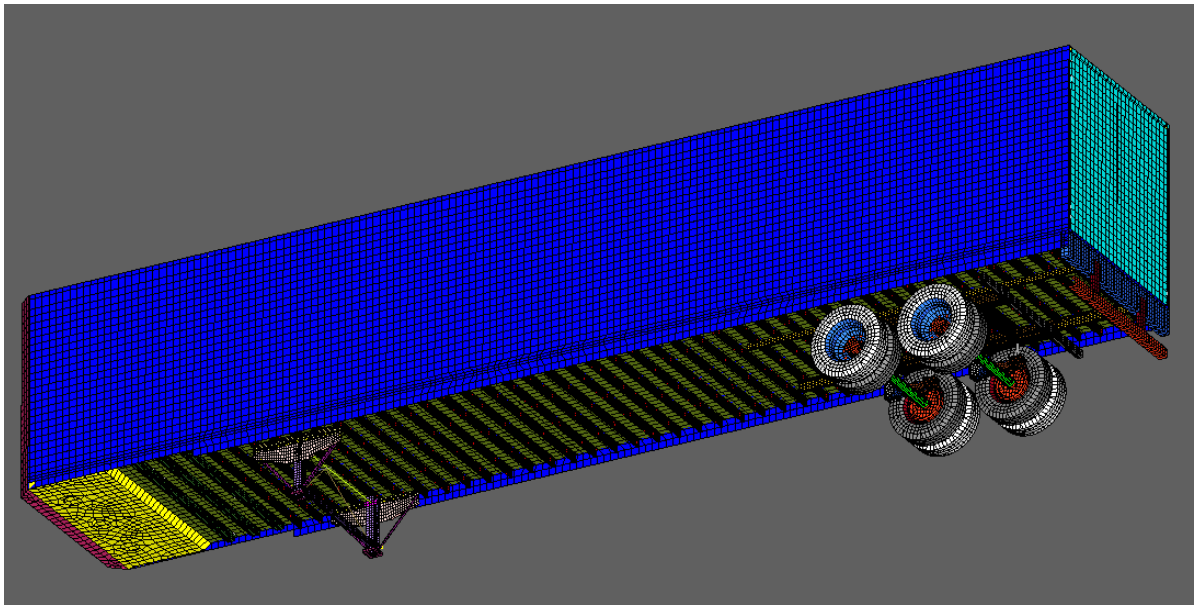

Figure 52. Illustration. Overall View of Trailer FE Model.

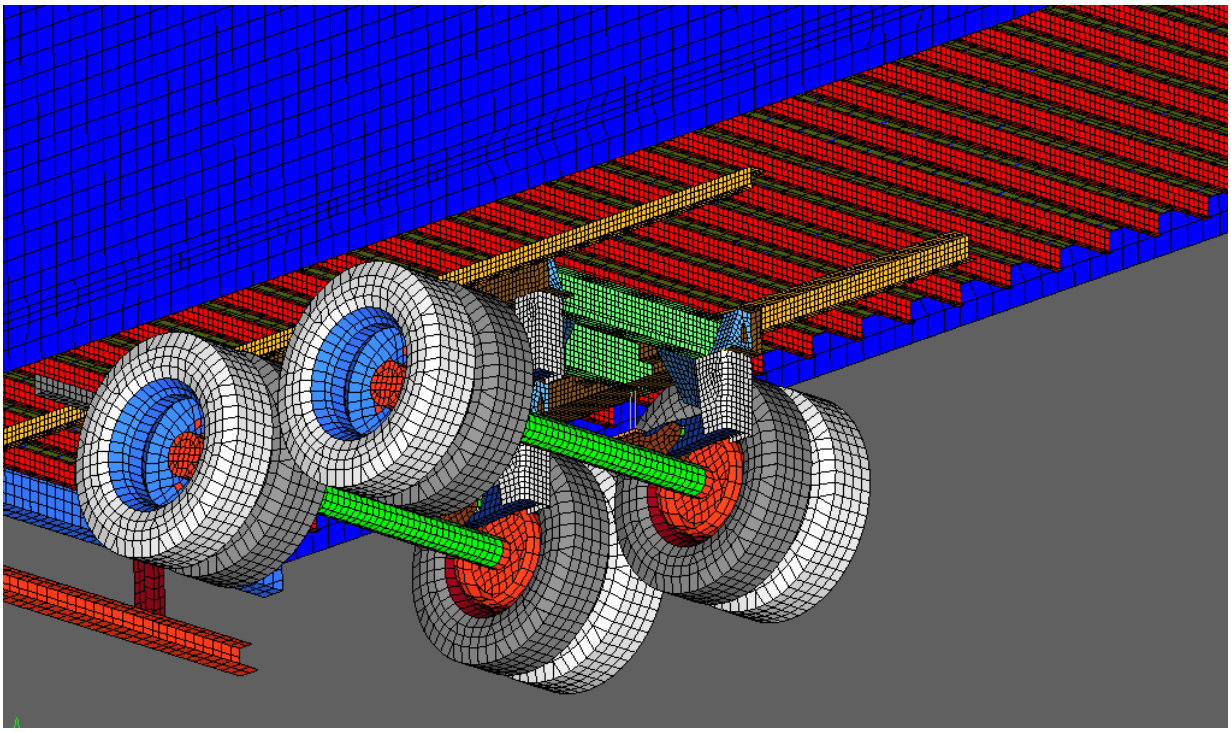

Figure 53. Illustration. Detail View of the Undercarriage of the Trailer FE Model.

Trailer Ballast

The trailer ballast was modeled based on pictures and data from MwRSF test report no. TRP-03-194-07 [7]. Figure 54 shows a photograph from MwRSF's test report looking in from the rear doors. It appears that the ballast (F-Shape concrete barriers) nearly fill the entire cargo area. It also appears that the ballast is cushioned on compliant material – probably so that the ballast itself will not add stiffness to the trailer.

The ballast in the FE model of the trailer is represented by 18 (3 x 6) coarsely-meshed blocks of elastic material of relatively low modulus, shown in figure 55. The blocks are in contact with one-another and in contact with the trailer floor and walls. The blocks are connected to the side walls with relatively low-stiffness springs.

The weight of the ballast can be changed by the user by changing the density of the material. For these initial analyses the density was set such that the weight of the ballast is 49,767 lb (22,575 kg). The center of gravity of the ballast is located at 72.5 in (1,842 mm) in the vertical direction based on data from MwRSF test report no. TRP-03-194-07.

Figure 54. Photograph. Photograph from MwRSF's Test Report Looking in from the Rear Doors.

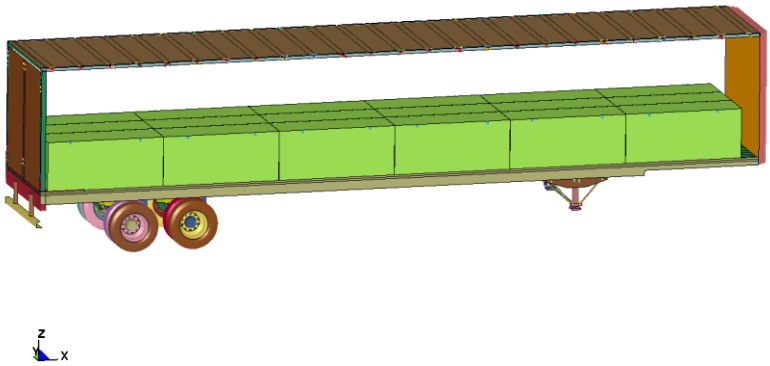

Figure 55. Illustration. FE Trailer Model (sides removed from view) Showing Ballast Model.

Tractor to Trailer Connection

The trailer model was connected to the tractor model in such a way as to simulate the kinematics of the real tractor-trailer interface. The tractor fifth-wheel/receiver was modified such that it could rotate in the pitch degree of freedom. The kingpin on the front of the trailer was connected to the fifth-wheel on the tractor via a spherical joint. Figure 56 shows the combined tractor-trailer model and figure 57 shows a more detail view of the fifth-wheel connection.

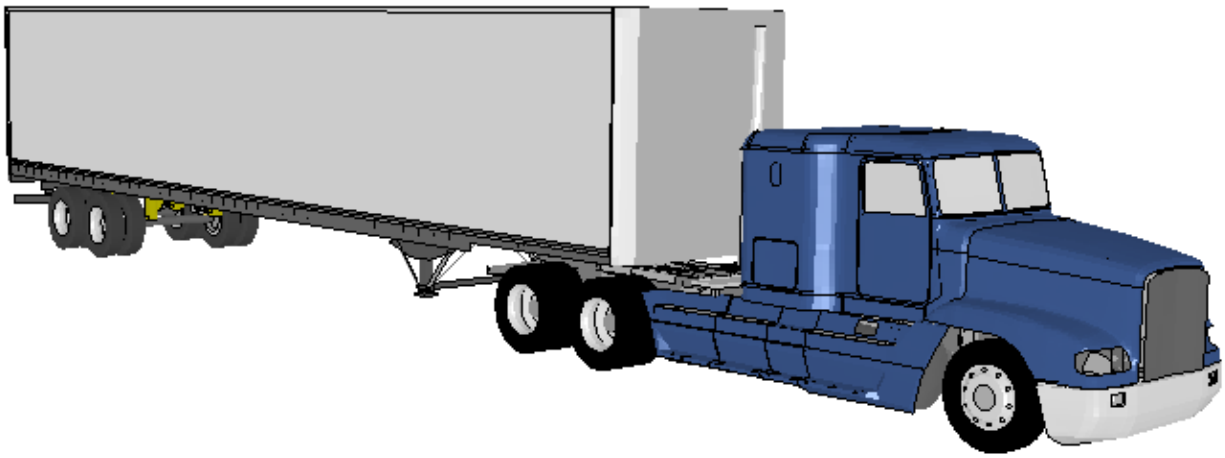

Figure 56. Illustration. Isometric View of Combined Tractor-Trailer Model.

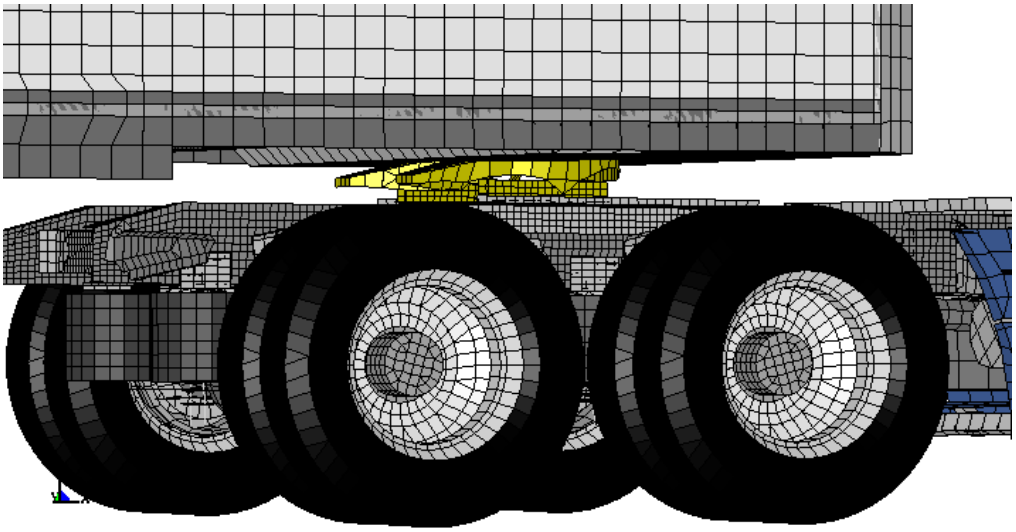

Figure 57. Illustration. Close-up view of Fifth-Wheel and Connection of Tractor to Trailer.

Initial Assessment of Tractor-Trailer Model

The combined tractor-trailer model was run to assess the basic functionality of the model. A recent full scale crash test that was run by MwRSF[7] was chosen for this initial point of comparison for the tractor-trailer model. Figure 58 shows an overall view of the tractor-trailer FE model with MwRSF's TL-5 Vertical Faced Concrete Median Barrier. A new concrete barrier FE model was created based this barrier for the simulation.

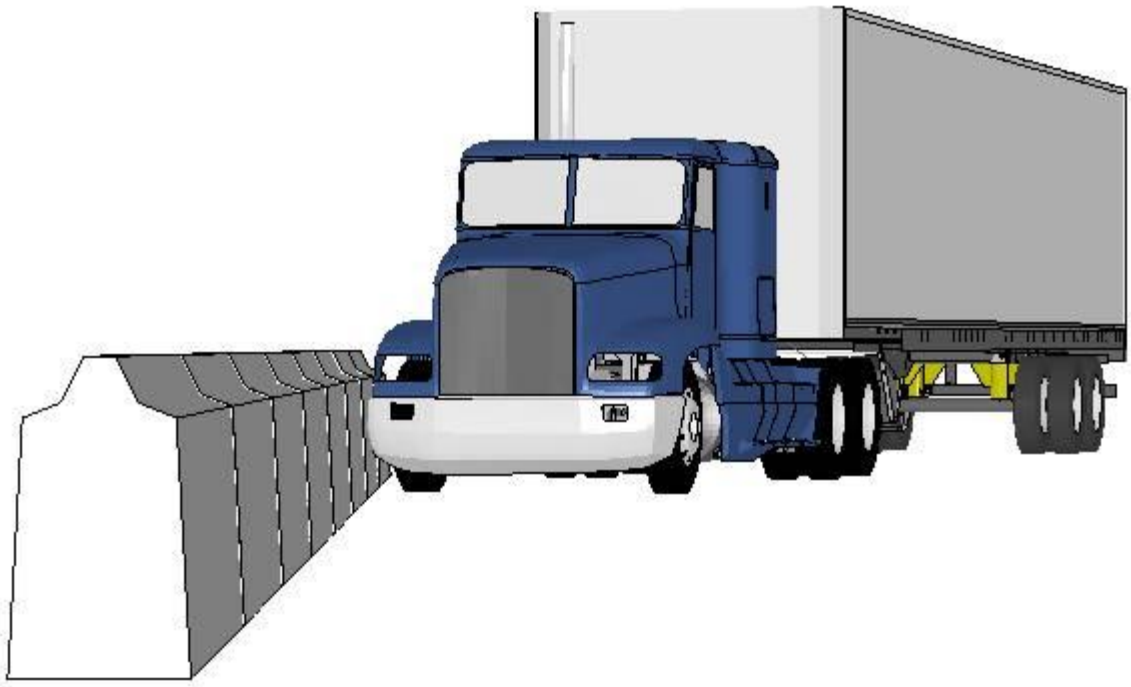

Figure 58. Illustration. Overall View of Tractor-Trailer FE Model with MwRSF TL-5 Vertical-Face Concrete Barrier.

The simulation was set up as a TL-5-12 test; 49.7 mph (80 km/hr) vehicle velocity at a 15° impact angle. The tractor-trailer FE model ran without terminating with a run-time error, and functioned as-expected in terms of tractor-trailer connectivity and vehicle to barrier contact. No detailed comparison of simulation-to-test physical parameters or other evaluation of model fidelity was done. A more in-depth comparison of the tractor-trailer model to this crash test is anticipated for the next phase of the Effort, Phase B.

SUMMARY AND ASSESSMENT

An FE model of a tractor-trailer developed by the NCAC has been evaluated and necessary modifications have been made to the model to enhance its fidelity. This model was created for the purpose of simulating tractor-trailer crash events with particular emphasis on those crash events involving roadside safety hardware (e.g., bridge rails, median barriers, etc.). This report has documented the modifications that were made to the FE models by Battelle in Phase A of the project and provided discussion of the validity of the enhanced model. The evaluation and correction of material properties and inertial properties of the tractor were carried out by ORNL and are documented in Chapter 4 of this report. Chapter 4 also documents the development of the web-based User's Manual.

The accuracy of the enhanced tractor FE model (version 07-1226b) was assessed by comparing simulation results to a full-scale crash test of a Freightliner FLD120 tractor impacting a 42-inch tall F-shape concrete barrier. This test was conducted at the FOIL under the auspices of the NCAC. It was selected for use in this assessment of the FE model because it was the only test that has been conducted that involved a tractor without a trailer impacting a barrier at an oblique angle.

The tractor vehicle used in the full-scale test did not exactly match the tractor that the FE model was based on. Further, the test vehicle was significantly modified prior to the test including removal of several parts. Only the exhaust stack and a section of the sleeper in the FE model were removed for the simulation to partially account for some of the differences. The model of the barrier was also idealized to be rigid, whereas the test barrier experienced some lateral displacement during impact.

Even with these discrepancies, the FE model was able to effectively capture all the important phenomenological events during the impact related to vehicle kinematics. For a more direct comparison, all the components removed from the test vehicle will need to be removed from the model and a more accurate representation of the barrier will need to be modeled. Once the additional modifications by ORNL have been implemented, the model will be modified to correspond as closely as possible to the test vehicle. The analysis will be rerun with those modifications in Phase B. Development of a valid barrier model, however, is out of scope of this project and any influence of this discrepancy will have to be considered in the assessment of the tractor model's accuracy.

The development of a semi-trailer was accomplished during Phase A of this project. The original semi-trailer model developed by NCAC was determined to be inappropriate for use in simulations of NCHRP Report 350 Test Level 5 (TL-5) crash tests, based on comparison of the model's geometry with the requirements specified in Report 350 and with semi-trailers used in

previous TL-5 crash tests. The original trailer model was far from complete so a decision was made to create the new trailer model.

The new trailer model was developed based primarily on the geometry of a 53-ft Stoughton trailer. The CAD geometry was obtained through a collaborative effort between Research team and Digimation. Research team staff visited a local Freightliner dealer and surveyed the trailers on their lot. Photographs and measurements were taken and provided to Digimation for use in developing the CAD geometry. This geometry was then used by the Research team to develop the FE mesh of the semi-trailer.

CHAPTER 4. TRACTOR-TRAILER MATERIAL AND INERTIAL PROPERTIES EVALUATION

The objective of the conducted research was to evaluate the performance and accuracy of the FE model for a tractor-trailer vehicle developed by the National Crash Analysis Center at the George Washington University. The models were developed with the objective to conduct computational simulations of safety barrier performance primarily for the impact scenarios as described in National Cooperative Highway Research Program (NCHRP) Report 350[8]. Recent examples of similar work can be found for example in references [9-11]. The original tractor-trailer model consisted of separate models of the tractor and the trailer. The file names were Tractor_V01b.key (figure 59) and Trailer_V00c.key (figure 60) for the tractor and trailer, respectively. The combined tractor-trailer model is shown in figure 61.

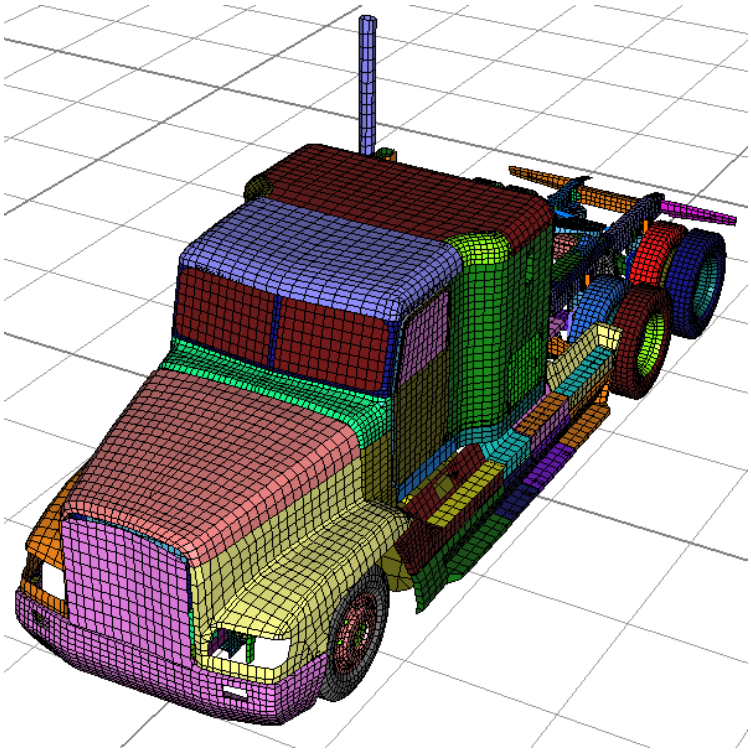

Figure 59. Illustration. Trailer FE Model (Tractor_V01b.key).

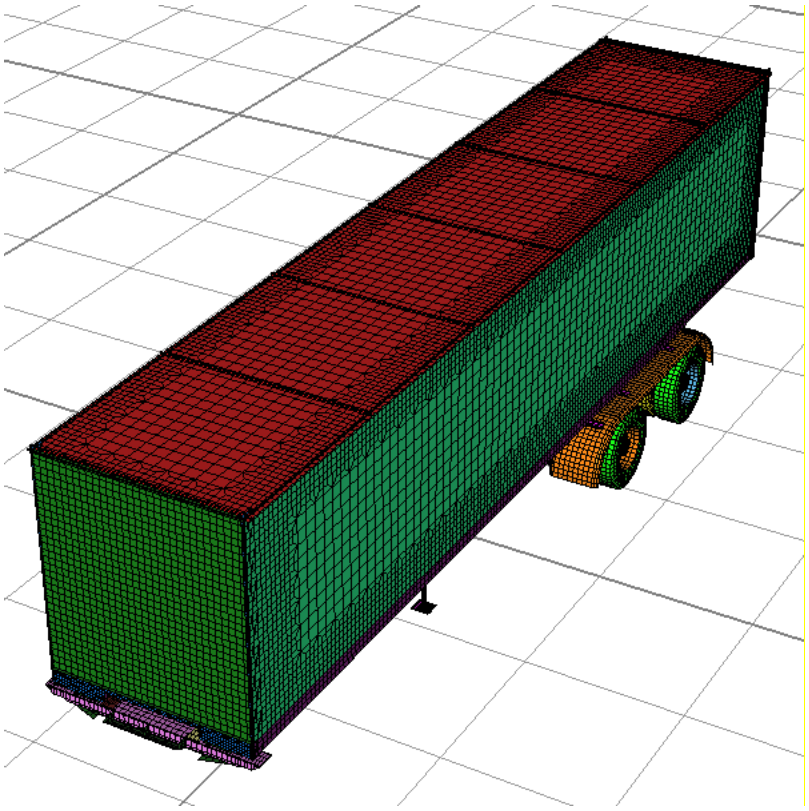

Figure 60. Illustration. Trailer FE Model (Trailer_V00c.key).

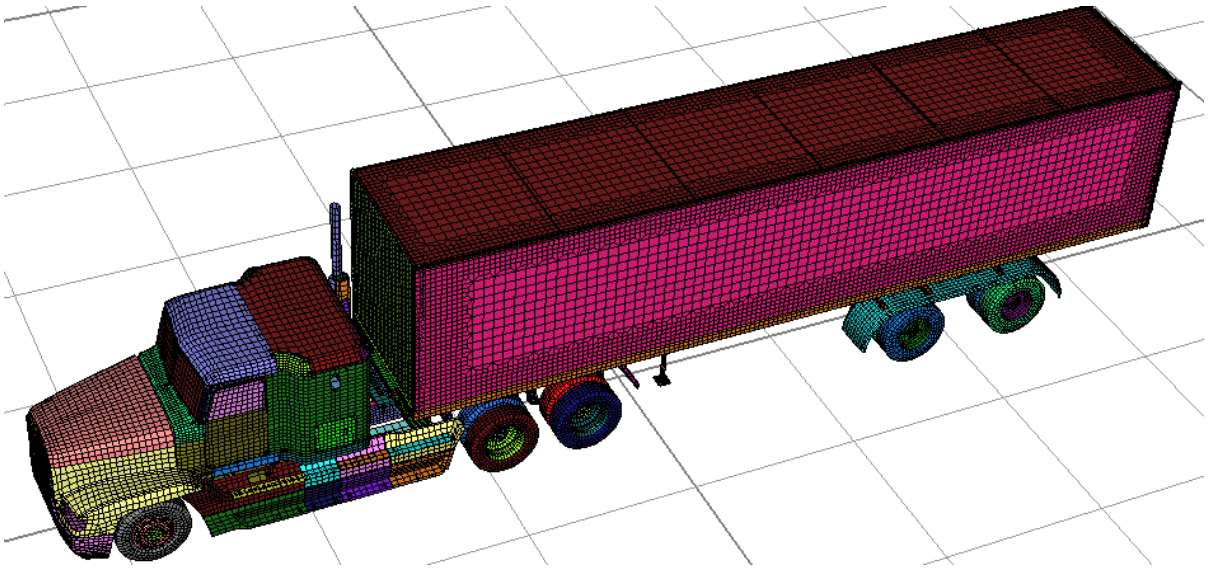

Figure 61. Illustration. Combined FE Tractor-Trailer Model.

Of the two models, the tractor model was advanced enough that it could be used for crash simulation and pass the baseline computational simulations. The trailer model, however, contained essentially FE discretized geometry, but without structural integrity and kinematics necessary for viable simulations. The tractor model had more deficiencies than initially anticipated when the original project plan was developed and, therefore, the original scope of work for the project was modified to concentrate initially on the tractor model.

ANALYSIS OF THE TRACTOR MODEL

The tractor model can be assessed from two perspectives. The first addresses the FE approaches and techniques used in the model and their fidelity with respect to the modeled objects. The original purpose of the model was to be used as a bullet object with its target as the primary object of interest. As such, many components of the vehicle were originally simplified so that their models would provide sufficiently accurate impact forces on the barrier but not necessarily replicate the deformation in the tractor. However, the availability of the model begets new applications, and, together with the drive for a better accuracy on ever-faster computers, it was necessary to update the model so that it can meet these requirements. From the second perspective, we evaluated the model's ability to simulate impact tests conducted for evaluation of various roadside safety barriers using similar vehicles. The available tests were documented in references [12-19]. These tests were used to evaluate the capability of various roadside barriers to contain and deflect heavy tractor-trailer trucks. The tests were conducted using different vehicle brands, models and trailers. While general performance similarities in the class of tractor vehicles are expected, direct comparisons of the tractor FE model performance with tractor-trailer tests cannot be reasonably done without a reasonably capable trailer FE model. Therefore, tractor FE model modifications and performance evaluations were based on the test conducted by NCAC [20] during the original model evaluation. The setup of the test is shown in figure 62.

Figure 62. Photograph. Test configuration for test in Ref. 20.

The vehicle make and model used in the FE development and test was a Freightliner FLD120 dual tandem tractor with a wheelbase of 5516 mm, which is longer than the maximum

recommended value in Reference 1. The test vehicle had several components removed, most notably the hood, sleeper, stairs, exhaust, seats, battery box, batteries, and the gearshift.

The two main areas for improvement in the tractor model were found to be: (a) suspension, and (b) material properties and masses. Both directly affect the overall kinematics performance of the vehicle. Matching the overall kinematics of the vehicle with the model is the baseline requirement, and where the original model had serious deficiencies. The suspension model modifications were performed by the Battelle researchers and reported in Chapter 3 of this report. The material model modifications and inertial properties were performed by the ORNL and are reported in the following chapters. .

Material Assignments in the Original Tractor Model

In the original model, each part had its own material model. For a model that has 361 parts, that results in 361 material models. Such an approach makes model maintenance and modification rather cumbersome, especially since there are just a few different materials in the model. The material models with permanent deformation capabilities (elasto-plastic), and therefore capable of absorbing crash energy are shown in figure 63.

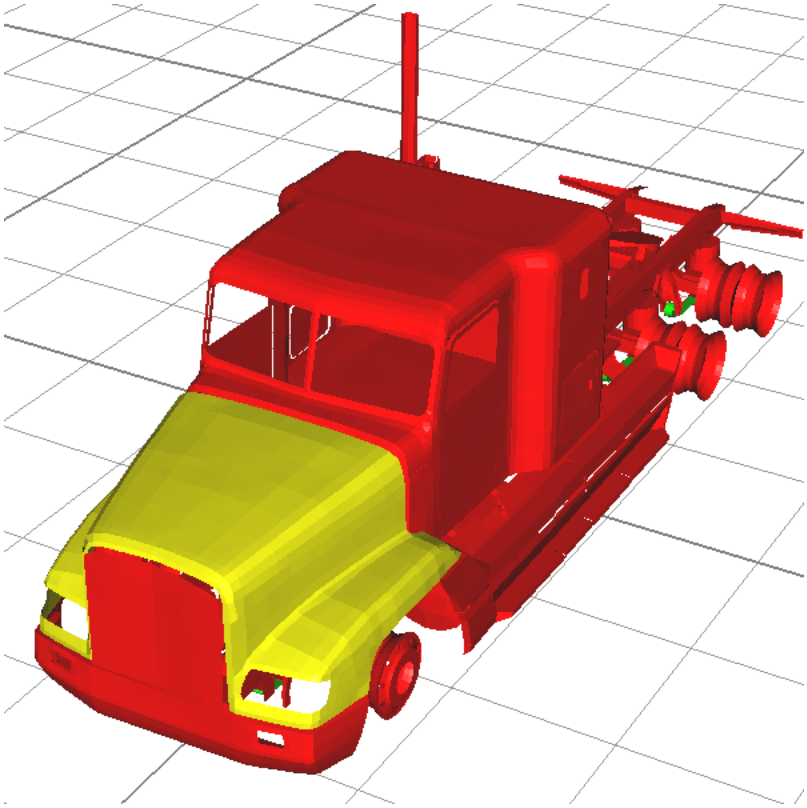

Figure 63. Illustration. Elasto-plastic materials in the original model.

The material models for elasto-plastic materials are implemented using LS-DYNA model *MAT_PIECEWISE_LINEAR_PLASTICITY which describes flow stress in material as a function of permanent (plastic) strain. The 297 separately defined elasto-plastic materials in the

original tractor model use one of three piecewise linear flow stress-strain curves shown in figure 64.

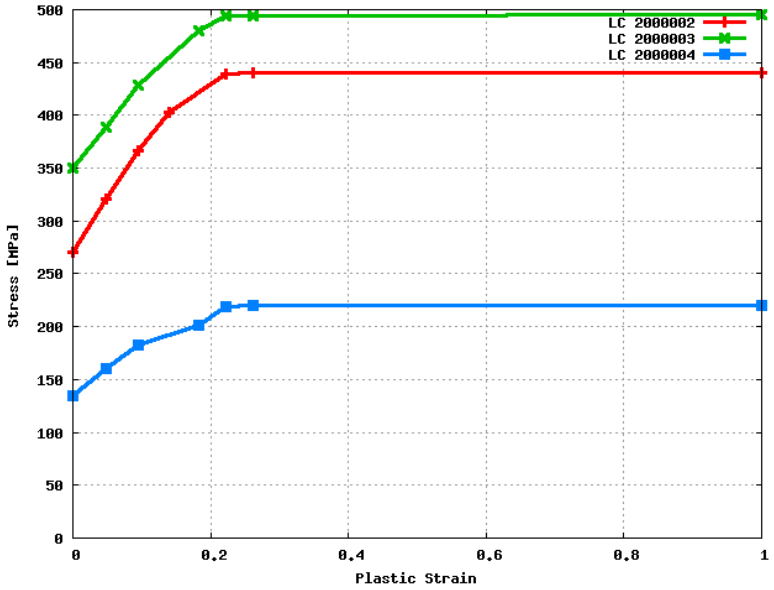

Figure 64. Chart. Flow stress curves in the original model. Labels denote load curve number in the model used for definition of relation between flow stress and plastic strain.

The parts with material that correspond to flow stress of 275 MPa and the load curve 2000002 are shown in figure 65.

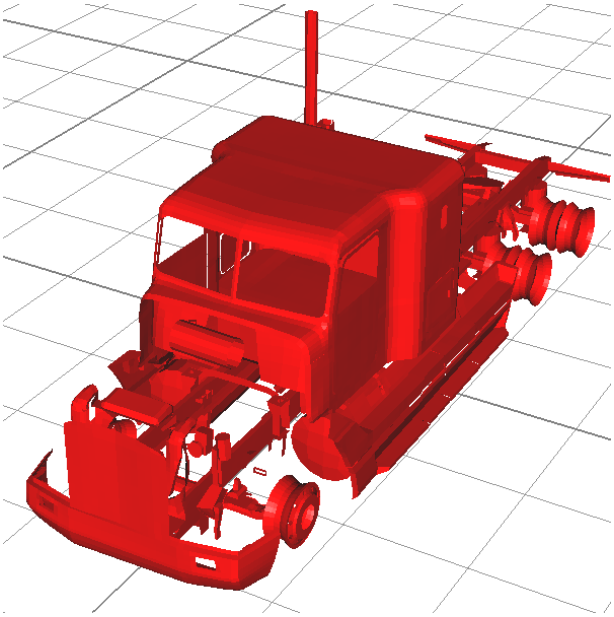

Figure 65. Illustration. Elasto-plastic material with yield stress of 270MPa.

The above group includes parts made of very dissimilar strength materials. For example, tractor frames are made of micro-alloyed steels that have flow strength much higher than 270 MPa., typically above 690 MPa. Bumpers, axles, brackets, and fasteners also have higher yield stress

than specified in the model. On the other hand, body parts are usually made of much softer materials.

The parts with material that correspond to flow stress of 350 MPa and the load curve 2000003 are shown in figure 66 These parts are the suspension leaf springs which are usually much more stronger materials of at least double yield stress than specified here.

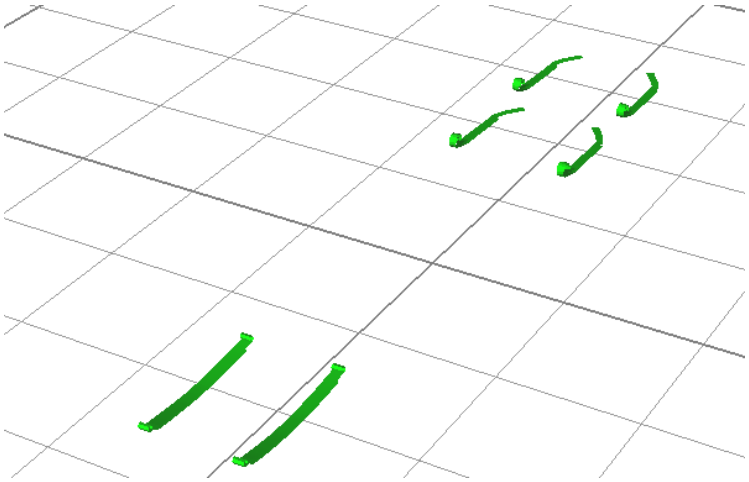

Figure 66. Illustration. Elasto-plastic material with yield stress of 350MPa.

The parts with material that correspond to flow stress of 140 MPa and the load curve 2000004 are shown in figure 67.

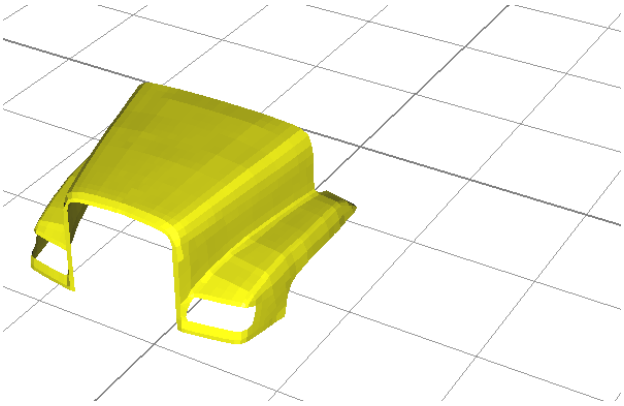

Figure 67. Illustration. Elasto-plastic material with yield stress of 140 MPa.

The material that is used for the hood in this vehicle is usually Sheet Molded Compound (SMC), reinforced with short glass fibers, which has markedly different properties than specified.

Some steel parts had densities changed from steel values, presumably to account for discrepancy in the overall model inertia properties. Many parts usually not made of steel, such as aerodynamic bumpers, chassis side fairing, and hood, had steel properties in the model. This

modeling decision was probably due to the lack of material information and material testing facilities.

Inertial Properties of the Original Tractor Model

From the perspective of vehicle dynamics, the tractor-trailer vehicle can be viewed as an assembly of rigid bodies interconnected by suspensions and hitches [21]. Springs connect two main characteristic sets of masses, unsprung and sprung, while hitches connect sprung masses of the tractor to the sprung mass of the trailer. In the tractor-trailer system, the tractor is only a small part of the total, fully laden heavy truck. However, its kinematics play an important role during the impact as it guides the load-dominant trailer mass through the hitch. Stability and dynamics of heavy vehicles has been extensively studied [21-28]. To investigate the original FE model mass distribution we first had to classify parts in the model into two main characteristic groups. The sprung and unsprung masses for the original model are shown in figure 68.

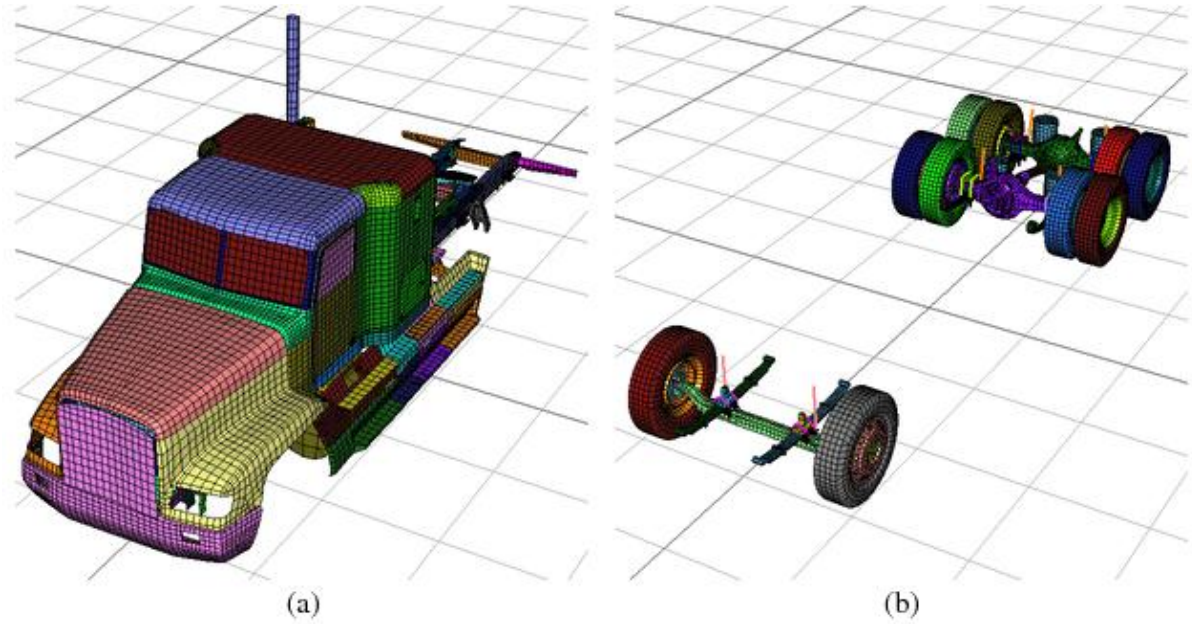

Figure 68. Illustration. Sprung (a) and unsprung mass (b) in the original FE model.

In tractor-trailer systems, unsprung masses are remotely located from the overall center of gravity [21], and since their inertial moments around their own centers of gravity are relatively low, their mass is their most important inertial property. Sprung masses, which include payload, have the dominating effect on heavy truck stability and dynamics, such as dynamic rollover. The sprung mass roll moment of inertia is regularly used for characterization of vehicle properties. Centers of gravity for the entire vehicle, sprung, and unsprung masses are also base indicators of the vehicle inertia and dynamics [21-23, 27].

Over the years, empirical formulas have been developed to estimate inertial properties of heavy trucks, tractors and trailers. Reference [21] lists formulas for sprung mass estimate and its moments of inertia. The sprung weight of the typical tandem axle tractor can be estimated as:

$$W_s = 11,800 + 1,000(L - 190)/30$$

Figure 69. Equation. Sprung Weight of the Typical Tandem Axle Tractor.

where Ws denotes sprung mass in pounds and L denotes the wheelbase in inches. The sprung mass roll inertia can be estimated as:

$$I_{xx} = 2.178W_s$$

Figure 70. Equation. Sprung Mass Roll Inertia.

where Ixx is the roll inertia with units in-lbs-sec2. The horizontal center of gravity with respect to the front axle of the tractor can be estimated as:

$$X_{cg} = 55 + (L - 190)/2$$

Figure 71. Equation. Horizontal Center of Gravity with Respect to the Front Axle of the Tractor.

where all the units are inches. Radius of gyration for mass is also often used for inertial characterization. Measurements are reported for unsprung and total masses.

$$R = \sqrt{I_{xx}/W}$$

Figure 72. Equation. Radius of Gyration for Mass.

The height of center of gravity of sprung mass for typical tractors is 44 inches.

Typical weights for the unsprung masses (axles with tires and brakes) are given as:

Tractor front axle components = 1,200 lbs
Tractor drive axle components = 2,300 lbs

Estimates for other heavy vehicles are also provided in reference [21] together with measured values for different vehicle brands and types. The above formulae are based on simplified models and can be used only as rough estimates. The inertial properties for the Freightliner FLD120 tractor could not be found except for the weights measured before the test [20]. The most detailed measurements of a tractor that are often used in literature come from reference [27]. However from discussions with one of its main authors (Steven M. Karamihas), it turns out that the measured roll moment of inertia is most likely in error, and he is currently reviewing the measurements.

A program was written at ORNL that analyzes the inertial properties of the FE model for different part sets. The main complication in this calculation is that the mass of parts that participates in the constraints is taken out of the mass of the part and assigned to a nodal rigid body that becomes a new nodal rigid body property with separate inertial properties. For example, the total mass of the original model was about 7.5 Tons, out of which 10%, 0.73 Tons were in nodal rigid bodies. Table 21 lists masses and inertias around the centers of gravity for the total, unsprung and sprung masses of the original model. The system axes are as follows: x – longitudinal direction of the truck, y – width direction, z- height direction. The origin of the coordinate system is on the pavement level below the centre of the front axle on the ground level. Reference range values are provided, where available. The reference values are from references [21, 22, 23] and [27].

Table 21. Inertia characteristics of the original FE model.

Inertia Property	Unsprung Mass		Sprung Mass		Total Vehicle	
	Model	Reference	Model	Reference	Model	Reference
Mass (kg)	2,760	2,631	4,763	5,760	7,523	4,932-8,164
X center of gravity (mm)	4,338		1,518	1,740	2,553	1,457-3,327
Y center of gravity (mm)	-21		13		0	
Z center of gravity (mm)	495		1,062	1,118	854	782-1,403
Roll moment, I_{xx} (kg m^2)	1,431		2,115	2,519-2,869	4,110	3,164-10,791
Pitch moment, I_{yy} (kg m^2)	14,603		18,139		47,198	14,875-53,878
Yaw moment, I_{zz} (kg m^2)	15,834		18,135		47,865	14,875-53,878

The original model values are generally within the bounds provided in the references. The mass and the roll moment of the sprung mass in the model are lower than the reference values, which is most likely due to omission of components during model development. The modifications of the parts densities may have been motivated by this difference.

MODIFICATIONS OF THE TRACTOR MODEL

Two main areas of improvement of the original tractor model were suspension and material models. The suspension model improvements are reported in detail in Chapter 3 of this report. The chapter also compares performance of the new model that includes all improvements by Battelle and ORNL researchers with test [20] and the original model. Here, we report on the material assignments in the new model and corresponding constitutive material models employed. All the model modifications and model editing are implemented using computer programs and scripts. Such an approach allows for simple version control; modifications can be turned on and off as needed; and parametric studies can be performed automatically.

New Material Assignments in the Enhanced Tractor Model

As described in Chapter 3, the original tractor model had material-to-part assignments inadequate for crash simulations. For example, compared to the actual vehicle, the original model had significantly lower yield for frame and the leaf springs, and higher yield for tractor body. During crash, parts undergo permanent, plastic, deformation that dissipates impact energy, and the model must have accurate material yield and flow stresses description if we were to have reasonable expectations of accuracy.

In the new model, new materials and constitutive model parameters are assigned to the following part systems:

1. Frame
2. Leaf springs
3. Driveshafts
4. Fasteners, brackets
5. Body, structural bumpers
6. Hood, aerodynamic bumpers, chassis side fairing

In the following, we describe the new material-to-part assignments, sources of information, and the references for the material parameters used.

Frame Material

Heavy truck frames are made of High Strength Low Alloy (HSLA) steels of 690 to 760 MPa yield stress or Aluminum alloys 6061-T6 or 2014-T6 [29]. The photographs from the crash test used for the model development and verification [20] indicate a steel frame. HSLA-100 (690MPa) properties were taken from references [30-32]. The properties of HSLA-100 are highly dependent on heat treatment employed, and as that information was not available, an average value in the range was used. In addition, the frame FE element discretization was too coarse to model localized deformation under off-axis compression. The model of the frame rails for the enhanced model was refined in two steps as shown in figure 73.

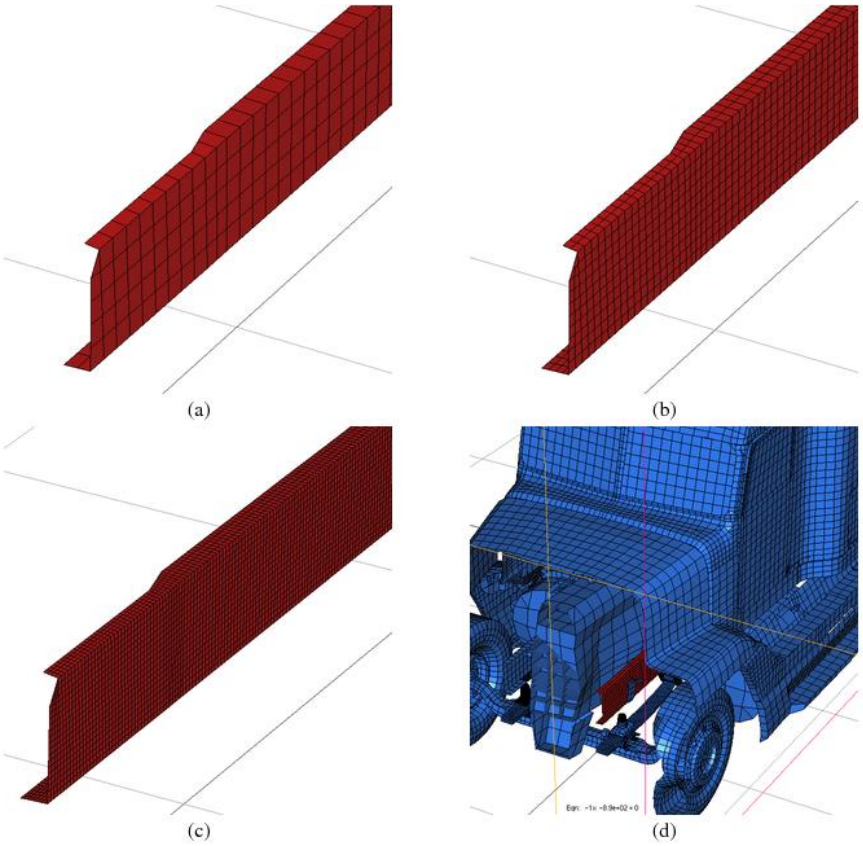

Figure 73. Illustration. FE mesh refinement, (a) original mesh, (b) 1st step, (c) 2nd step, (d) frame location.

Leaf Springs

Leaf springs incorporate axle guiding and suspension in one component [33]. The leaf springs are primarily designed to maximize their service life and fatigue properties. They operate on relatively high working stresses and are located close to the road surface and so are exposed to corrosive media and abrasion. Leaf springs have high material hardness (HRC 50/52), and therefore, they are highly susceptible to minute surface and internal flaws [34]. Fatigue performance [35-37] is the critical design requirement for leaf springs and they undergo complex thermo-mechanical processing [35,37,38], such as hot forming, quenching, shot peening, presetting, etc. For example, shot peening imparts tensile plastic deformation of a surface layer – produced as a sum of numerous indentation expansions and results in compressive residual stresses at the surface. This residual stress in the skin region is approximately half of the yield strength for the heavily work-hardened surface. Residual and applied stresses superimpose themselves, effectively lowering net surface stress that improves the service performance. The modern leaf springs have variable thickness, called tapered or parabolic leaf springs. They are designed to have constant bending stress along their length direction that is achieved by a variable thickness of the leaf according to a parabolic equation from thin end zones to a thicker middle part. The material is SAE 5160 steel or Japanese equivalent SUP9A [38]. The yield stress, flow curve and fracture properties of the leaf springs can vary significantly due to the processing and in-service history [38], so a simple model with average values from the literature

has been implemented. Example of tempering effect on the SUP9A steel properties is shown in figure 74.

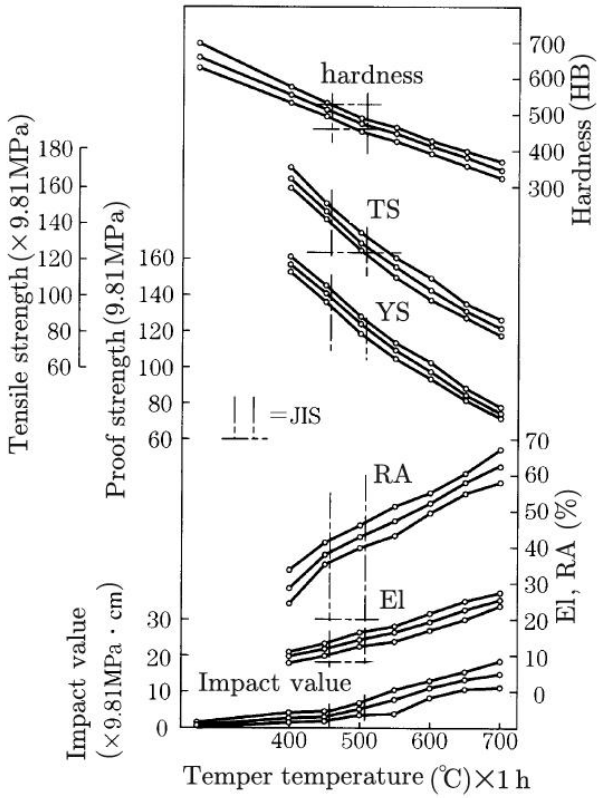

Figure 74. Chart. Effect of tempering temperature on properties of leaf spring steel [37] .

The prescribed minimum values for yield stress and strength are 1079MPa and 1226MPa , respectively, with minimum elongation of 9%. Accounting for residual stresses (e.g. shot peening) and in-service effect (e.g. surface cracks), require detailed testing protocol, which was beyond the scope of this project phase.

Driveshafts, Bars, Cast Parts

For the driveshaft and bar materials, we selected high carbon 51CrV4 steel. These are the standard steels with properties available in online materials databases, such as reference [39]. Cast steel properties were used for the rear axle.

Fasteners, Bolts, Brackets

Fasteners [40] are specified in the vehicle service manual [29] as SAE Grade 5 or SAE Grade 8. SAE Grade 8 was used on critical connections, such as U-bolts. Brackets were set to 5160 steel.

Body, Structural Bumpers, Wheel Hubs

The tractor body [41] is mostly made of mild steel, such as Drawing Quality Special Killed (DQSK) and Interstitial Free (IF) steels. Reinforcements and brackets are made of stronger materials, but since those were not present in the original model, only the mild steel materials were used. Structural bumper and wheels are usually made of HSLA steels, such as HSLA 340MPa.

Hood, Aerodynamic Bumpers, Chassis Side Fairing

On new tractor designs, such as Freightliner SLD, non-structural components on the truck body [41] such as hood, aerodynamic bumpers and chassis side fairing are made of plastic and glass fiber reinforced polymer composites. Sheet moulding compound (SMC) composites and Acrylonitrile-Butadiene-Styrene (ABS) plastics are commonly used materials. We have assumed glass fiber reinforced polyester SMC, 30 weight percent glass. The model is formulated as piecewise linear plasticity model for simplicity. More realistic material models for composites [42-44] will be used in the next phase of the project. The Chassis side fairing on Freightliner SLD tractor can be made of steel or fiberglass and ABS. The current model uses mild steel since the exact material could not be determined from the test photographs [20].

Summary of Material Model Parameters

The summary of material assignments for the new model is shown in figure 75. Model materials are defined in a separate file that is loaded into the main model file.

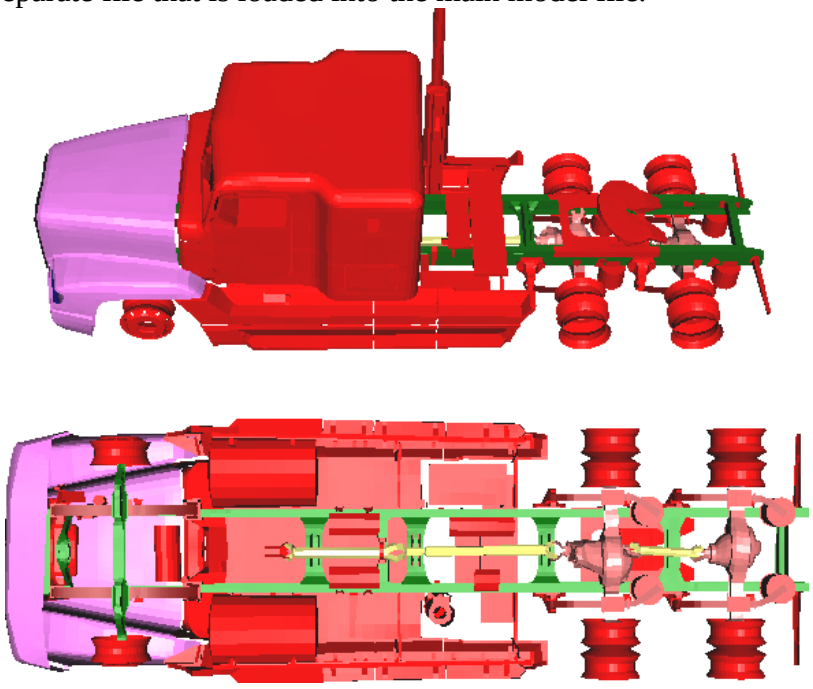

Figure 75. Illustration. Material assignment in the enhanced model.

Material parameters for elastoplastic models defined as piecewise linear stress strain curves are shown in figure 76.

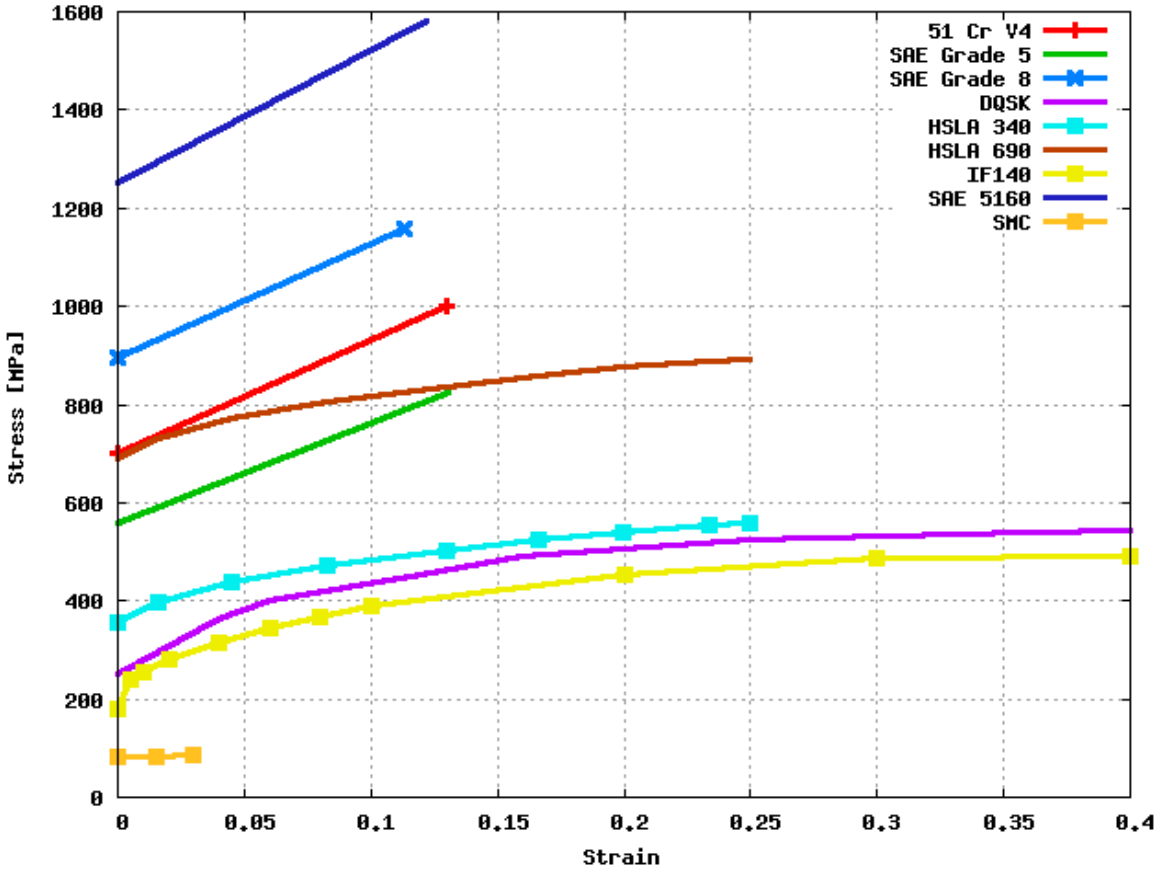

Figure 76. Chart. Elasto-plastic material parameters for the enhanced model.

The enhanced model may be further improved by application of more advanced material models for steel [45], plastic [42], and special parts such as cabin mounts [46], and windshield [47]. Details of leaf spring thermo-mechanical treatment may also provide marked improvement in its response.

Inertia Properties for the Enhanced Tractor Model

The parts in the new model were assigned to the two main vehicle dynamics sets as it was done for the original model. The sprung and unsprung masses are shown in figure 77.

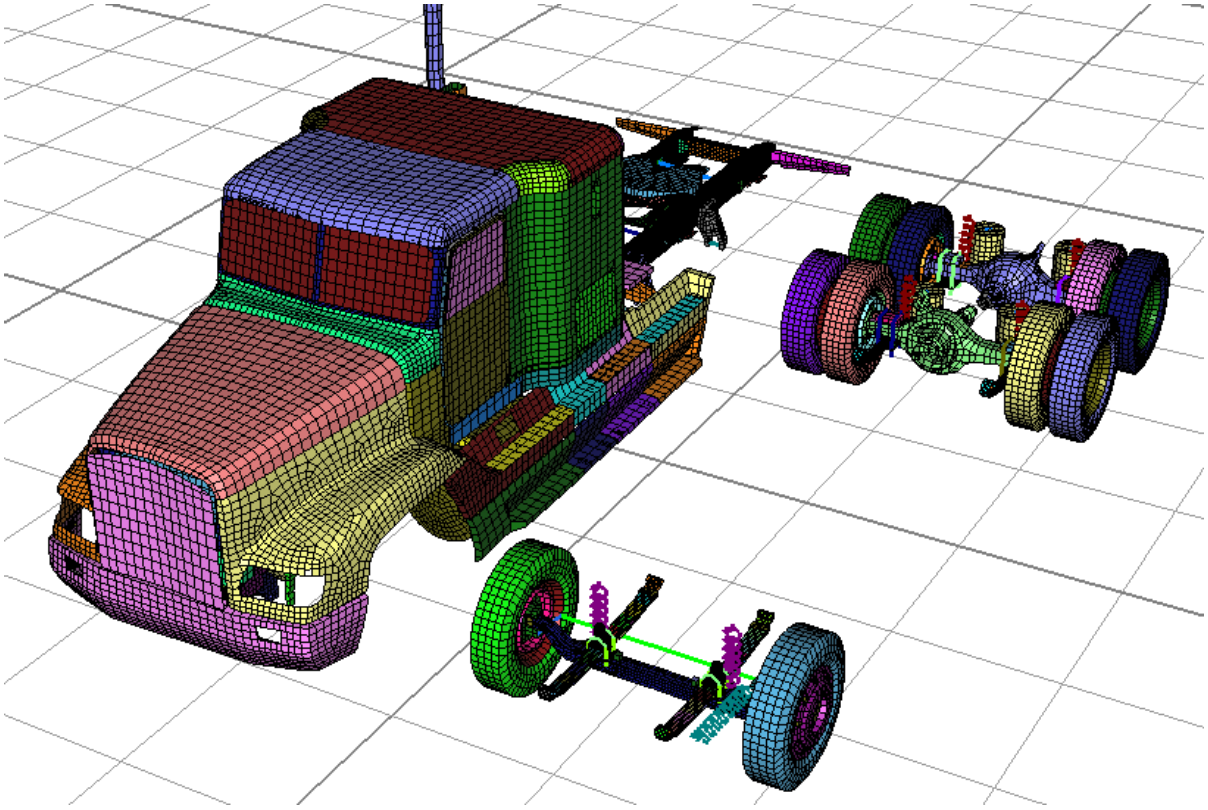

Figure 77. Illustration. Sprung (left) and unsprung (right) mass sets in the enhanced model.

The inertia properties of the modified tractor model are listed in table 22 together with reference values from the literature.

Table 22. Inertia characteristics of the enhanced FE model.

Inertia Property	Unsprung Mass		Sprung Mass		Total Vehicle	
	Model	Reference	Model	Reference	Model	Reference
Mass (kg)	2,757	2,631	4,955	5,760	7,712	4,932-8,164
X center of gravity (mm)	4,448		1,497	1,740	2,552	1,457-3,327
Y center of gravity (mm)	-21		22		7	
Z center of gravity (mm)	498		1,047	1,118	851	782-1,403
Roll moment, I_{xx} (kg m^2)	1,550		2,294	2,519-2,869	4,379	3,164-10,791
Pitch moment, I_{yy} (kg m^2)	13,709		17,712		47,381	14,875-53,878
Yaw moment, I_{zz} (kg m^2)	15,054		17,665		47,815	14,875-53,878

The overall change of the inertia properties compared to the original model is not significant. The markedly better performance of the enhanced model is primarily due to the vastly improved FE sub-models for the suspension and models for deformation of the critical structural parts of the tractor. The distribution of masses can now be better handled due to our ability to evaluate the inertial effect of parts modifications. The inertial modifications are primarily needed for the sprung mass with which we can tune the target inertial properties. This capability will be used in the second phase of the project to conduct a parametric study of the inertial properties on the tractor on its interaction with roadside safety barriers.

DEVELOPMENT OF THE WEB-BASED DOCUMENTATION

We have developed a base project web site and an web-based user manual for the tractor FEA model [48], similar to that developed previously for the SUT model [49]. The current web technologies allow for development of a dynamic web server system that can continuously be updated as the work on the project progresses and new versions of the model evolve. Current capabilities include base Web documentation structure, template strategy, base scripts, database, and management strategies for dynamic delivery of the content.

Modern vehicle FE models contain a large number of submodels, parts, components, and systems with complex properties, interaction, connectivity, and spatial and functional relations that are best described using interactive, cross-linked documentation that mimics the relations in the model. The new web technologies allow us to go beyond static, linear flowing information, and allow users to explore the model to his or her own preferences and a level of expertise.

Current Status

For a dynamically generated web user manual system, a big part of the overall work is the design and organization of the underlying database system and basic data structures that form the foundation of the system. As stated above, constant updates to the model in the project as well as likely future updates would make a static system very labor intensive and would inevitably become obsolete due to tendency of model developers to procrastinate on documentation updates. So, from the practical perspective, the web manual system should be easy to use and maintain; new versions of the model should not require manual modification of the web user manual data. Our solution is to develop a system that dynamically parses and generates model user manual data, provides multiple paths for model exploration, combines multimedia documentation, and enables visual exploration of the model. To that goal we have developed a basic database system, data types, templates, and user queries forms for content generation. The first version of the system is available on the World Wide Web [48]. The system implements basic viewing for model's part structure, FE element types, material properties, contact interfaces and simulation results. The full functionality to the web site will be built up during future phases of the project.

Figure 78 shows the interface for the FE element types. Users can currently select entities by their labels. The visually driven selection and information delivery, similar to the Virtual Reality Modeling Language (VRML) interface from the previous SUT web user manual [49] will be implemented during the next phase of the project. The evolving technologies in Web3D [50] will

be explored to build upon the previously developed VRML based system. Limited editing of the model will also be enabled to allow for model customization.

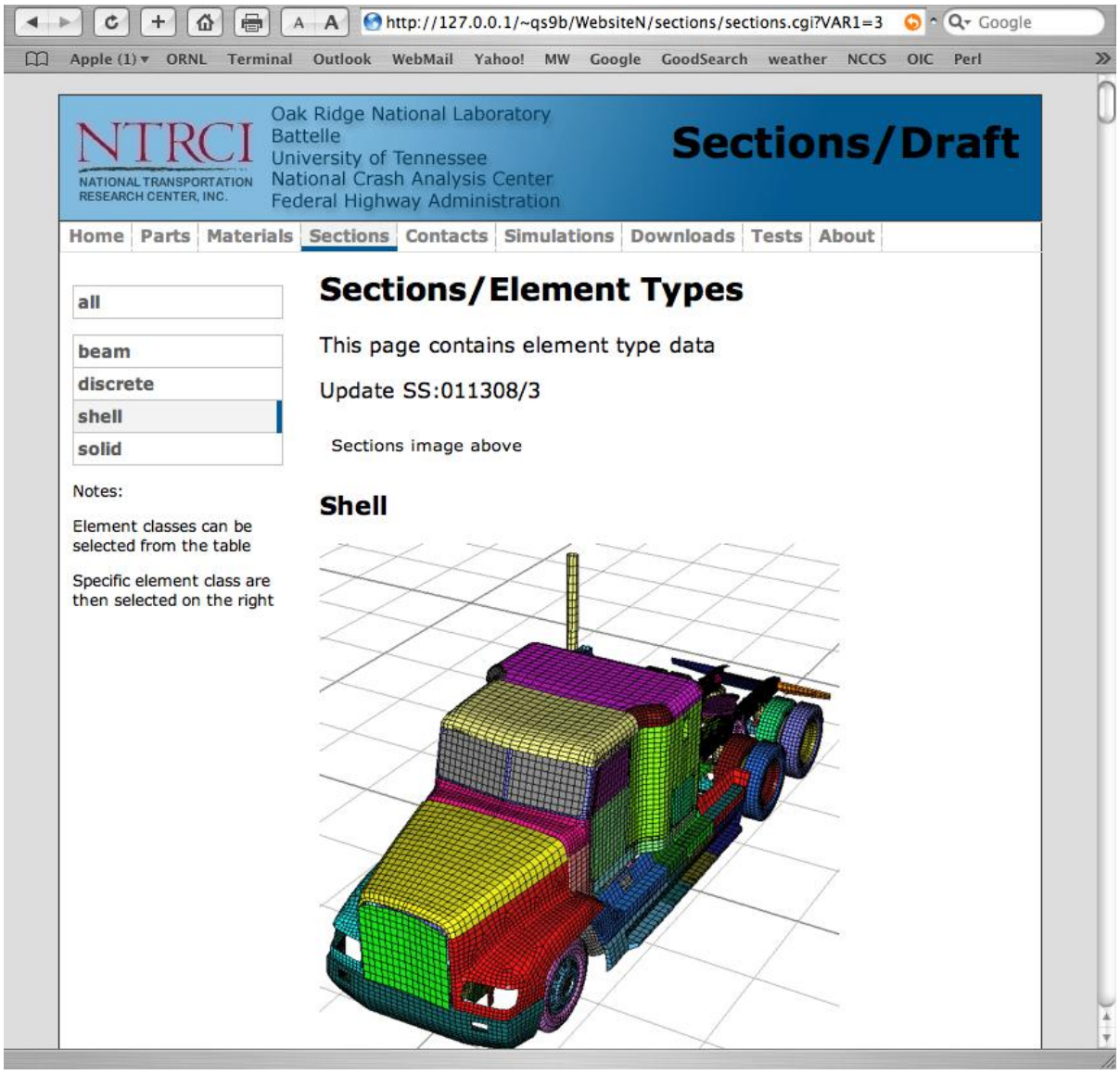

Figure 78. Screen Shot. Web-based model manual.

SUMMARY

The original heavy truck-trailer Finite Element (FE) method model developed by the National Crash Analysis Center for the US Department of Transportation Federal Highway Administration has been analyzed to determine areas for its further improvement. The FE model consisted of separate models for the tractor and the trailer. The trailer model was found to be inadequate for conducting FE simulations and the focus was directed on tractor model enhancements. Several shortcomings in the tractor model have been found, most critically in the areas of vehicle suspension and materials. The inertia characteristics of the model were also compared with the values reported in literature due to mismatch of the kinematics of the original FE model with the impact test data.

This document describes the analysis of the material models, and the new material sub-models and material-to-part assignment for the enhanced FE tractor model. The new FE model has new material models for suspension, frame, body, bumpers, fasteners, brackets, and axles. Further improvements are possible by implementing better material models based on mechanical testing and better constitutive models. Suspension modifications have been implemented by Battelle researchers and documented in Chapter 3 of this report. An inertia analysis program has been developed to allow for the evaluation of model modification effects on the overall kinematics of the vehicle. We have developed a base version of the World Wide Web user manual for the model. The manual allows for interactive analysis of the model and its capabilities. As a possible extension of this capability, reasonable capabilities for model modification and generation can also be made possible in order to tailor the model to the needs of the user. For example, capabilities to tailor the moments of inertia, material substitution, part deletion, wheelbase length, etc., can be implemented to generate FE models with user-defined properties. Of course, such capability should be limited to a reasonable set of options of interest for a particular model.

CHAPTER 5. SUMMARY OF PLANS FOR PHASE B OF THE INVESTIGATION

The evaluation and modifications of the combined tractor-trailer model have not yet been completed. A preliminary evaluation of the modified tractor and trailer FE model was initiated, but could not be completed in the first phase of the program. A major objective of Phase B of the project will be to validate the combined tractor-trailer models by simulating full-scale crash test(s) identified in the literature and comparing simulated vehicle behavior and failure modes to those reported in the crash test(s).

Once the performance of the tractor-trailer FE model is considered acceptable, the model will be provided to the other Centers of Excellence (COEs) in roadside safety, viz., Texas Transportation Institute (TTI), MwRSF, Worcester Polytechnic Institute (WPI), and ARA-Sacramento. Use of the beta version by the COEs is encouraged so that deficiencies not identified by the NTRCI Finite Element Analysis Team can be brought forth to better improve the tractor-trailer FE model. They may have applications for the tractor-trailer FEA model that could reveal unsuspected or previously unobserved kinematic behavior and/or failure modes of the tractor-trailer combination in impact situations. All comments and suggestions from the COEs will be

assessed and discussed with NCAC and FHWA for further action, including implementation into the model if deemed appropriate.

Also, a primary objective of the study is to determine the overall fidelity of the tractor-trailer FE model. Thus, an acceptable level of fidelity for the model will need to be established based on expected applications. The current level of geometric detail in the model limits its use to applications involving low vehicle deformations (e.g., roadside safety type applications-redirective impact on barriers) or applications involving the vehicle as simply a source of impact energy, where results are not significantly sensitive to vehicle damage (e.g., homeland security type applications). Since a primary use for the model will be to simulate TL-5 impacts into roadside safety barriers, the validation criteria for assessing model performance will be based on test data obtained from the literature involving full-scale TL-5 tests.

A summary of crash test data from a number of full-scale crash tests involving tractor-trailer impacts into roadside safety barriers is compiled in Chapter 2 of this report. Only those tests involving rigid barriers will be considered in the evaluation so that the mechanics of the impact can be isolated to the response of the vehicle. Unfortunately, none of those tests involve the specific tractor type that the FE model was based on. Furthermore, most of the tests were focused on performance of a barrier system rather than the vehicle, and consequently, very little information was provided in the reports regarding damage and response of the vehicles. The electronic data (e.g., accelerometer, rate gyros, photos, videos, etc.) corresponding to these tests will be synthesized to discern as much information as possible relating to the vehicle's response during impact in order to establish the validation criteria.

The vehicle dimensions may also need to be altered to meet Report 350 requirements before being applied in the analysis of roadside safety structures. NCHRP Report 350 does not require a specific make or model for the test vehicle, but rather provides recommended properties for the test vehicles to represent various classes of vehicles. For example, NCHRP Report 350 Test Level 5 requires that the maximum tractor wheel base not exceed 189 inches for the 36000V vehicle (79,366-lb tractor/van-trailer), which cannot be attained with a traditional style tractor with a sleeper-cab. The current model's wheel base length is 217.2 inches (5.52 m) and includes a sleeper-cab. It is recommended that the development/enhancement of the model continue based on its current geometry and that the model be validated using data obtained from FOIL/NCAC Test No. 03008. Once the model is validated, it can then be modified to meet length requirements of Report 350 by removing a section of the sleeper and the frame of the tractor. However, any permanent changes to the FE model (such as reduced length) will be at the agreement of FHWA, NCAC and the COEs.

In summary, the objectives of the next phase of effort are:

1) Complete preliminary evaluation and modifications of the combined tractor-trailer model based on a qualitative comparison to test data.
2) Provide model to COE community for beta testing.
3) Validate combined tractor-trailer model performance by comparison of the computer simulation results to the results of full-scale crash tests.

CHAPTER 6. REFERENCES

1. Ross, H.E., D.L. Sicking, and H.S. Perrara, "Recommended Procedures for the Safety Performance Evaluation of Highway Appurtenances," *National Cooperative Highway Research Program Report No. 350*, Transportation Research Board, Washington, D.C., 1993.
2. Presentation at Summer 2007 COE Workshop at Livermore Software Technology Corporation (LSTC) in Livermore, CA.
3. Clarke, C.K. and G.E. Borowski, "Evaluation of a Leaf Spring Failure," Paper No. 1547-7029, ASM International, August 31, 2005.
4. Orengo, F., M.H. Ray and C.A. Plaxico, "Modeling Tire Blowout in Roadside Safety Hardware Simulations Using LS-DYNA," Proceedings of IMECE'03 2003 ASME International Mechanical Engineering Congress & Exposition, Washington, D.C., November 16-21, 2003.
5. Marzougui, D., "Freightliner into 42 in. F-Shape concrete barrier at 25 degrees," Test Setup Report, Test No. 03008, Federal Outdoor Impact Laboratory, McLean, Virginia, August 28, 2003.
6. Polivka et al., "Development, Testing, and Evaluation of NDOR's TL-5 Aesthetic Open Concrete Bridge Rail," Report No. TRP-03-148-05, Midwest Roadside Safety Facility, Lincoln, Nebraska, 2005.
7. Rosenbaugh, S.K., Sicking, D. L., Faller, R. K., "Development of a TL-5 Vertical Faced Concrete Median Barrier Incorporating Head Ejection Criteria", Midwest Roadside Safety Facility, University of Nebraska-Lincoln (2007).
8. Ross, H. E., Sicking, D .L., Perrara, H. S., "Recommended procedures for the safety performance evaluation of highway appurtenances," National Cooperative Highway Research Program Report No. 350, Transportation Research Board, Washington, DC, 1993.
9. Borovinsek, M., Vesenjak, M., Ulbina M., Ren, Z., "Simulation of crash tests for high containment levels of road safety barriers", Engineering Failure Analysis, v 14, n 8, p 1711-8, 2007.
10. Itoh, Y., Liu, C., Kusama, R., "Dynamic simulation of collisions of heavy high-speed trucks with concrete barriers", Chaos, Solitons & Fractals, v 34, n 4, p 1239-44, 2007.
11. Atahan, A. O., "Crashworthiness analysis of a bridge rail-to-guardrail transition", Accident Analysis & Prevention", Accident Analysis & Prevention, In Press, 2007.
12. Alberson, D. C, Zimmer, R. A., Menges W. L., "NCHRP report 350 compliance test 5-12 of the 1.07-m vertical wall bridge railing", Research study 405511-2, Texas Transportation Institute, College Station, TX, 1996.
13. Plivka, K. A., Faller, R. K., Rohde, J. R., Holloway J. C., Sicking D. L., "Development, testing and evaluation of NDOR's TL-5 aesthetic open concrete bridge rail", MwRSF research report TRP-03-148-05, Midwest Roadside Safety Facility, Lincoln, NE, 2005.
14. Hirsch, T. J., Fairbanks, W. L., Buth, C. E., " Modified type T5 bridge rail to redirect busses and trucks", Research report 416-1F, Texas Transportation Institute, College Station, TX, 1984.
15. Mark, K. K., Campise, W. L., "Test and evaluation of Ontario "Tall wall" barrier with an 80,0000-pound tractor-trailer", Project no. RF 71620, Texas Transportation Institute, College Station, TX, 1990.
16. Campise, W. L., Buth, C. E., "Performance limits of longitudinal barrier systems", Contract no. DTFH61-82-C-00051, Texas Transportation Institute, College Station, TX, 1985.
17. Mak, K. K., Beason, W. L., Hirsch, T. J., Campise W. L., "Oblique angle crash tests of loaded heavy trucks into an instrumented wall", Report DOT HS 807 256, Texas Transportation Institute, College Station, TX, 1988.
18. Hirsch, T. J., Arnold, A., "Bridge rail to restrain and redirect 80,000 lb. trucks", Research report 230-4F, study TTI-2-5-78-230, Texas Transportation Institute, College Station, TX, 1981.
19. Buth, C. E., Hirsch, T. j., Menges, W. L., "Testing of new bridge rail and transition designs", Contract no. DTFH61-86-C-00071, Texas Transportation Institute, College Station, TX, 1997.

20. Marzougui, D., “Freightliner into 42 in. F-Shape concrete barrier at 25 degrees,” Test Setup Report, Test No. 03008, Federal Outdoor Impact Laboratory, McLean, VA, 2003.
21. Fancher, P. S., Ervin, R. D., Winkler, C. B., Gillespie, T. D., "A factbook of the mechanical properties of the components for single-unit and articulated heavy trucks. Phase I. Final report", University of Michigan, Ann Arbor, Transportation Research Institute, Report Number: UMTRI-86-12, 1986.
22. Winkler, C. B., "Inertial properties of commercial vehicles - descriptive parameters used in analyzing the braking and handling of heavy trucks. Volume 2.", University of Michigan, Ann Arbor, Transportation Research Institute, Report Number: UM-HSRI-81-19-2, 1981.
23. Winkler, C. B., "Inertial properties of commercial vehicles - descriptive parameters used in analyzing the braking and handling of heavy trucks. Volume 2. Second edition. Final report", University of Michigan, Ann Arbor, Transportation Research Institute, Report Number: UMTRI-83-17, 1983.
24. Fancher, P. S., Winkler, C. B., Bernard, J. E., "Simulation of the braking and handling of trucks and tractor trailers. Summary report: motor truck braking and handling performance study", Highway Safety Research Institute, Ann Arbor, MI, Report Number: UM-HSRI-PF-73-2, 1973.
25. Fancher, P. S., Ervin, R. D., Gillespie, T. D., Winkler, C. B., Segel, L., "Heavy truck stability: synthesis/program plan development. Final report", University of Michigan, Ann Arbor, Transportation Research Institute, Report Number: UMTRI-86-3, 1985.
26. Winkler, C. B., , "Experimental determination of the rollover threshold of four tractor-semitrailer combination vehicles. Final report", University of Michigan, Ann Arbor, Transportation Research Institute, Report Number: UMTRI-87-31, 1987.
27. Winkler, C. B., Bogard, S. E., Karamihas, S. M., Parameter measurements of a highway tractor and semitrailer. Final technical report, Report Number: UMTRI-95-47, University of Michigan Transportation Research Institute, 1995.
28. Kamnik, R., Boettiger, F., Hunt, K., "Roll dynamics and lateral load transfer estimation in articulated heavy freight vehicles", Proc. Instn Mech. Engrs Vol. 217 Part D: J. Automobile Engineering, p 985-97, 2003.
29. “Heavy-duty trucks service manual, Group 31-32.15”, Freightliner LLC, Portland OR, 1994.
30. Prabal, K. R., Ratan, I. G, Ashok, K. P, "Influence of Heat Treatment Parameters on Structure and Mechanical Properties of an HSLA-100 Steel", Steel Research (Germany), v 73, n 8, p 347-355, 2002.
31. Koss, D. A., Chae, D., "Damage accumulation and failure of HSLA-100 steel", Materials Science and Engineering A, v 366, n 2, p 299-309, 2004.
32. Xue, Q., Benson, D., Meyers, M.A., Nesterenko, V.F., Olevsky, E.A., "Constitutive response of welded HSLA 100 steel", Materials Science and Engineering A, v 354, p 166-79, 2003.
33. Kaiser, B., Berger, C., "Fatigue behaviour of technical springs", Mat.-wiss. u. Werkstofftech. v 36, n 11, p 685-96, 2005.
34. Clarke, C. K., Borowski, G. E., "Evaluation of a leaf spring failure", Journal of Failure Analysis and Prevention, Volume 5(6) December 2005, JFAPBC, v 6, p 54-63, 2005.
35. Landgraf, R.W. and Francis, R.C., "Material And Processing Effects On Fatigue Performance Of Leaf Springs", 1979 SAE Congress and Expos., Document number: 1979017, 1979.
36. Yang, Z., Wang, Z., "Cyclic creep and cyclic deformation of high-strength spring steels and the evaluation of the sag effect: Part I. Cyclic plastic deformation behavior", Metallurgical and Materials Transactions A, v 32, n 7, p 1687-98, 2001.
37. Reguly, A., Strohaecker, T.R., Krauss, G., Matlock, D. K., "Quench Embrittlement of Hardened 5160 Steel as a Function of Austenitizing Temperature", Metallurgical and Materials Transactions A, v 35A, p 153-62, 2004.
38. Yamada, Y. Ed., "Materials for Springs", Springer, 2007.
39. “MatWeb”, www.matweb.com.

40. Jones, F., Ryffel, H., Oberg, E., McCauley, C., Heald, R., "Machinery's Handbook", Industrial Press, 2004.
41. Schmit, D., "Design of a Medium and Heavy-Duty Truck Cab Shell", Commercial Vehicle Engineering, Congress and Exhibition, Rosemount, IL, October 26-28, 2004, SAE paper 2004-01-2637, 2004.
42. Lee, H.K.; Simunovic, S.; Shin, D.K., "A computational approach for prediction of the damage evolution and crushing behavior of chopped random fiber composites " Computational Materials Science, v 29, n 4, p 459-74, 2004.
43. Morozov, E. V., Morozov, K.E., Selvarajalu, V., "Progressive damage modelling of SMC composite materials", Composite Structures, v 62, p 361-6, 2003.
44. Oldenbo, M., Varna, J., "A Constitutive Model for Non-linear Behavior of SMC, Accounting for Linear Viscoelasticity and Micro-Damage", Polymer Composites, p85-97, 2005.
45. Rusinek, A., Zaera, R., Klepaczko, J.R., "Constitutive relations in 3-D for a wide range of strain rates and temperatures - Application to mild steels", International Journal of Solids and Structures, v 44, n 17, p 5611-34, 2007.
46. Ward, C. H., "The Application of a New Cab Mounting to Address Cab Shake on the 2003 Chevrolet Kodiak and GMC TopKick", International Truck and Bus Meeting and Exhibition Detroit, MI, SAE paper 2002-01-3102, 2002.
47. Du Bois, P. A., Kolling, S., Fassnacht, W., "Modelling of safety glass for crash simulation", Computational Materials Science, v 28, n 3-4, p 675-83, 2003.
48. “Tractor Trailer Model”, http://thyme.ornl.gov/FHWA/Tractor/index.cgi
49. “Single Unit Truck FEM Model”, http://thyme.ornl.gov/FHWA/F800WebPage/description
50. “Web3D Consortium”, http://www.web3d.org